

AD-A034 005

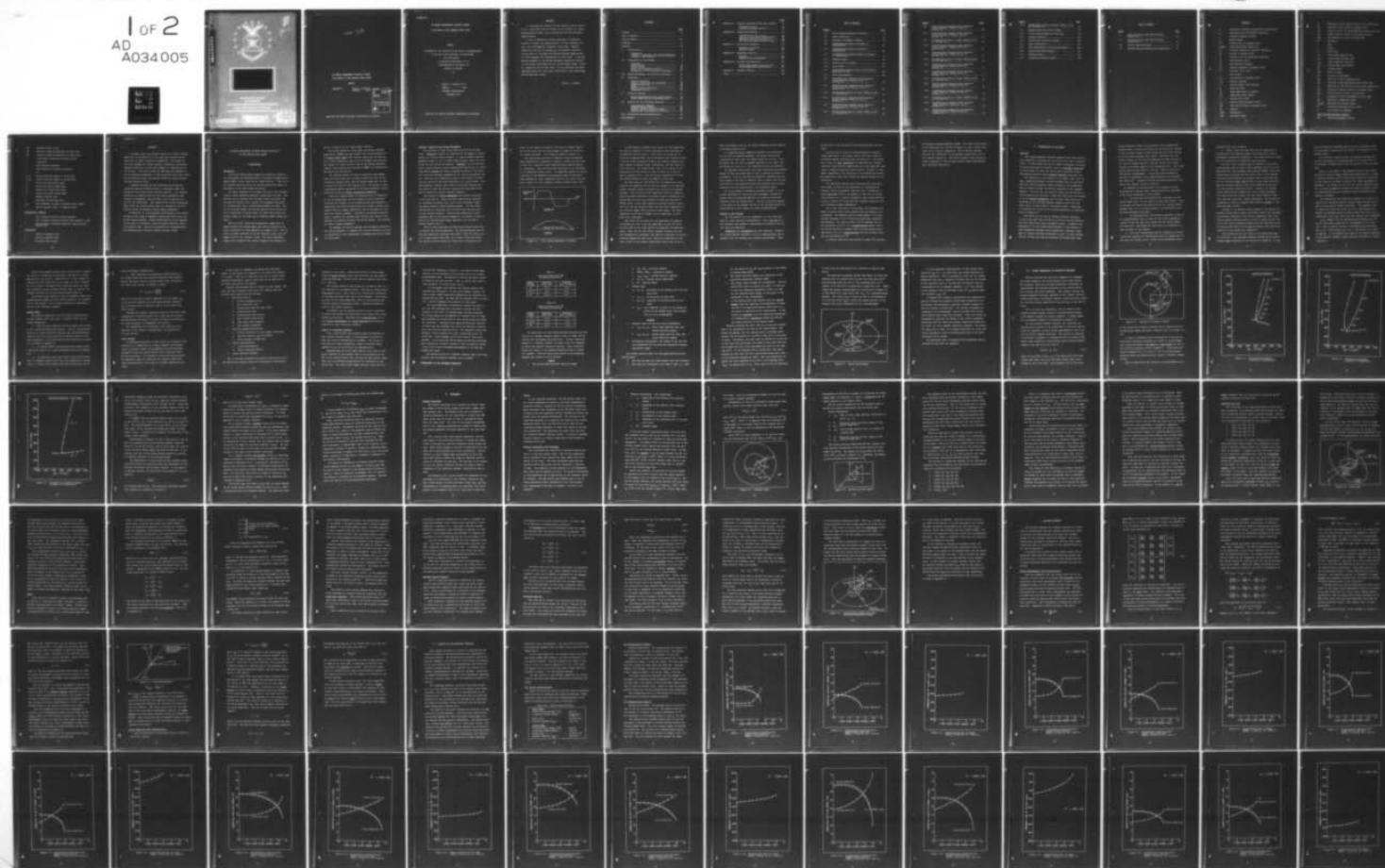
AIR FORCE INST OF TECH WRIGHT-PATTERSON AFB OHIO SCH--ETC F/G 22/3
AN ENERGY MANAGEMENT GUIDANCE SCHEME APPLICABLE TO THE INTERIM --ETC(U)
DEC 76 J L ROBERTS

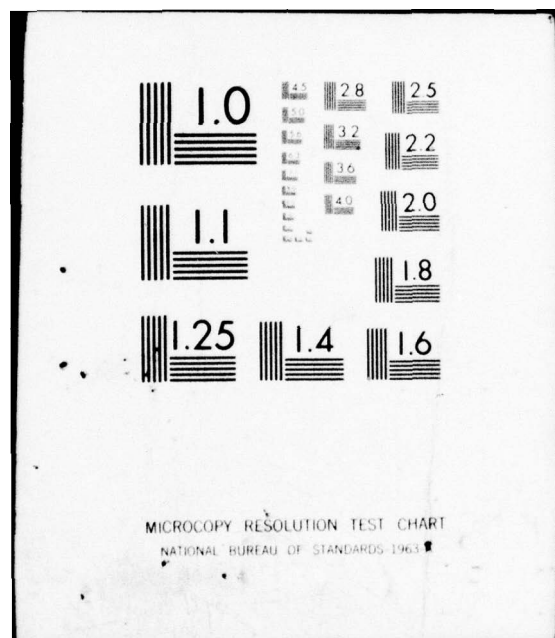
UNCLASSIFIED

6A/EE/76-1

NL

1 OF 2
AD
A034005



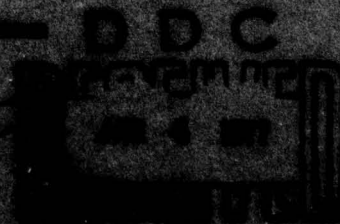
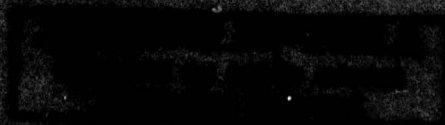


ADA034005



UNITED STATES AIR FORCE
AIR UNIVERSITY
AIR FORCE INSTITUTE OF TECHNOLOGY
Wright-Patterson Air Force Base, Ohio

Copy available to the public
upon request by the requester




See 1473

AN ENERGY MANAGEMENT GUIDANCE SCHEME
APPLICABLE TO THE INTERIM UPPER STAGE

THESIS

GA/EE/76-1

Jackie L. Roberts
Captain USAF

ACCESSION for	
NTIS	White Section <input checked="" type="checkbox"/>
DPC	Buff Section <input type="checkbox"/>
UNANNOUNCED	<input type="checkbox"/>
JUSTIFICATION	
BY	
DISTRIBUTION/AVAILABILITY CODES	
Dist.	AVAIL. and/or SPECIAL
	

Approved for public release; distribution unlimited

AN ENERGY MANAGEMENT GUIDANCE SCHEME

APPLICABLE TO THE INTERIM UPPER STAGE

THESIS

Presented to the Faculty of the School of Engineering
of the Air Force Institute of Technology

Air University

in Partial Fulfillment of the
Requirements of the Degree of
Master of Science

by

Jackie L. Roberts, B. S.

Captain USAF

Graduate Astronautics

December 1976

Approved for public release; distribution unlimited

Preface

In selecting the subject of this thesis it was my desire to do a study which may be helpful to the overall U.S. Space Transportation System, and in particular the Interim Upper Stage program.

I wish to express my sincere gratitude to Professor Richard M. Potter, my thesis advisor, for his interest, advise, and encouragement throughout this study. Special thanks are also due the members of the Reusable Launch Vehicles Office of the Space and Missile Systems Organization, for their guidance and sponsorship of this thesis. I am also greatly indebted to the Boeing Aerospace Company for providing up-to-date information on the Interim Upper Stage. Finally, thanks are due my wife, Wynn, for her patience and understanding during the long lonely hours while I was researching and writing this thesis.

Jackie L. Roberts

Contents

	<u>Page</u>
Preface.....	ii
List of Figures.....	v
List of Tables.....	viii
Notation.....	ix
Abstract.....	xii
I. Introduction.....	1
Background.....	1
Guidance, Targeting, and Energy Management.....	3
Outline of the Problem.....	6
II. Formulation of the Scheme.....	9
Overview.....	9
Dynamic Model.....	13
Error Sources.....	14
Choice of a Transfer Scenario.....	16
Explanation of the Prelaunch Targeting.....	17
III. Energy Management by Trajectory Matching.....	23
IV. Targeting.....	31
Overall Objective.....	31
Mission Constraints and Variables.....	32
Targeting Step One.....	39
NS01A.....	41
Maximum Payload Missions.....	45
Targeting Step Two.....	46
V. Accuracy Analysis.....	51
Thrust Misalignment Error Sensitivities....	51
Thrust Magnitude Error Sensitivities.....	56
VI. Results for the Reference Missions.....	59
Geosynchronous Mission.....	61
Subsynchronous Mission.....	61
Transfer Between Coplanar Orbits.....	83
Observations Concerning the Results.....	85
VII. Conclusions and Recommendations.....	90
Bibliography.....	92

	<u>Page</u>
Appendix A: Computer Simulation Algorithm Summary..	93
Targeting Portion.....	93
Accuracy Analysis Portion.....	94
Appendix B: Trajectory Matching.....	95
Calculation of ΔV_1 and ΔV_2	95
Limits of First Burn Plane Change....	97
Impulsive Transfer Derivation.....	99
The Functional Relationship $\Delta V_2(\psi_1)$..	108
Appendix C: Finite Burn Dynamics.....	112
Equations of Motion.....	112
Transfer Angle.....	114
Appendix D: Targeting Step Two.....	117
Phasing.....	117
Mission Delay Retargeting.....	120
Appendix E: Accuracy Determination.....	122
Thrust Misalignment Sensitivities....	122
Thrust Magnitude Sensitivities.....	127
Appendix F: Computer Listing.....	128
Vita.....	150

List of Figures

<u>Figure</u>		<u>Page</u>
1-1	Prior Energy Management Proposals.....	4
2-1	Epoch Conditions.....	21
3-1	Coplanar non-Hohmann Transfer.....	24
3-2	Geosynchronous Mission Allowable ΔV Combinations.....	25
3-3	Subsynchronous Mission Allowable ΔV Combinations.....	26
3-4	Geosynchronous Coplanar Mission Allowable ΔV Combinations.....	27
4-1	Transfer Angle.....	34
4-2	Thrust Direction Angles.....	35
4-3	Local Frame.....	40
4-4	Relationship Between Local and Geocentric- Equatorial Frames.....	49
5-1	Worst Misalignment.....	56
6-1	Geosynchronous Insertion Error Sensitiv- ities (Position) ($PROP_1=17,300$ lb, $PL=1000$ lb).....	62
6-2	Geosynchronous Insertion Error Sensitiv- ities (Velocity) ($PROP_1=17,300$ lb, $PL=1000$ lb).....	63
6-3	Geosynchronous Time of Flight ($PROP_1=17,300$ lb, $PL=1000$ lb).....	64
6-4	Geosynchronous Insertion Error Sensitiv- ities (Position) $PROP_1=17,300$ lb, $PL=2000$ lb).....	65
6-5	Geosynchronous Insertion Error Sensitiv- ities (Velocity) ($PROP_1=17,300$ lb, $PL=2000$ lb).....	66
6-6	Geosynchronous Time of Flight ($PROP_1=17,300$ lb, $PL=2000$ lb).....	67

<u>Figure</u>		<u>Page</u>
6-7	Geosynchronous Insertion Error Sensitiv- ities (Position) ($PROP_1=17,300$ lb, PL=3000 lb).....	68
6-8	Geosynchronous Insertion Error Sensitiv- ities (Velocity) ($PROP_1=17,300$ lb, PL=3000 lb).....	69
6-9	Geosynchronous Time of Flight ($PROP_1=17,300$ lb, PL=3000 lb).....	70
6-10	Geosynchronous Insertion Error Sensitiv- ities (Position) ($PROP_1=20,000$ lb, PL=1000 lb).....	71
6-11	Geosynchronous Insertion Error Sensitiv- ities (Velocity) ($PROP_1=20,000$ lb, PL=1000 lb).....	72
6-12	Geosynchronous Time of Flight ($PROP_1=20,000$ lb, PL=1000 lb).....	73
6-13	Geosynchronous Insertion Error Sensitiv- ities (Position) ($PROP_1=20,000$ lb, PL=2000 lb).....	74
6-14	Geosynchronous Insertion Error Sensitiv- ities (Velocity) ($PROP_1=20,000$ lb, PL=2000 lb).....	75
6-15	Geosynchronous Time of Flight ($PROP_1=20,000$ lb, PL=2000 lb).....	76
6-16	Geosynchronous Insertion Error Sensitiv- ities (Position) ($PROP_1=20,000$ lb, PL=3000 lb).....	77
6-17	Geosynchronous Insertion Error Sensitiv- ities (Velocity) ($PROP_1=20,000$ lb, PL=3000 lb).....	78
6-18	Geosynchronous Time of Flight ($PROP_1=20,000$ lb, PL=3000 lb).....	79
6-19	Subsynchronous Insertion Error Sensitiv- ities (Position) ($PROP_1=17,300$ lb, PL=4400 lb).....	80
6-20	Subsynchronous Insertion Error Sensitiv- ities (Velocity) ($PROP_1=17,300$ lb, PL=4400 lb).....	81

<u>Figure</u>		<u>Page</u>
6-21	Subsynchronous Time of Flight ($PROP_1=17,300$ lb, $PL=4400$ lb).....	82
B-1	Maximum First Burn Plane Change.....	97
B-2	Vector Relationships at First Burn.....	99
B-3	Transfer Geometry.....	102
B-4	Second Burn Coordinate System.....	103
B-5	Angle Definitions.....	107
B-6	Three-Dimensional Vector Relationships.....	108
B-7	Second Burn Relationships.....	111
C-1	Transfer Angle.....	115
D-1	Orientation Between Frames.....	118

List of Tables

<u>Table</u>		<u>Page</u>
I	Insertion Errors with IMU Initiated Second Burn.....	18
II	Insertion Errors with TOF Initiated Second Burn.....	18
III	Vehicle Specifications.....	60
IV	Maximum Payload Geosynchronous Transfers....	83

Notation

A	represents a matrix of sensitivity coefficients
a_T	semi-major axis of transfer trajectory
c	effective exhaust velocity
C_a	Central Angle
e_T	eccentricity of transfer orbit
$\hat{e}_r \hat{e}_\theta \hat{e}_z$	frame describing second burn
E_C	eccentric anomaly of transfer trajectory
E_T	energy of transfer orbit
F	denotes a set of n-nonlinear functions
F_g	gravitational force
g_0	gravitational constant
h_T	angular momentum of transfer orbit
H	altitude of an orbit
i	inclination
i_T	inclination of transfer orbit
I_{sp}	specific impulse
J	denotes pseudo-cost function
\dot{m}	mass flow rate
m_0	stage mass prior to ignition
m_f	stage mass after burnout
P	period of an orbit
P_s	synodic period between orbits
P_T	semi-latus rectum of transfer orbit
PL	payload
PROP	propellant
PQW	perifocal frame

r_2	magnitude of IUS position vector after second burn
\bar{r}_{1C}	position vector of IUS in parking orbit
\bar{r}_{1T}	position vector of IUS immediately after first burn
\bar{r}_{2C}	target position vector in the mission orbit
\bar{r}_{2T}	IUS position at start of second burn
ST	structure
t	time
T	thrust
t_0	epoch time
t_{b1}	first stage ignition time
t_{b2}	second stage ignition time
t_{ba}	first stage burn duration
t_{bb}	second stage burn duration
TA	transfer angle
TOF	time of flight
v_g	velocity-to-be-gained
\bar{v}_{1C}	velocity of IUS in parking orbit
\bar{v}_{1T}	velocity of IUS immediately after first burn
v_2	magnitude of IUS velocity vector after second burn
\bar{v}_{2C}	velocity of target position in mission orbit
\bar{v}_{2T}	IUS velocity at start of second burn
\bar{x}	represents thrust misalignment vector ($\Delta \bar{A}L$)
XYZ	geocentric-equatorial frame
$X_p Y_p Z_p$	IMU platform inertial frame
\bar{y}	represents insertion error vector
\bar{Y}	an n-vector of unknowns

Greek and Miscellaneous Symbols

$\Delta \bar{A}L$	thrust misalignment vector
-------------------	----------------------------

$\Delta \bar{M}$	insertion error vector
$\Delta \bar{V}_1$	velocity change accomplished by first burn
$\Delta \bar{V}_2$	velocity change accomplished by second burn
θ	total plane change angle between orbits
λ	eigenvalue
μ	gravitational parameter
v	true anomaly of transfer trajectory
π	Pi
φ_1, φ_2	thrust direction angles of first burn
φ_3, φ_4	thrust direction angles of second burn
ψ_1	first burn flight path angle
ψ_2	first burn plane change angle
ψ_3	second burn flight path angle
ψ_4	second burn plane change angle
ω	angular rotation rate
Ω	longitude of ascending node
ℓ_{02}	true longitude at epoch of mission orbit target
*	denotes nominal value, or targeted value

Mathematical Symbols

$\bar{}$	over a symbol denotes a vector quantity
$\dot{}$	over a symbol denotes derivative with respect to time
T	denotes matrix transpose operation (when used as a superscript)

Subscripts

1	refers to parking orbit
2	refers to mission orbit
k	iteration step counter

Abstract

A workable open loop guidance scheme for orbital transfer maneuvers is developed for a two stage solid-rocket vehicle which has no thrust termination capability. The scheme effectively manages any excess energy by matching a non-Hohmann transfer trajectory to the fixed energy (ΔV) capabilities of the vehicle. The entire burden of effecting the transfer is put on prelaunch targeting, so that during the burns the thrust can be directed along a precomputed direction using constant attitude maneuvers only.

A computer program has been developed which employs a nonlinear equation solving routine to accomplish exact targeting for the finite-thrust transfer maneuver. The transfer trajectory is characterized by six control parameters (the outputs of targeting), and the final orbit is defined by a set of "hit conditions". The values of the control parameters which drive the vehicle state vector to satisfy the hit conditions become the guidance system target parameters.

In addition, an error analysis is performed on the scheme throughout the range of possible trajectories which exist for excess energy missions. These trajectories are then compared on the basis of optimality, such as minimum insertion errors and transfer time. Results are presented for geosynchronous and subsynchronous transfers between circular orbits.

AN ENERGY MANAGEMENT GUIDANCE SCHEME APPLICABLE
TO THE INTERIM UPPER STAGE

I. Introduction

Background

The United States space program is currently focused on the development and implementation of the Space Transportation System (STS), better known as the "Space Shuttle". This is to be a system that will serve the routine operational space requirements in the 1980 decade and beyond.

The major component of the space shuttle is the "Orbiter" vehicle, which somewhat resembles a cargo-type aircraft. The orbiter will be boosted into low earth orbit, and after completing its mission, will re-enter the atmosphere and glide to a landing much like a conventional powered aircraft. Due to its size and weight, the orbiter vehicle can be placed in only a relatively low earth orbit, but will carry extra propulsive stages in its cargo bay to complete higher energy missions.

While in orbit, these extra propulsive stages will be placed outside the orbiter where they can be launched to deliver a satellite or other payload to a higher orbit. The low orbit is usually referred to as the "parking" orbit, and the higher orbit as the "mission" orbit. The extra propulsive stages, which complete the orbital transfer, are usually re-

ferred to jointly as the "upper stage" vehicle.

The United States Air Force Space and Missile Systems Organization (SAMSO) has been tasked with the development of an Interim Upper Stage (IUS) vehicle, which will be used until a fuller capability vehicle can be designed and produced. The "Burner II" space booster, made by the Boeing Aerospace Company, has recently been selected by SAMSO for modification and use as the IUS vehicle.

The baseline Burner II vehicle consists of two stages, where the first stage burn is used to place the IUS into an elliptical transfer orbit, and the second stage burn is used to insert the IUS into the mission orbit. The Burner II uses a propulsion system consisting of two solid propellant rocket motors which have no thrust termination capability.

Since the engines cannot be shutdown prior to depletion of all the propellant, and off-loading of solid propellant to tailor each mission to its minimum energy requirements is impractical, the solid rocket motors will usually produce more energy (velocity change capability) than is necessary to complete the orbital transfer. Therefore, any guidance scenario used to complete the transfer must involve some method of depleting (or somehow utilizing) the excess energy. This process is termed "energy management".

In summary, the overall guidance and navigation problem of the IUS is primarily to complete the orbital transfer; but this is complicated by the requirement of managing any excess energy in the process.

Guidance, Targeting and Energy Management

The meanings of these three terms should first be made clear. Targeting consists of computations done prior to launch, usually in a ground based computer, to supply mission dependent parameter values to the on-board flight program, where they are stored for use during the maneuver. Guidance, in the strictest sense, usually means on-board computations carried out in closed loop fashion during the actual thrusting portions of the maneuver to provide steering commands for the vehicle propulsion system. When the term targeting is used in this study, its meaning will adhere to the above definition in a strict sense. The term guidance, however, will often be used more loosely, and will tend to infer any and all computational processes necessary to effect the orbital transfer maneuver.

The concept of energy management was briefly introduced in the last section. There are many possibilities available for handling the excess fuel, both in the premission targeting and/or during on-board guidance phases. The fuel depletion problem is relatively new, but some work has been done on this concept recently. Several good examples are early proposals made by the Boeing Company for the Burner II (Ref 2), and by the Charles Stark Draper Laboratory for the Navy's Trident Missile (Ref 3).

Both of these proposals utilized maneuvering during burns to deplete the excess propellant. The Boeing proposal used an attitude modulation technique that would rotate the thrust vector to equal angles each side of a nominal thrust direction. The Trident scheme rotated the thrust vector through an arc

where the arc length is equal to the velocity change capability of the motor, and the chord length is equal to the velocity change necessary. Both ideas are shown in Figure 1-1.

The underlying objective of guidance (loose connotation again emphasized) is generally to place a vehicle on some form of free fall trajectory which satisfies given specifications or constraints. Here the free fall trajectory to be satisfied is the specified mission orbit. To completely specify an orbit, a maximum of six parameters (constraints) must be satisfied. These parameters, which completely describe the orbit, are normally chosen to be the classical orbital elements (Ref 1:58).

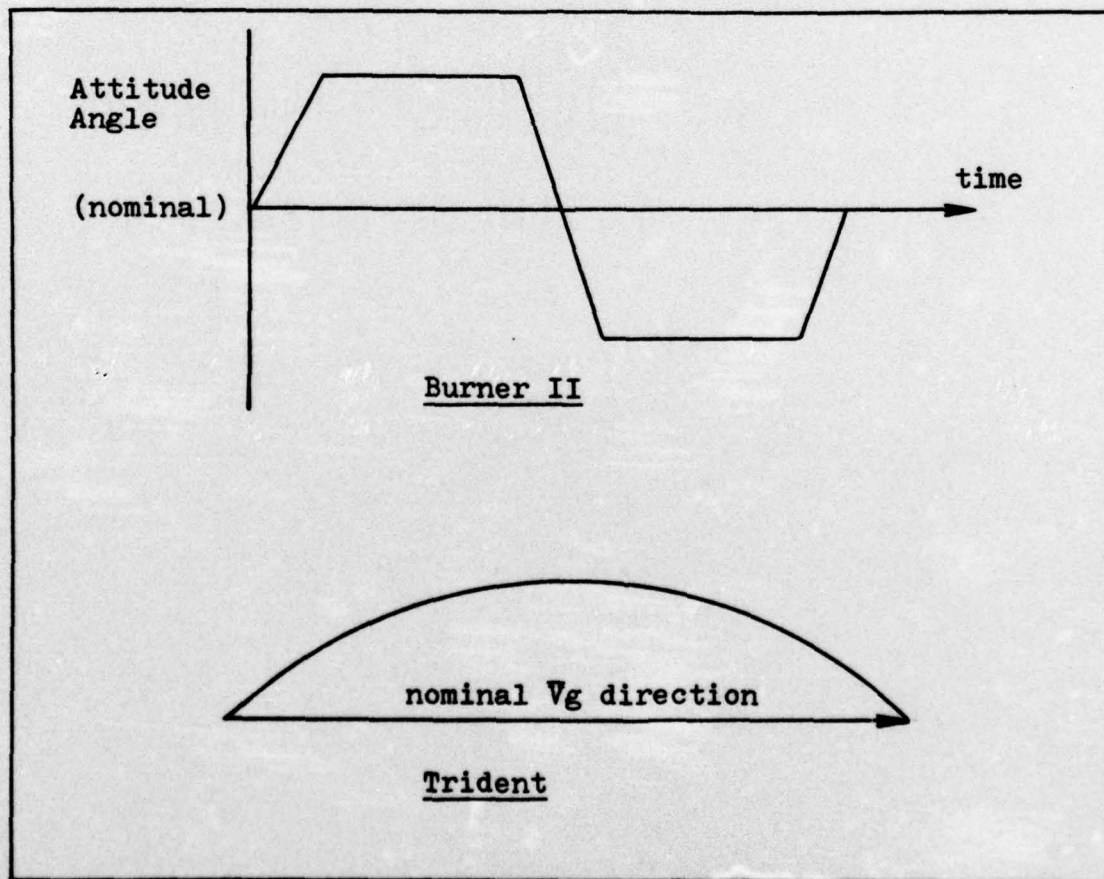


Figure 1-1. Prior Energy Management Proposals

In most guidance schemes (with thrust cut off capability) the idea is normally to effect thrusting in the direction of the desired velocity vector. This vector is called the velocity-to-be-gained (\bar{V}_g), and is defined at any instant of time to be the vector difference between the velocity required (at that instant to satisfy final constraints), and the actual vehicle velocity. The usual method, then, is to thrust in the direction of the \bar{V}_g vector in order to drive it to zero as soon as possible (i.e., with the minimum expenditure of fuel). The instant \bar{V}_g goes to zero the engine is shut down.

The main point is that thrust cut off capability, which controls the magnitude of the velocity change, is an important control variable usually available for velocity-to-be-gained guidance. With thrust cut off capability there are eight degrees-of-freedom available to satisfy mission constraints; assuming that the burns are constant attitude and directed at making up \bar{V}_g . These eight degrees-of-freedom (mission variables) are the two ignition times, and the three components of the velocity change ($\Delta\bar{V}$) vectors for each stage. The three components of $\Delta\bar{V}$ can be thought of as a magnitude, a pitch angle and a yaw angle.

When there is no thrust cut off capability two degrees-of-freedom are lost, since the magnitudes of each $\Delta\bar{V}$ vector are now fixed by the total amount of propellant on-board each stage. Thus, for the IUS orbital transfer problem, six mission variables are available (two ignition times and two thrust direction angles for each burn), which are sufficient to satisfy a total of six mission constraints; where most or all of

these constraints could be the orbital parameters which specify the desired mission orbit.

In comparing energy management guidance with conventional velocity-to-be-gained guidance, the former becomes more constrained in that since the engine cannot be cut off, it is necessary that the fuel is somehow depleted at the exact time the \bar{V}_g goes to zero (i.e., the required velocity is attained).

An important final point to be made concerning any guidance scheme is that the scheme must be able to satisfy accuracy requirements. That is, the overall navigation, guidance and control system of the IUS, in whatever form it takes, must be such that errors in the desired position and velocity vectors after insertion into the mission orbit, are acceptably small.

So in an attempt to design any guidance scheme, it is of overall importance to know how errors propagate through the scheme (and the resulting maneuver) to produce errors after insertion into the mission orbit. This is a practical measure of the worth of the scheme, and one of the deciding factors in consideration of that scheme for actual implementation.

Outline of the Problem

The IUS vehicle is to be expendable, so cost effectiveness is a most important consideration. Thus, low cost system (hardware and software) requirements for guidance and control would be desirable.

Simplicity and reliability are also important. Simplicity is particularly desirable to aid in understanding, and to minimize both the hardware and software requirements. These

points tend to lay the ground rules and guidelines for this study.

The goal was to devise an energy management guidance scheme applicable to the space shuttle IUS, which could be relatively simple, practical and cost effective. The scheme was to have the dual capability of completing the transfer using the fixed velocity capabilities of a two stage IUS, and using a transfer trajectory which would be "optimal" in some sense, depending on the objectives of the particular mission. An essentially "open loop" scheme was desired because of its simplicity.

One important question that this study was intended to help answer is that of the feasibility of completing the transfer (within acceptable insertion error tolerances) by using open loop control, as opposed to some form of closed loop control (e.g., explicit guidance), which would probably be more accurate, but also much more complex; simplicity and cost constraints again emphasized.

Due to the time limit on this study, only transfers between circular orbits, both coplanar and non-coplanar, were considered. The emphasis was on accomplishment of two particular transfers, both of which are potentially important IUS missions. The first is from a 160 nm parking orbit at an inclination of 28.5° , to a geosynchronous mission orbit. The second involves a transfer from a 160 nm parking orbit inclined at 57° , to a subsynchronous (12 hour) mission orbit with an inclination of 63° .

A computer simulation was created to target and evaluate

the proposed energy management scheme. The inputs and outputs of the simulation are listed in Chapter II, and a verbal flow chart can be found in Appendix A. The following chapters describe the formulation of the guidance scheme which led to the computer simulation. The actual computer code listing is found in Appendix F, and includes comment cards highlighting each important computation.

II. Formulation of the Scheme

Overview

The energy management scheme proposed herein was conceived with simplicity, practicality, and cost as the major considerations. In this scheme the entire burden of managing the excess fuel and effecting the transfer is put on prelaunch targeting, so that during the burns the thrust can be directed along a precomputed direction using constant attitude maneuvers only.

The highlight of this scheme is its simple "open loop" design, suggesting minimal on-board equipment for its execution. Only six mission parameter values (outputs of the targeting) need be stored on-board the IUS for execution of the transfer maneuver. They are the two ignition times, and two thrust direction angles for each burn. These six values will be referred to as the control parameters; and, as such, they could be implemented by the on-board guidance system to drive the IUS state vector to match that of the mission orbit. Targeting, to determine the values of the control parameters, is explained fully in Chapter IV.

Motivation for the use of constant attitude thrusting is due to the fact that the IUS is to have an Inertial Measurement Unit (IMU) which uses "strapdown" gyros. A possible disadvantage of the two aforementioned Burner II and Trident energy management proposals (and consequently a possible advantage of constant attitude thrusting) is that, in those schemes, vehicle turning rates during thrusting can become quite high,

and may adversely affect the accuracy of the strapdown IMU. Turning rates of as much as $7^{\circ}/\text{sec}$ for the Burner II (through a total attitude change of $\pm 90^{\circ}$ during the burn) were indicated by the Boeing proposal (Ref 2:319). Similarly for the Trident scheme, if the vehicle capability is 25% in excess of the velocity change required, then the vehicle must rotate through an attitude change of 125° during the burn. This would produce peak turning rates of $3-4^{\circ}/\text{sec}$. This is cited as a "significant disadvantage ... which may affect navigation accuracy or computation rates associated with the strapdown IMU" (Ref 3:10). Constant attitude thrusting completely eliminates this possible source of trouble.

In addition to the decision to use constant attitude thrusting only, several other considerations were important in the early formulation of this scheme:

1. The first was the criterion for initiation of the second stage burn; in the context of open loop control. That is, whether the second burn should occur at a certain preprogrammed time, or at a certain position, as indicated by the on-board navigation equipment.

As indicated above, the decision was made to base it on a predetermined time, so that the six control parameters consist of the two start burn times, and two thrust angles for each burn. The reason for this choice is explained in a later section of this chapter.

2. The next consideration was the necessity to include finite burn dynamics to realistically test the feasibility of the open loop design, and to obtain control parameter values

consistent with real hardware.

3. Lastly, since the IUS must have the capability of accounting for any mission delays, the scheme had to have a contingency retargeting capability. This would allow the transfer to be performed on consecutive opportunities.

The first idea considered was to formulate the problem using optimal control theory, where numerical solution of the associated Two Point Boundary Value Problem (TPBVP) would have automatically accounted for the finite burns. This formulation would have selected the transfer which effectively used all the velocity change capabilities of each stage, and also gave the minimum insertion error (cost function being position and velocity insertion errors). However, the optimal control approach was dropped for a more flexible procedure that would lend more insight into the actual maneuver execution, and also yield more output information. The concept of attempting to find the transfer that would be optimal in some sense was kept, however.

Instead of the optimal control approach, the mission constraints (values which define the mission orbit) are expressed as nonlinear functions of the control parameters, and a nonlinear equation solving routine is used to search out the values of the control parameters which cause the IUS state vector to exactly match that of the required mission orbit after termination of the second burn (insertion).

This process is the very heart of the scheme developed in this study. The nonlinear equation solving routine accomplishes exact targeting for the finite burn dynamics. It has

the most important advantage that there are no guidance algorithm-generated insertion errors (within the framework of the dynamic model).

The nonlinear equation solver is a general purpose subroutine developed by the mathematician M.J.D. Powell (Ref 7). Its callname is NS01A, and it will be referred to here by that name.

Early in the study, it was apparent that for most combinations of velocity change capabilities ($\Delta \bar{V}_1$ and $\Delta \bar{V}_2$), a range of possible transfer trajectories exists; where any trajectory in that range can be made to satisfy the energy management requirement. The reason for this is that in most cases the number of control parameters exceeds the number of mission orbital elements which must be satisfied, thus introducing extra degrees of freedom.

The observation that there will normally be a variety of trajectories available within a certain range led back to the idea of selecting an optimal trajectory. The parameter used to define this range was chosen to be the span between the minimum and maximum amounts of plane change that could be accomplished by the first burn, and still satisfy the constraints.

As an example, for the geosynchronous mission up to 10^0 of the total plane change may be accomplished by the first burn. This is based on Burner II specifications, which produce a $\Delta V_1 = 9453$ ft/sec, and a $\Delta V_2 = 7070$ ft/sec for a 3000 lb payload. So by sampling this range at one degree intervals, eleven possible transfer trajectories are available for direct comparison.

This is the standard method used in this study to compare the results of targeting for any given combination of energy capabilities, ΔV_1 and ΔV_2 . Sensitivities to error inputs are computed for each trajectory in the range, so that a comparison can be made to determine which trajectory gives the smallest insertion errors, minimum transfer time, or whatever the optimal criterion for any particular mission might be.

This section was intended to give the general reader some background and insight into the ideas involved in the formulation of this scheme. All of these concepts are explained in detail in the following chapters.

Dynamic Model

The system consisting of the IUS vehicle undergoing an orbital transfer about the earth, is modeled under the following assumptions:

1. Only two-body equations of motion apply, with thrust as the only perturbative acceleration. That is, any perturbations due to solar radiation pressure, and the gravitational effects of the sun, moon, and other celestial bodies are assumed negligible. The restricted two-body equations of motion are presented in Appendix C.
2. An inverse square gravitational field applies about a spherical earth (i.e., earth oblateness effects are negligible).
3. The mass flow rate (burn rate) of each solid rocket motor is assumed constant with time, thus producing a constant thrust. Initial thrust buildup and final thrust tail-off ef-

fects are assumed insignificant.

4. When computing the performance characteristics of each stage needed for the impulsive targeting first approximation, the ideal velocity equation (with later corrections for finite burn losses) is assumed to apply:

$$\Delta V = I_{sp} g_0 \ln \left(\frac{m_0}{m_f} \right) \quad (2-1)$$

where ΔV is the ideal velocity capability of the stage; I_{sp} is the specific impulse; g_0 is the gravitational constant; m_0 is the mass prior to ignition; and m_f is the final mass after burnout.

Although the computer simulation used for this study (and consequently the method itself) will accept any IUS vehicle specifications, the Burner II values, as given in Reference 2, are used throughout to standardize the results.

The assumptions and constraints, under which an error analysis of this scheme is accomplished, are described in the next section.

Error Sources

An underlying objective of this study is to determine the feasibility of completing the orbital transfer using simple open loop control; under the presumption that any additional software or Reaction Control System (RCS) correction burns, may be unnecessary. If insertion errors could be kept within an acceptable range (by using the most optimal trajectory), then implementation of this type of a scheme might prove feasible.

A major point of emphasis concerning this particular scheme is that within the framework of the model just stated, it is exact. That is, if there were none of the below listed unmodeled disturbance inputs, there would be no insertion error after execution of the scheme.

External disturbances will be present to some degree, however, and will introduce errors into the transfer maneuver.

The main error sources are as follows:

1. IMU errors (Ref 6)
 - a. Initial alignment errors
 - b. Gyro drift-rate bias
 - c. Acceleration-sensitive gyro drift
 - d. Accelerometer bias
 - e. Accelerometer scale factor
 - f. Gyro torquer scale factor
 - g. Gyro input axis alignment
 - h. Gyro torquer asymmetry
2. Velocity change perturbations
 - a. Vehicle structure and fuel weight deviations
 - b. Specific impulse (I_{sp}) deviations
 - c. Thrust profile fluxuations
3. Gravity perturbations
 - a. n-Body disturbances
 - b. Earth oblateness effects
4. Solar radiation pressure

Due to the time constraint involved in this study, all of the above error sources could not be included in the accuracy

analysis of the scheme. Those selected can be neatly summarized as thrust vector errors, and constitute the most significant disturbances. Thrust vector errors originate from sources 1. and 2.c.

The overall effect of IMU errors is to cause an error in the direction of the applied thrust. This may be termed thrust misalignment error. Error source 2.c. arises from variations in the mass flow rate (burn rate) of the engines. This causes an error in the thrust magnitude, which in turn perturbs the velocity change acceleration profile, ultimately causing an error in the burnout position.

In summary, the two general sources of error considered to affect this scheme are deviations in the thrust vector magnitude and direction. Insertion error sensitivities due to both thrust misalignment and thrust magnitude deviations are computed for each trajectory targeted.

Choice of a Transfer Scenario

Once it was decided that guidance would be performed using constant attitude burns, it was necessary to decide how best this could be implemented in hardware. The choice of selecting the control parameters, based on two burn times, appeared to be the best method, as explained here.

Assuming that the first stage ignition will occur at the proper position in any scenario (due to the proximity of the IUS to the orbiter vehicle with its position well known), then there are two different possibilities for initiation of the second burn. One where second stage ignition occurs when the

on-board IMU indicates it should, or one where second stage ignition occurs according to an on-board clock at a certain preprogrammed time. The question obviously was which scenario would be the most accurate. That is, which case would be least sensitive to thrust vector errors.

To investigate this question two similar computer simulations were developed. In both cases Hohmann transfer velocity change capabilities were assumed and the impulsive approximation was used. An ideal IMU was assumed (with no drift, etc.), and an alignment error present in both cases.

The first simulation initiated the second burn when either the IMU indicated that the proper altitude had been reached, or that 180° of transfer angle had been completed. The second simulation precomputed the transfer time of flight and initiated the second burn at that instant along the transfer trajectory. Insertion error sensitivities were computed for each case and combined into values for position insertion error and velocity insertion error. The transfers tested were between a 160 nm parking orbit and a synchronous orbit (at 19,323 nm). Plane changes of 0° , 28.5° and 57° were accomplished. In all cases the TOF initiated second burn performed more accurately, by about a factor of two, as shown in Tables I and II for a one milliradian misalignment of the IMU axes during both burns.

The logical choice of a transfer scenario then, from these results, was one based on transfer time of flight.

Explanation of the Prelaunch Targeting

Table I.

Insertion Errors with IMU
Initiated Second Burn

Plane Change	Position Error (nm)	Velocity Error (ft/sec)
0°	22.2	15.7
28.5°	22.2	14.5
57°	22.2	11.1

Table II.

Insertion Errors with TOF
Initiated Second Burn

Plane Change	Position Error (nm)	Velocity Error (ft/sec)
0°	12.6	7.5
28.5°	12.6	6.3
57°	12.6	2.9

The final form for this scheme followed directly from the choice of a transfer scenario based on time of flight as the criteria for initiating the second burn. Certain conditions needed to be defined, however, in order to lay the framework in which that scenario could be executed. These conditions become the inputs to the computer simulation used to target the transfer. Both the inputs and outputs of the targeting program were chosen to be as follows:

Inputs

1. IUS vehicle specifications (given by stage)

- a. ST_1, ST_2 - structure weights
 - b. $PROP_1, PROP_2$ - propellant loading
 - c. I_{sp1}, I_{sp2} - average specific impulses
 - d. T_1, T_2 - average thrust magnitudes
 - e. PL - payload weight
2. Orbital data
- a. H_1, H_2 - altitudes of the parking orbit and mission orbit
 - b. i_1, i_2 - inclinations of each orbit
 - c. Ω_1, Ω_2 - longitude of ascending node of each orbit
 - d. l_{02} - true longitude at epoch of the target position in the mission orbit (when rendezvous is to be accomplished)

Outputs

- 1. Targeted values of the six control parameters
 - a. $t_{b1}, \varphi_1, \varphi_2$ - first stage ignition time, and thrust direction angles
 - b. $t_{b2}, \varphi_3, \varphi_4$ - second stage ignition time, and thrust direction angles
- 2. Contingency retargeting - the values of the six control parameters for the next four sequential mission opportunity times.

The scheme operates under the following definitions and restrictions:

- 1. Both the parking orbit and mission orbit are circular.
- 2. The times are referenced to an "epoch" time, t_0 . That

is, the values of t_{b1} and t_{b2} are given in the number of seconds past epoch.

3. The thrust direction angles are referenced to the geocentric-equatorial inertial frame.
4. Only simple plane changes are accomplished. This requires that either Ω_1 and Ω_2 are equal, or that one or both are undefined (equatorial orbit), so that all the required plane change is just equal to the difference in the inclinations.
5. If the parking orbit and mission orbit are non-coplanar, then the targeting is accomplished to place the IUS in the specified mission orbit only (i.e., the point of insertion is not constrained). If the orbits are coplanar, then the targeting automatically accomplishes a rendezvous between the IUS and the target position in the mission orbit.

Properly defining the epoch time (t_0) allows the orbital data to be expressed in the form of the inputs above. The scheme presupposes that the parking orbit is already established, and the position of the IUS in that orbit is accurately known. Thereafter, the epoch time is defined to be any one of the times (the particular one chosen by the user) when the IUS crosses the line of the ascending node while in the parking orbit. If the parking orbit is equatorial, then epoch becomes the time that the IUS is positioned along the X axis of the geocentric-equatorial frame. With this definition of epoch, the true longitude of the IUS, in the parking orbit (l_{01}), is always equal to Ω_1 . Thus, only Ω_1 need be specified

to fully fix the IUS position as a function of time in that orbit.

The perifocal coordinate system (PQW frame) of either the parking orbit or mission orbit as used here will have the \bar{P} axis pointing along the line of the ascending node, if it exists, or if the orbit is equatorial, along the X axis. These frames and angular relationships are illustrated in Figure 2-1 as they might be at some epoch time (t_0), for a geosynchronous mission. The vector $\bar{r}_{1C}(t)$ tracks the IUS in the parking orbit, and the vector $\bar{r}_{2C}(t)$ tracks the target position in the mission orbit (when rendezvous is to be accomplished).

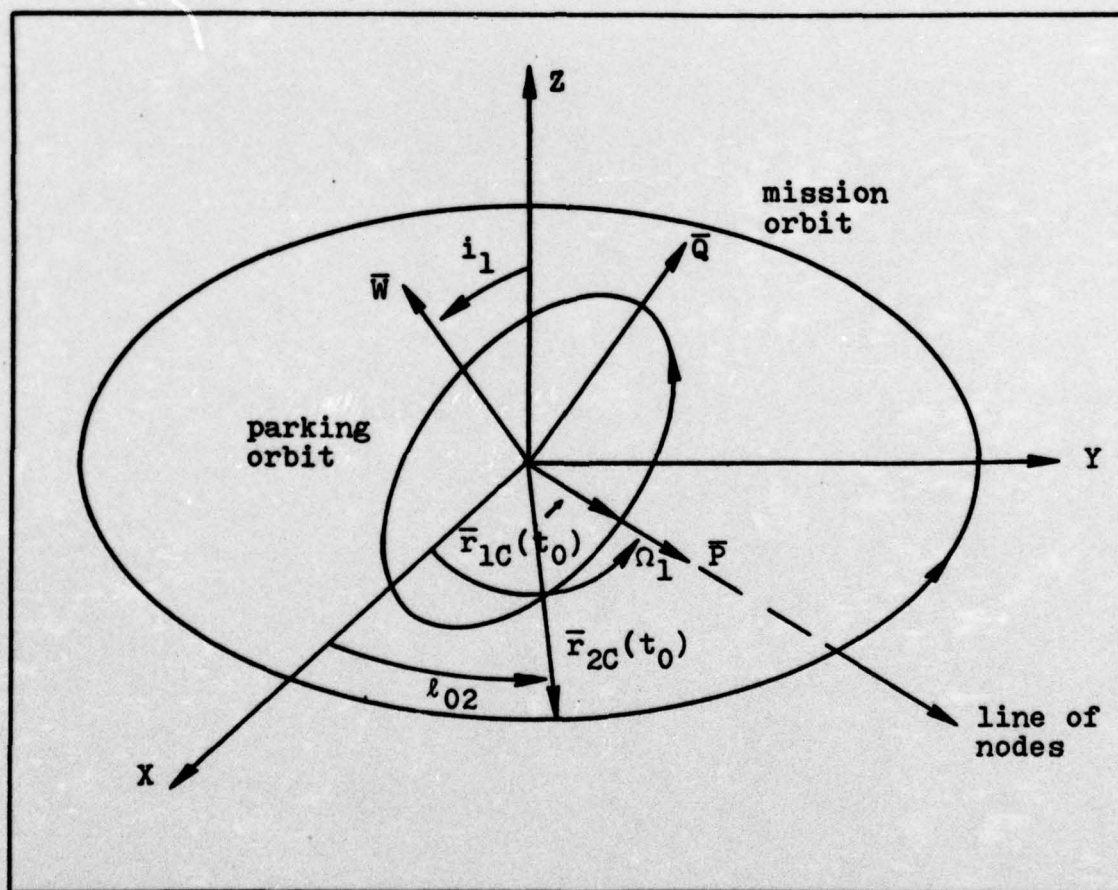


Figure 2-1. Epoch Relationships

It is an important characteristic of this scheme that a value for l_{02} (i.e., an epoch time, and target position) always be specified. This is necessary so that the six control parameters will have a reference to which they can be related. If the insertion point of the IUS into the mission orbit is unconstrained (for a coplanar transfer), or if the transfer is non-coplanar, then an arbitrary value for l_{02} may be used (for instance, $l_{02} = 0$).

It happens that transfer opportunities are regularly repetitive between non-coplanar orbits (when rendezvous is unnecessary), and synodically repetitive between coplanar orbits (to satisfy a rendezvous). This allows contingency re-targeting to be accomplished, since an endless list of possible mission start times are available. Thus, the scheme is programmed to generate the values of the control parameters associated with the first five mission opportunity times after epoch, for each transfer trajectory targeted. The reason for doing this is that, if a mission delay were to occur, the control parameters could be automatically reset to the next sequential set of values.

The algorithm used to accomplish this targeting task is presented in the next two chapters.

III. Energy Management by Trajectory Matching

Various possibilities have been suggested for managing the excess energy of the fixed-impulse solid rocket motors. The prominent ideas have included propellant offloading, adding ballast, and attitude modulation of the thrust vector; all of which have major drawbacks. This chapter explains the energy management technique employed by this scheme, which involves selecting a non-Hohmann transfer trajectory which "matches" the fixed energy capabilities (ΔV_1 and ΔV_2) of the IUS vehicle.

For a ΔV_1 and ΔV_2 combination, both in excess of the Hohmann (minimum energy) values for any particular mission, a non-Hohmann transfer is usually possible. A simple coplanar non-Hohmann transfer is illustrated in Figure 3-1.

For any orbital transfer maneuver, the insertion conditions may be related to the conditions at the first burn by using the impulsive velocity change approximation, and a series of orbital transfer equations. This series of equations is contained in Appendix B as Equations (B-11) through (B-28). Within these equations a relationship exists between possible values of ΔV_1 and ΔV_2 in the form of

$$\Delta V_2(\Delta V_1, \psi_1, \psi_2) \quad (3-1)$$

where for any value of ΔV_1 , ψ_1 is the associated first burn flight path angle, and ψ_2 is the plane change angle accomplished by the first burn. The consequent ΔV_2 is the value

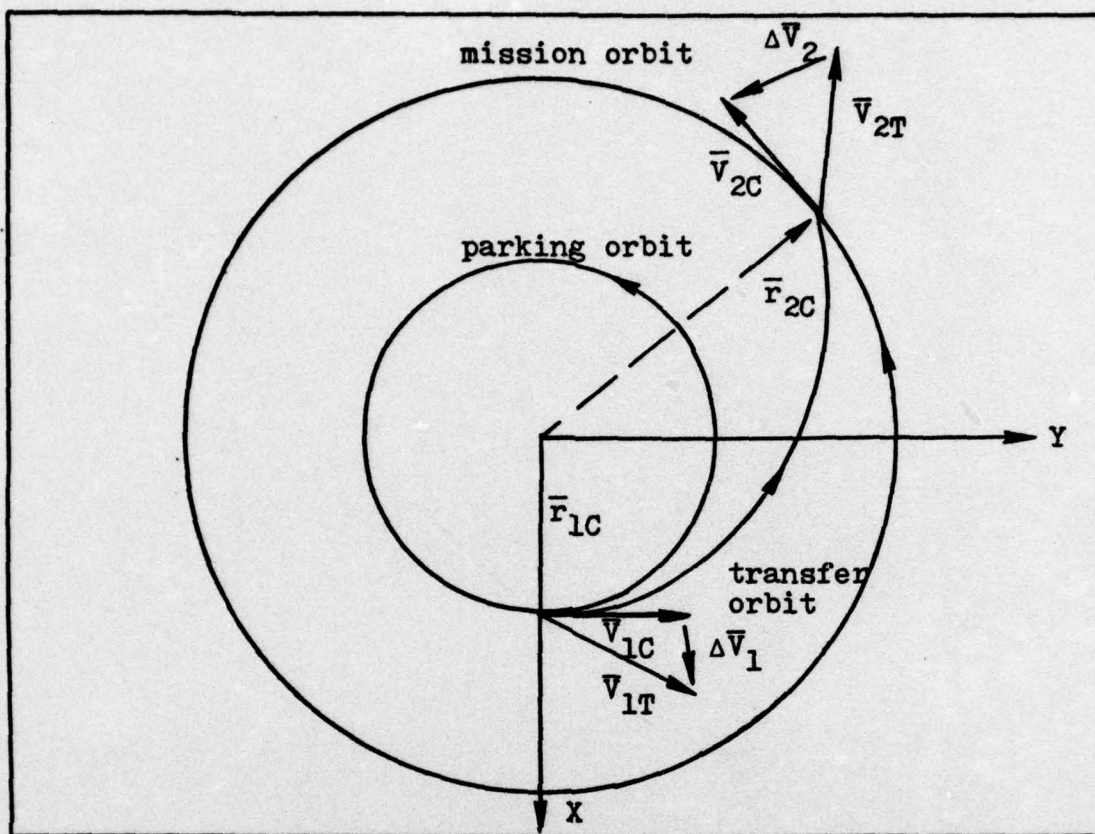


Figure 3-1. Coplanar non-Hohmann Transfer

of the second burn velocity increment which completes any remaining plane change and causes insertion into the mission orbit.

In order to determine which combinations of ΔV_1 and ΔV_2 would allow trajectory matching as a means of energy management, plots were made of allowable ΔV combinations for each of the reference missions listed in Chapter I. These plots are shown in Figures 3-2, 3-3, and 3-4, for the geosynchronous, subsynchronous, and geosynchronous coplanar transfers, respectively.

Each of these plots was obtained by accomplishing a two-

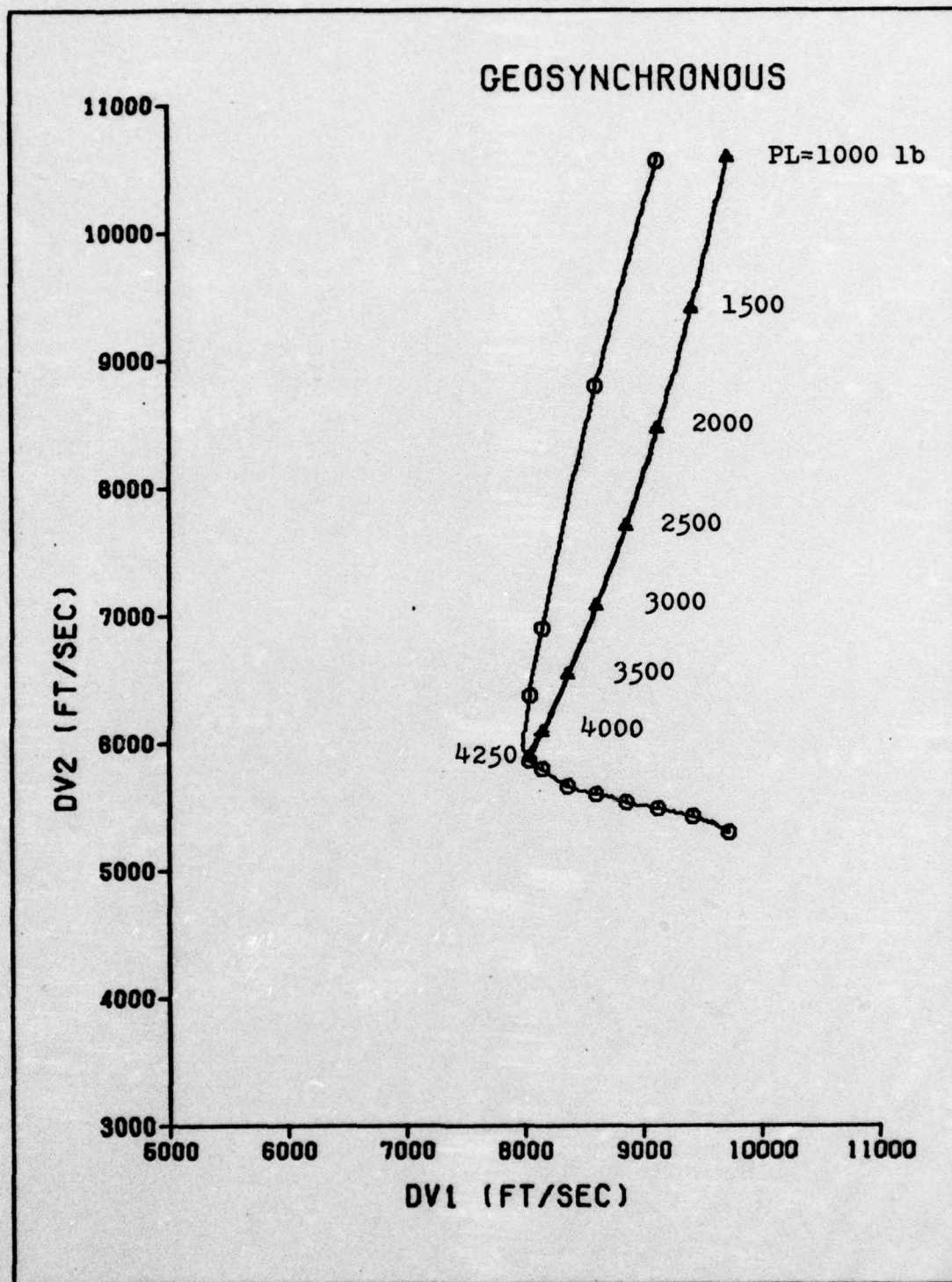


Figure 3-2. Geosynchronous Mission Allowable ΔV Combinations

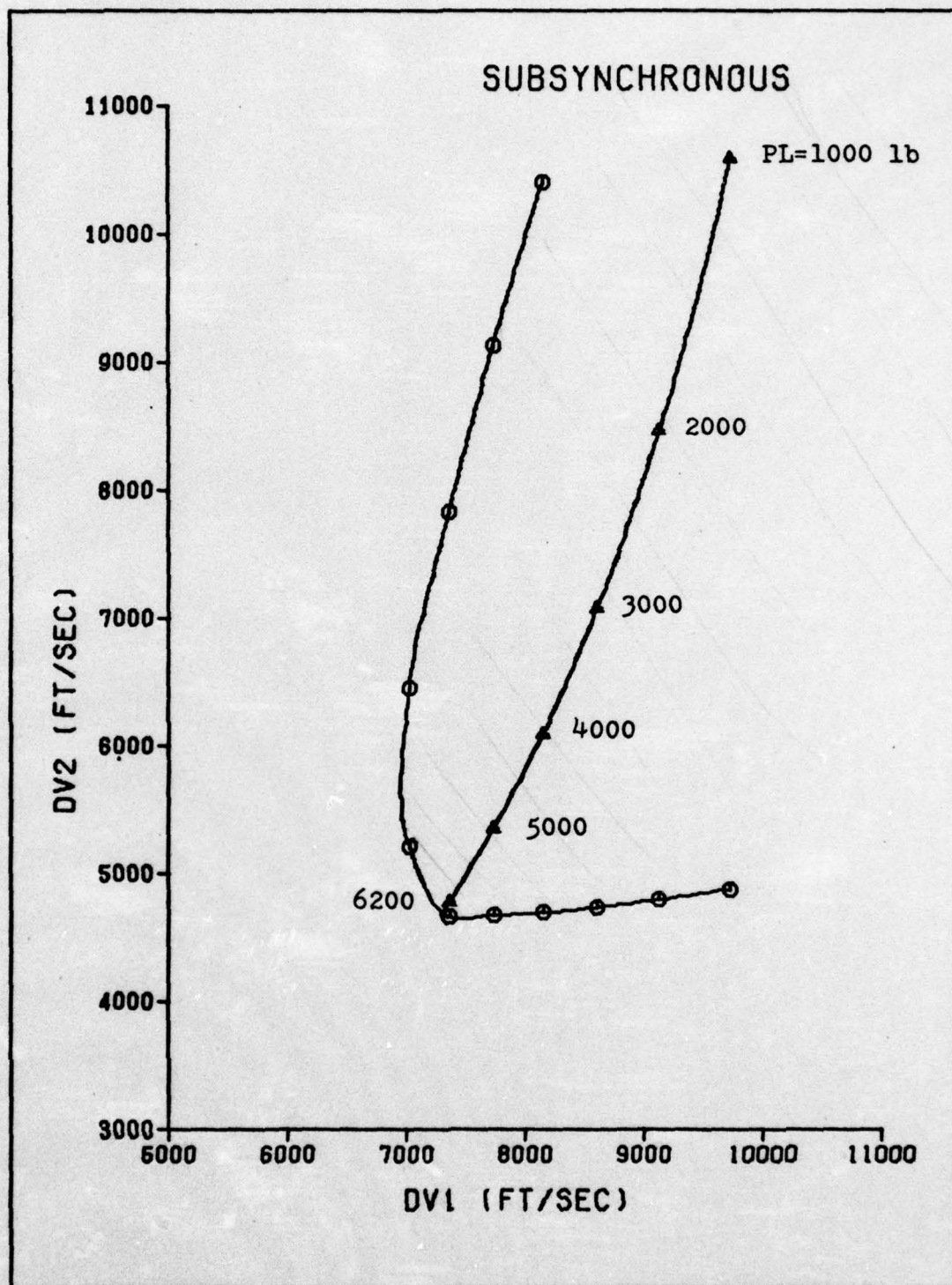


Figure 3-3. Subsynchronous Mission
Allowable ΔV Combinations

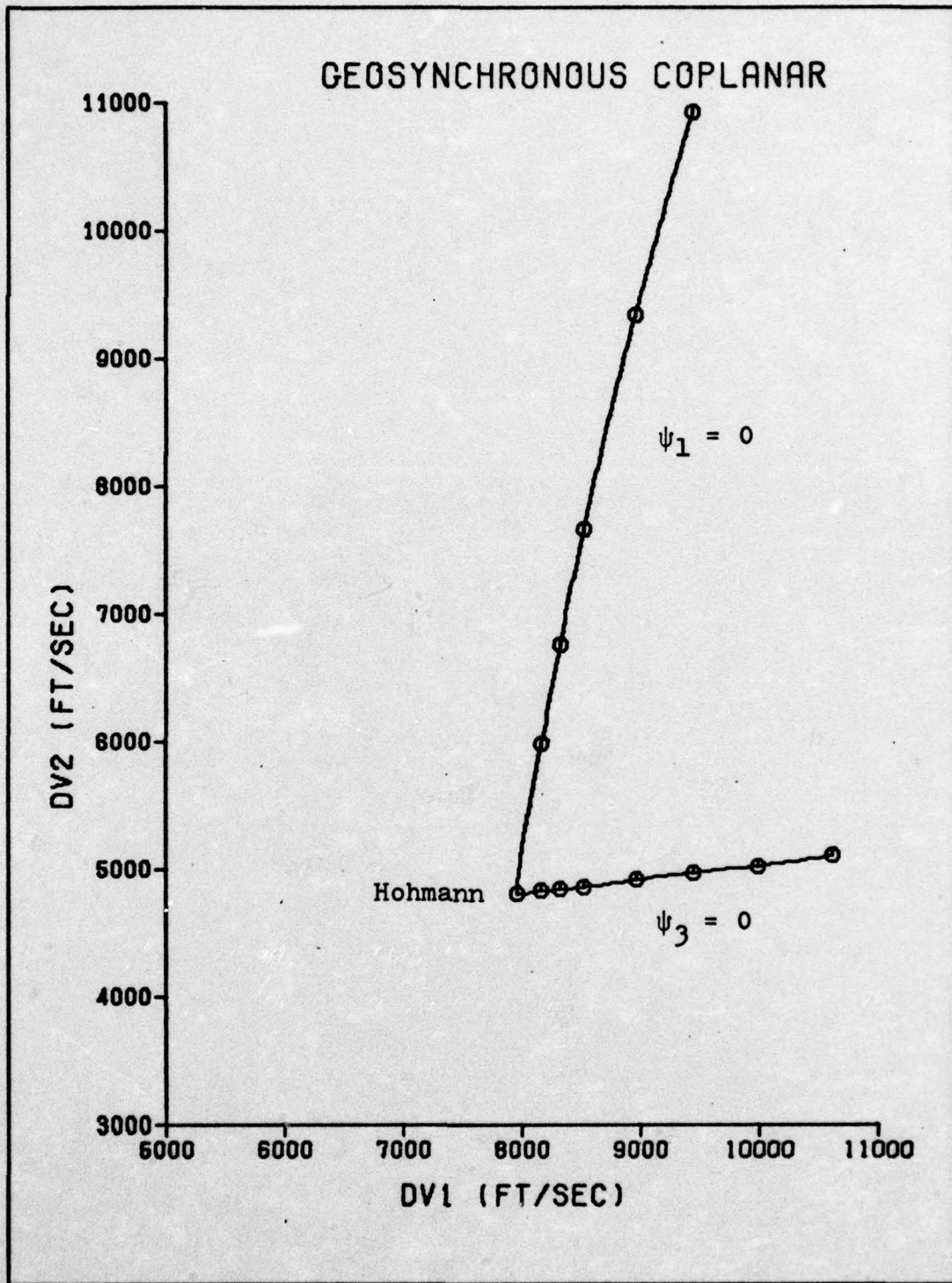


Figure 3-4. Geosynchronous Coplanar Mission Allowable ΔV Combinations

dimensional mapping through all allowable combinations of ψ_1 and ψ_2 for various values of ΔV_1 ; using the orbital transfer relationships of Equations (B-11) through (B-28). Using this procedure, the boundaries of the allowable regions become the maximum and minimum values that ΔV_2 may take on, for a set value of ΔV_1 .

It happens that the maximum possible value for ΔV_2 (given the value of ΔV_1) occurs where both ψ_1 and ψ_2 are equal to zero. The minimum possible ΔV_2 occurs where ψ_2 has its maximum value, and ψ_3 (second burn flight path angle) becomes equal to zero. A trajectory is possible for any value of ΔV_2 between these extremes.

Superimposed on Figures 3-2 and 3-3 are plots of the ΔV_1 and ΔV_2 resulting from various payload weights, using the Burner II as the IUS vehicle, with a first stage fuel load of 17,300 lbs and a second stage fuel load of 4700 lbs. It is apparent that the excess energy balance between ΔV_1 and ΔV_2 is primarily dependent on the payload weight.

The significance of these plots is that transfer trajectories may always be found that match any combination of ΔV 's selected from within the allowable regions. In the case of a coplanar transfer, the functional relationship of (3-1) reduces to

$$\Delta V_2(\psi_1) \quad (3-2)$$

for a fixed value of ΔV_1 . The trajectory matching procedure then consists of finding the solution of

$$\Delta V_2(\psi_1) = \Delta V_2^* \quad (3-3)$$

where ΔV_2^* is the fixed (known) value.

The analytical relationship of $\Delta V_2(\psi_1)$, contained in Equations (B-11) through (B-28), is highly nonlinear and transcendental in nature, and must be solved iteratively. To illustrate this, a closed form expression for $\Delta V_2(\psi_1)$ is derived in Appendix B, for a coplanar transfer.

For a transfer between coplanar orbits, only one trajectory exists which matches a given ΔV_1 and ΔV_2 combination, and remains within the plane of the orbits. It is often possible, however, to gain flexibility by thrusting out of plane with a portion of ΔV_1 and back into plane with a portion of ΔV_2 . It is interesting to note, though, that the minimum time of flight trajectory is always the one which remains in plane. The reason for this is that, in this case, all the available energy remains in the plane of the transfer trajectory.

For a transfer between non-coplanar orbits, an additional degree of freedom is introduced through the addition of ψ_2 , as expressed in Equation (3-1). A particular combination of ΔV_1 and ΔV_2 may now yield a variety of different trajectories, depending on the amounts of plane change accomplished during each burn. In this case, there will be a range of values for ψ_2 , any one of which will allow a solution to the remaining relationship of Equation (3-3).

The actual range over which ψ_2 may take on values depends on the excess energy balance between ΔV_1 and ΔV_2 (i.e., their coordinates within the allowable region). The upper and lower

limits, on the range of values ψ_2 may have, are always given by:

$$0^\circ \leq \psi_2 \leq \psi_{2\max} \quad (3-4)$$

A relationship for calculating $\psi_{2\max}$ is given in Appendix B. The actual range of ψ_2 (for finite burn trajectories, etc.) will always be somewhat less than this.

Thus, trajectory matching using the impulsive velocity change approximation becomes an important early step in the targeting process. Acceptable trajectories are found by fixing a value of ψ_2 , which is the parameter used to define the range of usable trajectories, and then accomplishing a one-dimensional search on ΔV_2 , for varying values of ψ_1 . When the solution to Equation (3-3) has been bracketed by this search procedure, a Regula-Falsi (Ref 4:178) iteration is accomplished to refine it exactly. During the targeting computations (described in Chapter IV) each value of ψ_2 , within the range (usually at 1° intervals), is sampled to generate all the possible trajectories.

The amount of flexibility in choosing possible trajectories depends entirely on the range of values ψ_2 may take on, which in turn depends on the energy balance between ΔV_1 and ΔV_2 . Only one trajectory is possible for a ΔV combination lying on a boundary of the allowable regions. This becomes the case for the maximum payload combination.

IV. Targeting

Overall Objective

The mission objective is to complete an orbital transfer between a low altitude parking orbit and a higher altitude mission orbit. The mission orbit can be defined by certain constraints, or "hit conditions", to which the IUS state vector must be driven in order to accomplish insertion into that orbit. The form of the mission constraints used in this targeting algorithm are chosen to conform with the energy management technique described in the last chapter.

For a vehicle with fixed-impulse capability, the payload weight is the governing parameter in fixing the actual values of ΔV_1 and ΔV_2 , and the consequent excess energy balance. With excess energy, a variety of trajectories are possible which would satisfy the mission constraints. The parameter ψ_2 (plane change angle accomplished by the first burn) was chosen to define the range of transfers possible using the available ΔV_1 and ΔV_2 . The idea was to fix values of ψ_2 at one degree intervals through the range so that a comparison of the resulting transfer trajectories could be made.

Specifying ψ_2 for a given transfer is equivalent to constraining the inclination of the transfer trajectory (i_T). For a fixed amount of first burn plane change (ψ_2), and the inclination of the parking orbit (i_1) specified, the inclination of the transfer orbit is the fixed sum of these two

angles.

In the targeting algorithm, the IUS vehicle state vector (three components of position, and three components of velocity) becomes a function of the six control parameters. Where necessary, the components of the IUS state vector are converted into the equivalent orbital elements for direct comparison with the mission constraints. The function of the targeting algorithm is to generate the values of the control parameters which drive the IUS state vector (and its corresponding orbital elements) to match the values of the mission constraints. The algorithm, as coded, will only target transfers between circular orbits. It would be straightforward, however, to include coding which would handle elliptical orbits also.

Mission Constraints and Variables

Six constraints are required to completely specify an orbit, in the most general case. Five of the constraints may be constants which specify the size, shape, and orientation of the orbit. The sixth constraint specifies the position within that orbit, and is, therefore, a function of time. The classical orbital elements are the parameters most often used to specify an orbit. The mission constraints in this algorithm, are a modification of the classical orbital elements. The IUS vehicle must satisfy some or all of these constraints after termination of the second stage burn (depending on the type of transfer - as will be explained).

Mission Constraints: (hit conditions)

1. r_2 - magnitude of the mission orbit position vector
2. V_2 - magnitude of the mission orbit velocity vector
3. e_2 - eccentricity of the mission orbit
4. i_2 - inclination of the mission orbit
5. Ω_2 - longitude of the ascending node of the mission orbit
6. TA^* - transfer angle

Of the six mission constraints shown, the first five are constants (both r_2 and V_2 are constant for a circular orbit), but the sixth is a function of time and needs some explanation. In essence, $TA(t)$ is the selected form of the orbital element which insures the insertion into the mission orbit at the desired position in that orbit. As used here, $TA(t)$ is defined to be the angle between the two vectors $\bar{r}_{1C}(t)$ and $\bar{r}_{2C}(t + TOF^*)$, where "t" is any particular time, and TOF^* is the orbital transfer time; that is, the time from initiation of the first stage burn to termination of the second stage burn.

Before the transfer, the position of the IUS vehicle is tracked by the vector $\bar{r}_{1C}(t)$, and the target position in the mission orbit is tracked by the vector $\bar{r}_{2C}(t)$. During the actual transfer, the target position will have shifted along its orbit from $\bar{r}_{2C}(t_{b1})$ to $\bar{r}_{2C}(t_{b1} + TOF^*)$, where t_{b1} is the time the transfer began (i.e., first stage igni-

tion time). This is illustrated in Figure 4-1 for the case of a simple coplanar transfer.

Satisfaction of the sixth constraint really means finding the correct first stage ignition time, such that

$$TA(t_{b1}) = TA^* \quad (4-1)$$

where TA^* is the angle between the vectors $\bar{r}_{1C}(t_{b1})$ and $\bar{r}_{2C}(t_{b1} + TOF^*)$. Thus, it is apparent that the constraint TA^* is dependent for its actual value on the transfer time of flight TOF^* , which in turn is dependent on the particular transfer trajectory.

Since TOF^* is really dependent on the two burn times, the true functional form of TA^* really is $TA^*(t_{b1}, t_{b2})$.

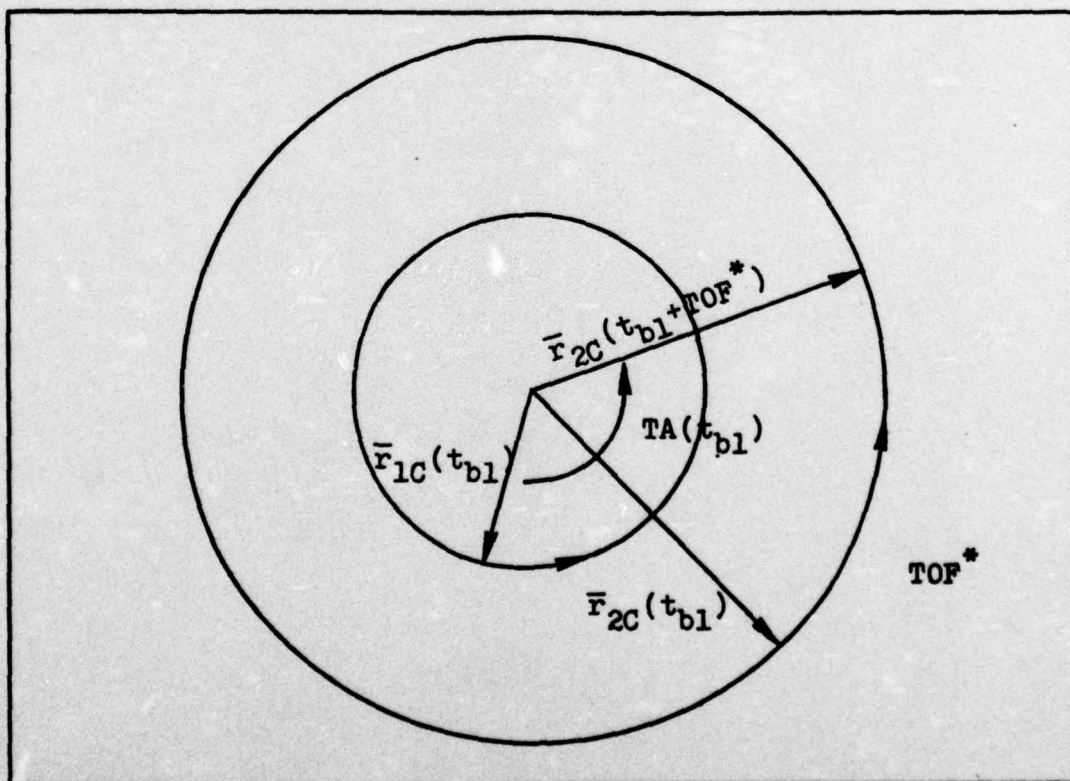


Figure 4-1. Transfer Angle

Satisfaction of TA^* may be thought of as insuring the proper "phase angle" at departure, to effect a rendezvous with the target position in the mission orbit.

The six control parameters are the variables used to satisfy the mission constraints, and are listed here:

Control Parameters:

1. t_{b1} - time of first stage ignition (referenced to epoch, $t_0 = 0$)
2. φ_1 - } inertial thrust direction angles of the
3. φ_2 - } first stage burn
4. t_{b2} - second stage ignition time (a function of transfer TOF)
5. φ_3 - } inertial thrust direction angles of the
6. φ_4 - } second stage burn

The thrust direction angles specify the constant attitude inertial orientations of the thrust vectors of each stage, \bar{T}_1 and \bar{T}_2 . The angles φ_1 and φ_2 define the direction of \bar{T}_1 , as shown in Figure 4-2. Similarly, the angles φ_3 and φ_4 specify the orientation of \bar{T}_2 .

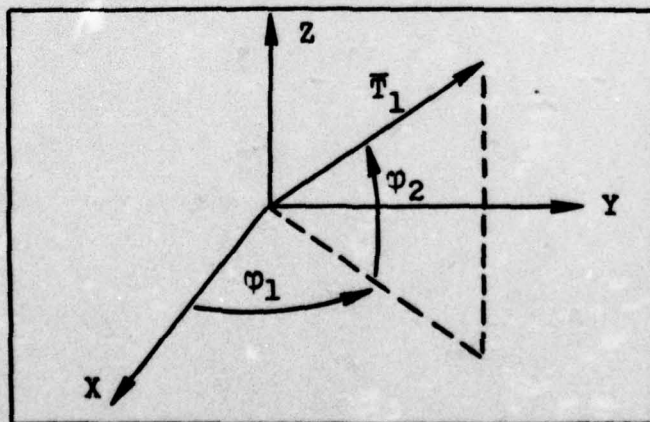


Figure 4-2. Thrust Direction Angles

The important point in the relationship between the mission constraints and the control variables is that unique values for the six control parameters specify unique values for the six constraints. That is, any combination of values, even selected arbitrarily, for the control parameters will produce some unique orbit (not necessarily circular) after the second burn. The task of the targeting algorithm then becomes one of generating the proper values of the control parameters such that their values drive the IUS vehicle to produce an orbit after second stage burnout which satisfies the constraints.

There are many ways to attack this problem, but the method decided upon here (which attempts to be conceptually straightforward), is to use two distinct steps in the solution process. The first step is to simply target the transfer in a general form, where only four of the constraints are satisfied. The four to be satisfied in this first step of targeting are r_2 , V_2 , e_2 , i_2 ; with Ω_2 and TA left free. The second step essentially satisfies proper phasing.

The decision to target the transfer in two steps can be explained best by looking at the functional relationship between the constraints and variables:

1. $r_2(\varphi_1, \varphi_2, t_{b2}, \varphi_3, \varphi_4)$
2. $V_2(\varphi_1, \varphi_2, t_{b2}, \varphi_3, \varphi_4)$
3. $e_2(\varphi_1, \varphi_2, t_{b2}, \varphi_3, \varphi_4)$
4. $i_2(\varphi_1, \varphi_2, t_{b2}, \varphi_3, \varphi_4)$
5. $\Omega_2(t_{b1}, \varphi_1, \varphi_2, t_{b2}, \varphi_3, \varphi_4)$
6. $TA(t_{b1}, t_{b2})$

Thus, it is apparent that there is decoupling between the first four constraints and the last two constraints, with respect to the variable t_{b1} . The first four constraints are not a function of t_{b1} . In other words, they are independent of the position in the parking orbit at which first stage ignition occurs and the transfer is initiated. Verification of the above constraint variable relationships through the interrelating equations is straightforward and will not be shown here.

Since there are six constraints and an equal number of variables, it might be possible to find a unique solution for the variables which would satisfy all six constraints, for even the most general non-coplanar transfers. However, due to the nature of the initial conditions (Chapter II, last section) and the energy management requirements incorporated in the governing relationships, a straightforward way of solving for values of the control parameters which would satisfy all six constraints in every case, was not apparent. From the familiarization gained in this study it seems most likely that a unique solution is only possible under certain circumstances.

The reason for the difficulty in finding a unique solution to satisfy all six constraints, is that one degree of freedom is "lost" when the parking orbit is specified before targeting (as is always the case in this scenario). Although the parameter t_{b1} is free, it is really the vector $\bar{r}_{10}(t)$ which must be completely free in order for a solution

to be possible which satisfies all six constraints. When the IUS position in the parking orbit is specified before targeting, $\bar{r}_{1C}(t)$ is no longer free with respect to time.

There is, however, a certain limited degree of freedom generated by the range of values ψ_2 may have, which in turn gives some flexibility in choosing a trajectory with a certain transfer angle. Here, even at best, a unique solution would involve a very narrow launch window for the space shuttle orbiter itself, and even then may allow only one mission opportunity, thus precluding a retargeting capability.

Since most missions will probably not involve a rendezvous requirement anyway, the targeting algorithm developed here assumes an arbitrary parking orbit already established. When satisfaction of the sixth constraint (rendezvous) is required between non-coplanar orbits, it may still be accomplished by a station-keeping maneuver within the parking orbit to obtain proper phasing for the targeted trajectory.

Thus, the path chosen in the formulation of this scheme was to satisfy only five of the six constraints (through the targeting algorithm) for general non-coplanar transfer missions. In step one of targeting the first four constraints are satisfied, and in targeting step two (phasing) either Ω_2 or TA^* is satisfied depending on the mission. If the transfer is between coplanar orbits, Ω_2 is never a constraint since it is always satisfied, and TA^* is enforced in this case as the fifth constraint. If the mission is a non-co-

planar transfer, then Ω_2 is satisfied in step two and TA^* (insertion position) is left free.

Targeting Step One

The first step of the targeting process involves finding the geometry of a trajectory which will satisfy the first four constraints, without regard to proper phasing. Leaving the last two constraints, Ω_2 and TA^* , free in this step leaves four constraints as functions of five variables:

1. $r_2(\varphi_1, \varphi_2, t_{b2}, \varphi_3, \varphi_4)$
2. $v_2(\varphi_1, \varphi_2, t_{b2}, \varphi_3, \varphi_4)$
3. $e_2(\varphi_1, \varphi_2, t_{b2}, \varphi_3, \varphi_4)$
4. $i_2(\varphi_1, \varphi_2, t_{b2}, \varphi_3, \varphi_4)$

In order to solve for unique values of the five variables which will satisfy these four constraints, an additional constraint equation (which is consistent with these four) is necessary. A logical and very convenient choice for the additional constraint was to use the inclination of the transfer trajectory $i_T(\varphi_1, \varphi_2)$, since it became an additional constraint anyway when a value for ψ_2 was fixed. In this sense, i_T might more aptly be called a design parameter, since its value is selected freely (from within the limits of its range). Once set, however, i_T functions as another constraint that the targeting must satisfy.

Since the first step of targeting involves constraints which can be satisfied regardless of where t_{b1} occurs in the parking orbit, a "local" inertial frame $(XYZ)_p$ is ini-

tially used. This local frame (as it will be called) is referenced to the first burn point, as shown in Figure 4-3. The X_ℓ axis always passes through the point of the first stage ignition. The frame is oriented such that the inclination of the parking orbit is always zero, and the inclination of the mission orbit is just equal to the absolute difference between the actual parking and mission orbit inclinations.

In this initial step, the impulsive velocity change approximation is used so that a trajectory may be targeted (in the local frame) to satisfy i_T , r_2 , V_2 , e_2 , and i_2 , using the orbital transfer relationships of Equations (B-11) through (B-28). In this approximation the thrust direction

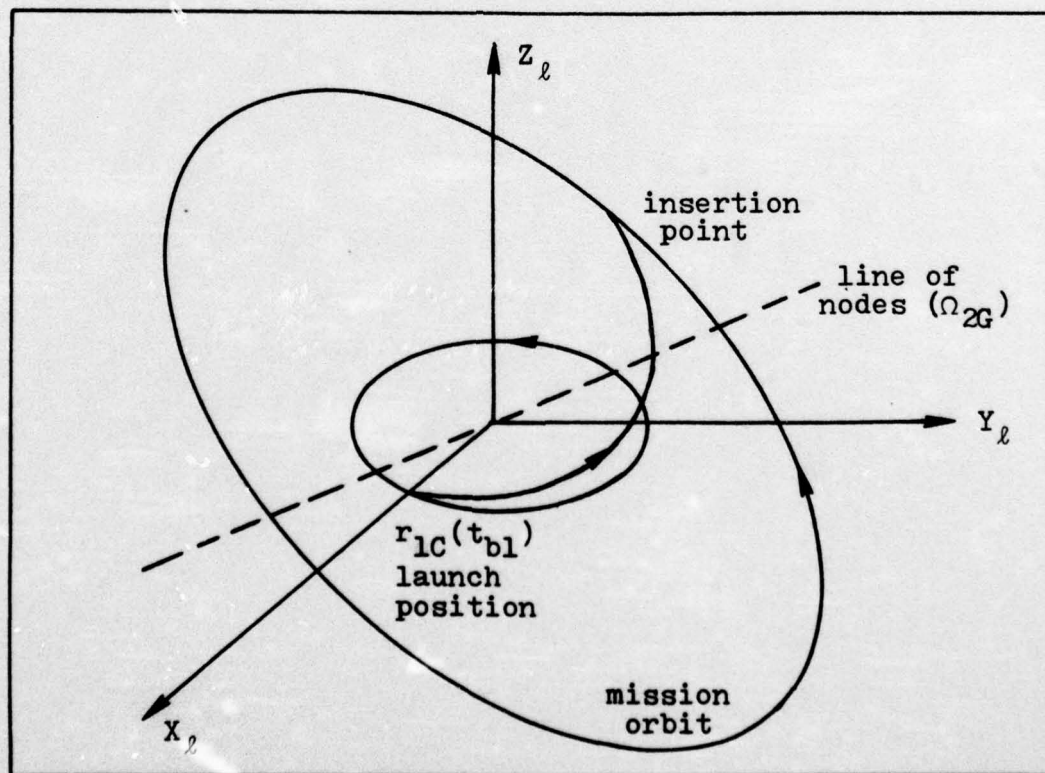


Figure 4-3. Local Frame

and associated $\Delta\bar{V}$ direction are by definition the same. Through these relationships, the impulsive directions of $\Delta\bar{V}_1$ (\bar{T}_1 direction) and $\Delta\bar{V}_2$ (\bar{T}_2 direction), as expressed in the local frame, are found which match an energy management transfer trajectory for a set value of ψ_2 . From this, the four thrust direction angles are determined with respect to the local frame. The consequent transfer time of flight (TOF) becomes an approximation to the second stage burn time (t_{b2}), as measured from a first burn referenced to $t_{b1} = 0$.

After approximate values for ϕ_1 , ϕ_2 , t_{b2} , ϕ_3 , and ϕ_4 are obtained through impulsive targeting, their actual values for the real finite burn dynamics are found using the nonlinear equation solving routine (NS01A), coupled with numerical integration of the equations of motion. Once NS01A has generated values for the five control parameters which correspond to the minimum value for ψ_2 (amount of first burn plane change), targeting for subsequent values of ψ_2 is expedited by using the values of the control parameters generated for the previous ψ_2 , as the initial inputs to NS01A. This gives shorter iteration times, as opposed to recompleting impulsive targeting at each step of ψ_2 .

NS01A

Since the five constraint variable relationships used in step one of targeting are highly nonlinear, a numerical solution technique must be employed. NS01A, a Fortran subroutine developed by Powell, is a highly effective numerical algorithm which solves a set of nonlinear algebraic equa-

tions. The NS01A subroutine itself is a standard listing which calls on another subroutine (call named CALFUN) in which the particular equations to be solved are contained. Only the fundamental characteristics of NS01A are described here. A detailed explanation of the algorithm and the actual Fortran listing can be found in Reference 7.

The nonlinear equations to be solved by NS01A are contained in CALFUN (which the user must write). The equations must be expressed in the standard form

$$\bar{F}(\bar{Y}) = \bar{0} \quad (4-2)$$

where \bar{Y} is an n-vector of the n unknowns, and \bar{F} denotes the set of n nonlinear functions, each expressed as the difference between the current value and the desired value of that function. Expressed in the CALFUN format of (4-2), the nonlinear equations to be solved by NS01A become:

$$\begin{aligned} F_1 &= i_T(\bar{Y}) - i_T \\ F_2 &= r_2(\bar{Y}) - r_{2C} \\ F_3 &= v_2(\bar{Y}) - v_{2C} \\ F_4 &= e_2(\bar{Y}) - 0 \\ F_5 &= i_2(\bar{Y}) - i_2 \end{aligned} \quad (4-3)$$

The values on the right of the minus sign are the actual values of the constraints for that particular transfer. They are usually referred to as the hit conditions. The \bar{Y} vector of unknowns is

$$\begin{aligned}
 & \left. \begin{aligned} Y_1 &= \varphi_1 \\ Y_2 &= \varphi_2 \\ Y_3 &= \varphi_3 \\ Y_4 &= \varphi_4 \end{aligned} \right\} \begin{aligned} &\text{thrust direction angles ex-} \\ &\text{pressed in the local inertial} \\ &\text{frame} \end{aligned} & (4-4) \\
 & Y_5 = \text{TOF (equivalent to } t_{b2})
 \end{aligned}$$

Given the equations from CALFUN in the form of $\bar{F}(\bar{Y})$, NS01A initially creates a pseudo-cost function as

$$J(\bar{Y}) = \bar{F}^T(\bar{Y}) \bar{F}(\bar{Y}) \quad (4-5)$$

where "T" denotes the transpose operation. This expression represents a vector multiplication of a (1 x n) vector times an (n x 1) vector which produces a quadratic scalar cost J; where $J \geq 0$ at all values of \bar{Y} .

A combination of either Newton-Raphson or gradient type iteration steps are employed to find the minimum of the function $J(\bar{Y})$ to within a certain accuracy (ACC), selected by the user. To start the numerical solution process, the user must supply NS01A with an initial guess for \bar{Y} . Iteration then proceeds between NS01A, which checks for

$$J(Y) \leq \text{ACC} \quad (4-6)$$

and CALFUN, which computes the values of $\bar{F}(\bar{Y})$ for each iteration. Since the minimum of J is zero, the values of \bar{Y} which minimize (4-5) are the solution values to the nonlinear equations (4-2).

The NS01A algorithm is quite efficient in that it em-

employs a Newton-Raphson technique, but automatically switches to the method of steepest gradient when it detects possible divergence of the Newton-Raphson steps. So NS01A essentially uses a gradient step when the initial guess of \bar{Y} is far from the actual solution, then provides quadratic convergence via Newton-Raphson steps when nearer the solution.

Several difficulties are inherent in the application of a general purpose subroutine to this specific problem. First, the values of the \bar{Y} variables must be about the same order of magnitude in order to ensure convergence. Since four of the variables are angles expressed in radians, and Y_5 is a TOF expressed in seconds, the usual value of Y_5 is many orders of magnitude different from the other components of \bar{Y} . This necessitated scaling the TOF variable. The proper choice of the scaling factor greatly aided convergence.

The most critical problem, however, in the application of NS01A to the trajectory targeting process, was its sensitivity to the initial guess of \bar{Y} . Unless this guess was fairly close to the actual solution, convergence would not occur.

The problem of good initial guesses was overcome by first targeting the transfer using the assumption that the burns were impulsive. This method generated values of \bar{Y} which were sufficiently close to the actual values necessary for the real finite burn case, thus facilitating convergence by NS01A.

Since targeting is done to satisfy the actual finite

thrusting, a numerical scheme must be used to integrate the resulting nonlinear vector differential equations of motion (Appendix C, Equation C-7). Here again a general purpose subroutine combination called SET/STEP is employed for this purpose. Thus, CALFUN calls upon SET/STEP to integrate the equations of motion resulting from the current values of \bar{Y} .

The user must supply SET/STEP with the integration step-size. Then SET initializes the differential equations, and STEP integrates them one step at a time. A classical Runge-Kutta method is used for the first three steps, and then a fourth order Adams-Bashforth-Adams-Moulton predictor corrector scheme is applied to succeeding points.

NS01A gave convergence in as few as 20 iterations, or at the most 90 iterations depending on how closely the impulsively targeted values of \bar{Y} were to the actual values for the particular transfer trajectory being targeted.

Maximum Payload Missions

The hit conditions employed in CALFUN are not unique. Indeed, many different forms were tried, and their convergence properties compared, before selecting the set used in (4-3). There, constraining the inclination of the transfer trajectory was simply a convenient method of sampling the range of trajectories possible for excess energy missions.

When targeting a transfer for near maximum payload (for the given ΔV_1 , ΔV_2), constraining the amount of first burn plane change is too restrictive. The range of possible trajectories narrows considerably for payloads near maximum;

and reduces to one at some limiting value. In these cases it is difficult to predict what i_T should be.

An alternate set of hit conditions is used for targeting missions where the payload is near or at maximum. This set also has good convergence properties, and does not constrain i_T :

$$\begin{aligned} F_1 &= V_x(\bar{Y}) - V_x \\ F_2 &= V_y(\bar{Y}) - V_y \\ F_3 &= V_z(\bar{Y}) - V_z \\ F_4 &= e_2(\bar{Y}) - 0 \\ F_5 &= i_2(\bar{Y}) - i_2 \end{aligned} \tag{4-7}$$

The first three hit conditions now become the components of the velocity vector, \bar{V}_{2C} . These component values are calculated at each call of CALFUN to correspond to the orientation of $\bar{r}_2(\bar{Y})$, generated by that iteration of NS01A.

This set of hit conditions will also converge equally well for lower payloads, but the range of possible trajectories present in this case (by not specifying ψ_2) will produce a non-unique solution.

Targeting Step Two

This step may be thought of as selecting the IUS launch time for proper phasing between the orbits. Step one of targeting solves for five of the variables, referenced to the local frame. Once values for these five variables are fixed, the last two constraints are then functions of the only var-

iable left free in step one (the launch time), leaving

$$\Omega_2(t_{b1}) \quad (4-8)$$

$$TA(t_{b1}) \quad (4-9)$$

Thus, two independent equations in one unknown now remain. Since the equations are independent, a value for t_{b1} cannot, in general, be found which will satisfy both relationships. At this point then, either (4-8) or (4-9) is satisfied depending on the type transfer involved.

In the case of a three-dimensional transfer, satisfying TA^* without also satisfying Ω_2 would be meaningless. So, if the transfer is between non-coplanar orbits, the targeting in this step automatically satisfies (4-8) and leaves (4-9) free. If the transfer is between coplanar orbits, then a t_{b1} which satisfies (4-9) is found instead.

Two points are worthy of emphasis here. First, even if the parking orbit and mission orbit are coplanar, the transfer orbit itself can be non-coplanar. An out-of-plane transfer trajectory is often possible because of excess energy. In this case, a component of ΔV_1 is depleted by thrusting out of plane (creating a non-coplanar transfer orbit), and a component of ΔV_2 is likewise utilized to regain the initial plane. For this transfer, (4-9) is still satisfied.

The second point is that even though a coplanar transfer is necessary, rendezvous (i.e., satisfaction of TA^*) may not be required. In this case, a t_{b1} must still be

selected so that a reference location is specified for final computation of corresponding thrust direction angles. If rendezvous is not a necessary part of the mission, this may be accomplished by simply specifying some arbitrary value for ℓ_{02} ; such as $\ell_{02} = 0^\circ$. This, in turn, generates an arbitrary $TA(t_{b1})$, which when solved yields a t_{b1} . Here any value of t_{b1} will do just as well if rendezvous is unnecessary, and it gives a reference point in the parking orbit needed to compute the actual thrust direction angles expressed in the geocentric-equatorial frame.

The value of t_{b1} , once determined, represents the absolute time in seconds after the epoch time when the first opportunity for transfer occurs. The actual time for second stage ignition, then, now becomes

$$t_{b2} = t_{b1} + TOF^* - t_{bb} \quad (4-10)$$

where TOF^* is the total time in seconds from first stage ignition to second stage burnout (as previously computed in targeting step one), and t_{bb} is the fixed burn time of the second stage.

The next operation carried out in step two of targeting is to translate the values of the thrust direction angles expressed in the local frame from targeting step one, to their values expressed in the geocentric-equatorial frame. This can be done through appropriate coordinate transformations once t_{b1} is known. As explained earlier, given the orbital elements of the parking orbit, $\bar{r}_{1C}(t)$ may be computed

in the geocentric-equatorial frame. When t_{b1} is known, the inertial position for first stage ignition is fixed as \bar{r}_{1C} (t_{b1}). That vector, in turn, fixes the orientation between the local frame and the geocentric-equatorial frame, as shown in Figure 4-4, for the example of a geosynchronous transfer mission.

The last step in targeting is to compute the next four sequential times when the mission transfer could occur, and the corresponding thrust direction angles for each time. The reason for this is so these values could be stored on-board the IUS and sequentially used as necessary if mission delays occur. Here the usefulness of doing the original targeting

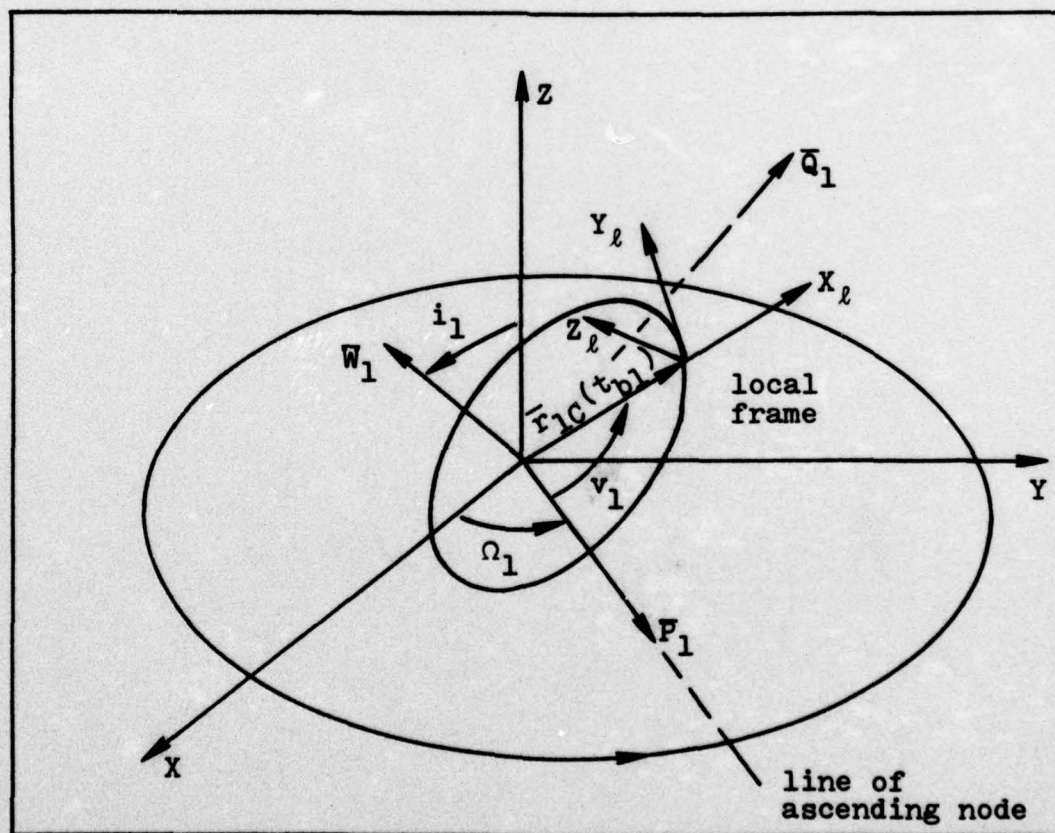


Figure 4-4. Relationship Between Local and Geocentric-Equatorial Frames

in a local frame is apparent. When each of the next four t_{b1} times is determined, it is only necessary to go through the same coordinate transformation for each new $\bar{r}_{1C}(t_{b1})$ position, rather than retarget the whole mission again. The fact that five sequential times are chosen here is completely arbitrary. Any number of parameter value sets could equally well be calculated in this way.

If the transfer is between non-coplanar orbits, the interval between successive mission opportunity times is just equal to the period of the parking orbit, and the thrust direction angles remain the same. This is because the transfer must be initiated at only one position in the transfer orbit. If the transfer is between coplanar orbits, then the interval between successive t_{b1} times is just equal to the synodic period of the two orbits, and the values of the thrust direction angles are different at each opportunity.

The actual calculations discussed in this section may be found in Appendix D.

V. Accuracy Analysis

The accuracy analysis is a separate operation in itself which is incorporated into the computer simulation in order to evaluate the effectiveness of the open loop transfer scheme for each transfer trajectory targeted. The error sources were discussed in Chapter II, and the actual computations involved in calculating the error sensitivities can be found in Appendix E.

To evaluate the accuracy of the overall scheme, and in particular each trajectory targeted using this scheme, sensitivities due to thrust misalignment and sensitivities due to thrust magnitude deviations, are calculated for each trajectory.

Thrust Misalignment Error Sensitivities

With the assumption that the thrust vector can be accurately directed along the pretarget IMU indicated inertial directions, any thrust misalignment then is caused by misalignment between the IMU platform inertial frame ($X_p Y_p Z_p$) and the actual geocentric-equatorial frame (XYZ). The sensitivities due to thrust vector misalignment are expressed in matrix form and relate thrust alignment errors during the burns to errors in position and velocity after the second burn (insertion). The misalignment is assumed the same for each burn. Expressed in matrix notation, this gives

$$\overline{\Delta M} = \frac{\partial \overline{M}}{\partial \overline{A L}} \overline{\Delta A L} \quad (5-1)$$

where $\overline{\Delta M}$ is a (6 x 1) "miss" vector (insertion error vector), $\overline{\Delta AL}$ is a (3 x 1) thrust misalignment vector, and $(\partial \overline{M} / \partial \overline{AL})$ is a (6 x 6) matrix of sensitivity coefficients. Written out in full this expression is

$$\begin{bmatrix} \Delta r_{xi} \\ \Delta r_{yi} \\ \Delta r_{zi} \\ \text{---} \\ \Delta V_{xi} \\ \Delta V_{yi} \\ \Delta V_{zi} \end{bmatrix} = \begin{bmatrix} \frac{\partial r_{xi}}{\partial AL_x} & \frac{\partial r_{xi}}{\partial AL_y} & \frac{\partial r_{xi}}{\partial AL_z} \\ \frac{\partial r_{yi}}{\partial AL_x} & \frac{\partial r_{yi}}{\partial AL_y} & \frac{\partial r_{yi}}{\partial AL_z} \\ \frac{\partial r_{zi}}{\partial AL_x} & \frac{\partial r_{zi}}{\partial AL_y} & \frac{\partial r_{zi}}{\partial AL_z} \\ \text{---} & \text{---} & \text{---} \\ \frac{\partial V_{xi}}{\partial AL_x} & \frac{\partial V_{xi}}{\partial AL_y} & \frac{\partial V_{xi}}{\partial AL_z} \\ \frac{\partial V_{yi}}{\partial AL_x} & \frac{\partial V_{yi}}{\partial AL_y} & \frac{\partial V_{yi}}{\partial AL_z} \\ \frac{\partial V_{zi}}{\partial AL_x} & \frac{\partial V_{zi}}{\partial AL_y} & \frac{\partial V_{zi}}{\partial AL_z} \end{bmatrix} \begin{bmatrix} \Delta AL_x \\ \Delta AL_y \\ \Delta AL_z \end{bmatrix} \quad (5-2)$$

where the subscript "i" denotes "at insertion". All the individual components and sensitivities are expressed with respect to the local frame. This enables a more meaningful comparison of results between diverse transfers. The units of the individual sensitivities are nm of position error per milliradian of thrust misalignment; or, ft/sec of velocity error per milliradian of thrust misalignment.

With the sensitivities in this form, however, it is

difficult to draw a standard of comparison for evaluating the accuracies of individual trajectories, to determine which one from a group of possible trajectories would give the lowest insertion errors. A great deal of thought went into how best to use the information provided by the thrust misalignment sensitivity matrices to compare trajectory accuracies.

This dilemma was finally resolved by deciding upon a "worst case" comparison. But before explaining this method it is instructive to look at the dilemma in the light of what the sensitivities mean. The overall miss vector ($\overline{\Delta M}$) can be broken into two components; one for position error, $\overline{\Delta r}$, and the second for velocity error, $\overline{\Delta V}$, as the partitioning in (5-2) shows. Taking for example the position error vector $\overline{\Delta r}$ (same for velocity), the error is expressible as

$$\begin{aligned}\overline{\Delta r} &= \Delta r_{xi} \bar{i} + \Delta r_{yi} \bar{j} + \Delta r_{zi} \bar{k} \\ &= \left(\frac{\partial r_{xi}}{\partial AL_x} AL_x + \frac{\partial r_{xi}}{\partial AL_y} AL_y + \frac{\partial r_{xi}}{\partial AL_z} AL_z \right) \bar{i} \\ &\quad + \left(\frac{\partial r_{yi}}{\partial AL_x} AL_x + \frac{\partial r_{yi}}{\partial AL_y} AL_y + \frac{\partial r_{yi}}{\partial AL_z} AL_z \right) \bar{j} \\ &\quad + \left(\frac{\partial r_{zi}}{\partial AL_x} AL_x + \frac{\partial r_{zi}}{\partial AL_y} AL_y + \frac{\partial r_{zi}}{\partial AL_z} AL_z \right) \bar{k}\end{aligned}\tag{5-3}$$

where the magnitude of the position error is

$$\Delta r = \sqrt{\Delta r_{xi}^2 + \Delta r_{yi}^2 + \Delta r_{zi}^2}\tag{5-4}$$

Equation (5-4) in turn depends on the actual components

of the misalignment vector

$$\overline{\Delta AL} = AL_x \bar{i} + AL_y \bar{j} + AL_z \bar{k} \quad (5-5)$$

Thus, as seen from studying Equation (5-3), the actual value of Δr for any particular transfer is dependent on the particular magnitudes (and even the signs) of the individual components of $\overline{\Delta AL}$. But $\overline{\Delta AL}$ is a completely random variable! At best, only a tolerance (or upper limit) on the magnitude of $\overline{\Delta AL}$ may be known.

Assuming an arbitrary orientation and magnitude for $\overline{\Delta AL}$, and using this same value to compute a subsequent Δr for each trajectory, is one possible approach. However, this approach is still inadequate in that there is no way of knowing whether or not this arbitrary $\overline{\Delta AL}$ has the same effect on each of the widely diverse trajectories. Also, there would be no way of predicting whether a "worse" $\overline{\Delta AL}$ direction might be possible. This approach, however, is meaningful if a guaranteed worst alignment direction were used based on the sensitivity characteristics of each trajectory.

Although there is no way of predicting the actual orientation of the random thrust misalignment vector, it is valid to say that there will be in every case a "worst possible" orientation. That is, there will be some orientation of the $\overline{\Delta AL}$ vector, which (for any fixed magnitude) will cause the greatest insertion errors. This concept, then, is implemented here.

The sensitivity matrix of each transfer is reduced to

two "worst case" sensitivities; one for position error and one for velocity error. To explain how the worst case sensitivities are found, the example of insertion position error can again be used. Derivation of the worst case velocity error sensitivity is exactly the same. Using a more simplified notation to convey the concept, let

$$\bar{y} = A \bar{x} \quad (5-6)$$

where $\bar{y} = \Delta \bar{r}$, the insertion position error vector; $\bar{x} = \Delta \bar{A} \bar{L}$, the thrust misalignment vector; and A is the matrix of sensitivity coefficients, $(\partial \bar{r}_i / \partial \Delta \bar{A} \bar{L})$, which transforms the vector \bar{x} into the vector \bar{y} .

Now the question of a worst misalignment direction may be put in this form: For a fixed specified magnitude of the vector \bar{x} , what is the maximum possible magnitude of the vector \bar{y} . Since a sensitivity is desired, this equates to asking what orientation of the unit thrust misalignment vector goes through the vector transformation of (5-6) to give the maximum length of the insertion position error vector.

With the assumption that the thrust misalignment is strictly due to misalignment between the XYZ frame and the $X_p Y_p Z_p$ frame, the worst possible orientation of the thrust misalignment vector is along the "Euler angle" axis direction which produces the "worst" misalignment between these two frames, in the sense of causing maximum insertion error. This is illustrated in Figure 5-1.

As derived in Appendix E, the maximum possible magnitude of \bar{y} caused by some \bar{x} is obtained from

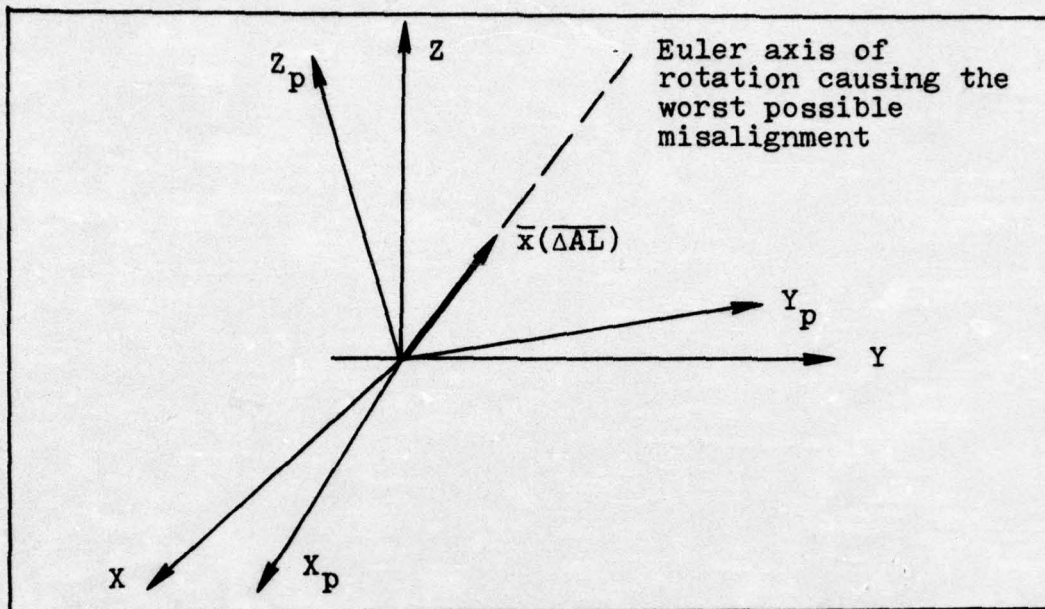


Figure 5-1. Worst Misalignment

$$|\bar{y}|_{\max} = \sqrt{\lambda_{\max}} |\bar{x}| \quad (5-7)$$

where λ_{\max} is the largest eigenvalue of the $A^T A$ matrix.

Thus, by computing the eigenvalues of the symmetric matrix $A^T A$ formed from the respective position or velocity error sensitivity matrices, the two worst case sensitivities are obtained. From these, and a value for the magnitude of the worst thrust misalignment expected, the upper bounds of the associated insertion errors are obtained directly. These values may then be compared between an assortment of trajectories as a valid and direct measure of their respective accuracies.

Thrust Magnitude Error Sensitivities

Vehicle performance is calculated using the ideal velocity (ΔV) equation

$$\Delta V = I_{sp} g_0 \ln \left(\frac{m_0}{m_f} \right) \quad (2-1)$$

where I_{sp} is the specific impulse of the solid propellant; g_0 is the gravitational constant ($32.14644 \text{ ft/sec}^2$); m_0 is the vehicle mass at ignition; and m_f is the vehicle mass at burnout. From (2-1) it can be seen that the ΔV provided by a specific stage is a function only of the propulsion parameters (I_{sp} and propellant weight), and the inert (empty) weight of the vehicle.

It is assumed here that fairly tight tolerances can be maintained on I_{sp} , fuel weight and the structure weight of the vehicle so that the magnitude of ΔV for each stage is not subject to error. However, a deviation in the thrust profile of either engine is possible without any variation in its total impulse (ΔV). That is, the total velocity change can be equal to that expected, but the acceleration profile may vary. This would be caused by a variation in the solid propellant burn rate, thus causing a deviation in the thrust magnitude. This can be seen from the thrust equation

$$T = -c\dot{m} \quad (5-8)$$

where c is the effective exhaust velocity; and \dot{m} is the mass flow rate. The mass flow rate equation (assuming constant \dot{m}) is

$$m(t) = m_0 - \dot{m}t \quad (5-9)$$

Evaluating this equation at the burnout time (t_b), and solving for t_b , gives the total burn time as

$$t_b = \frac{m_0 - m_f}{\dot{m}} \quad (5-10)$$

So a variation in the magnitude of T will be associated with a change in the burn time. A variation in the burn time will affect the position at burnout. This can be a major source of insertion error since (as discussed in Chapter I) the required velocity to hit the target is a function of the burnout position.

As with thrust direction error, the thrust magnitude error is in general a random variable. However, bounds on this error should be predictable from studying the statistical characteristics of the engine performance. With this in mind, sensitivities are calculated for both an overall plus and an overall minus 1% error in the thrust magnitude. For each sensitivity it is assumed that both engines have the same thrust error.

VI. Results for the Reference Missions

This chapter presents the results of targeting and the accuracy analysis of the geosynchronous and subsynchronous reference missions. The geosynchronous mission is given the greatest emphasis. The results for this mission are presented for two different fuel load combinations; each with four different payload weights. In addition, the results for a coplanar (geosynchronous) transfer are included - along with an expanded explanation of some of the intermediate targeting and error analysis steps - since this maneuver is easily visualized.

For targeting purposes, arbitrary values were assumed for λ_{02} (true longitude at epoch of the mission orbit target position), and Ω_1 (longitude of the ascending node of the parking orbit). The values obtained for the six control parameters for each mission are not included here, since they are based on arbitrary initial conditions and the selected plane change split between burns.

The results of the error analyses are presented in graphical form for most missions. Insertion error sensitivities are plotted against the first burn plane change angle, for the various fuel and payload combinations. The sensitivities due to thrust misalignment are the "worst case" values. The units on the position and velocity insertion error sensitivities due to thrust misalignment are nautical miles and ft/sec, per milliradian of thrust vector misalignment; and similarly for insertion error sensitivities due to thrust magnitude

variations, per $\pm 1\%$ variation. The last plot for each mission shows the transfer time of flight versus first burn plane change angle.

In all cases except two, the maximum value of the first burn plane change angle shown on the plots is within 1° of its absolute maximum. The two exceptions are shown in Figures 6-7, 6-8, 6-9, and in Figures 6-16, 6-17, 6-18, where the maximum value of the first burn plane change angle was iterated to within $.1^\circ$ of its absolute maximum.

The last section in this chapter summarizes the overall results, and gives some general observations concerning this scheme.

IUS Vehicle Specifications

Table III lists the values of the IUS vehicle parameters which were used in targeting the reference missions. These values are based (with some minor simplifications) on the Burner II specifications as given in Reference 2.

Table III. Vehicle Specifications

<u>First Stage:</u>	
Total Structure Weight (ST_1)	2437 lb
Propellant Weight ($PROP_1$)	17,300 lb or 20,000 lb
Thrust (T_1)	41,923.4 lbf
Specific Impulse (I_{sp1})	291.8 sec
<u>Second Stage</u>	
Total Structure Weight (ST_2)	1362 lb
Propellant Weight ($PROP_2$)	4700 lb
Thrust (T_2)	14,345.6 lbf
Specific Impulse (I_{sp2})	300.8 sec

The Geosynchronous Mission

Mission Description: the parking orbit is circular, at an altitude of 160 nm and is inclined 28.5° . The mission orbit is equatorial, and at an altitude of 19,323 nm.

Figures 6-1 through 6-9 show the results for a fuel load combination of $PROP_1 = 17,300$ lbs, $PROP_2 = 4700$ lbs; and payload (PL) weights of 1000, 2000, and 3000 lbs. Similarly, Figures 6-10 through 6-18 show the comparable results for a fuel loading of $PROP_1 = 20,000$ lbs, $PROP_2 = 4700$ lbs.

To obtain results for payloads very near maximum, the alternate hit conditions given in Equation 4-7 were employed. In these cases, the amount of first burn plane change is left free to seek its optimum value. Table IV lists the maximum payload results for the two different fuel load combinations.

The retargeting period is 5427 seconds for all the geosynchronous non-coplanar transfer missions.

The Subsynchronous Mission

Mission Description: The parking orbit is at an altitude of 160 nm, and inclined 57° . The mission orbit is at an altitude of 10,900 nm, and has an inclination of 63° . The longitudes of the ascending nodes, Ω_1 and Ω_2 , are equal.

The subsynchronous transfer mission will be used for placement of the Department of Defense Navstar Global Positioning System (GPS). The total payload weight is forecast to be 4400 lbs. The results for a subsynchronous mission with this amount of payload are shown in Figures 6-19, 6-20, and 6-21. The fuel loading for this transfer was $PROP_1 =$

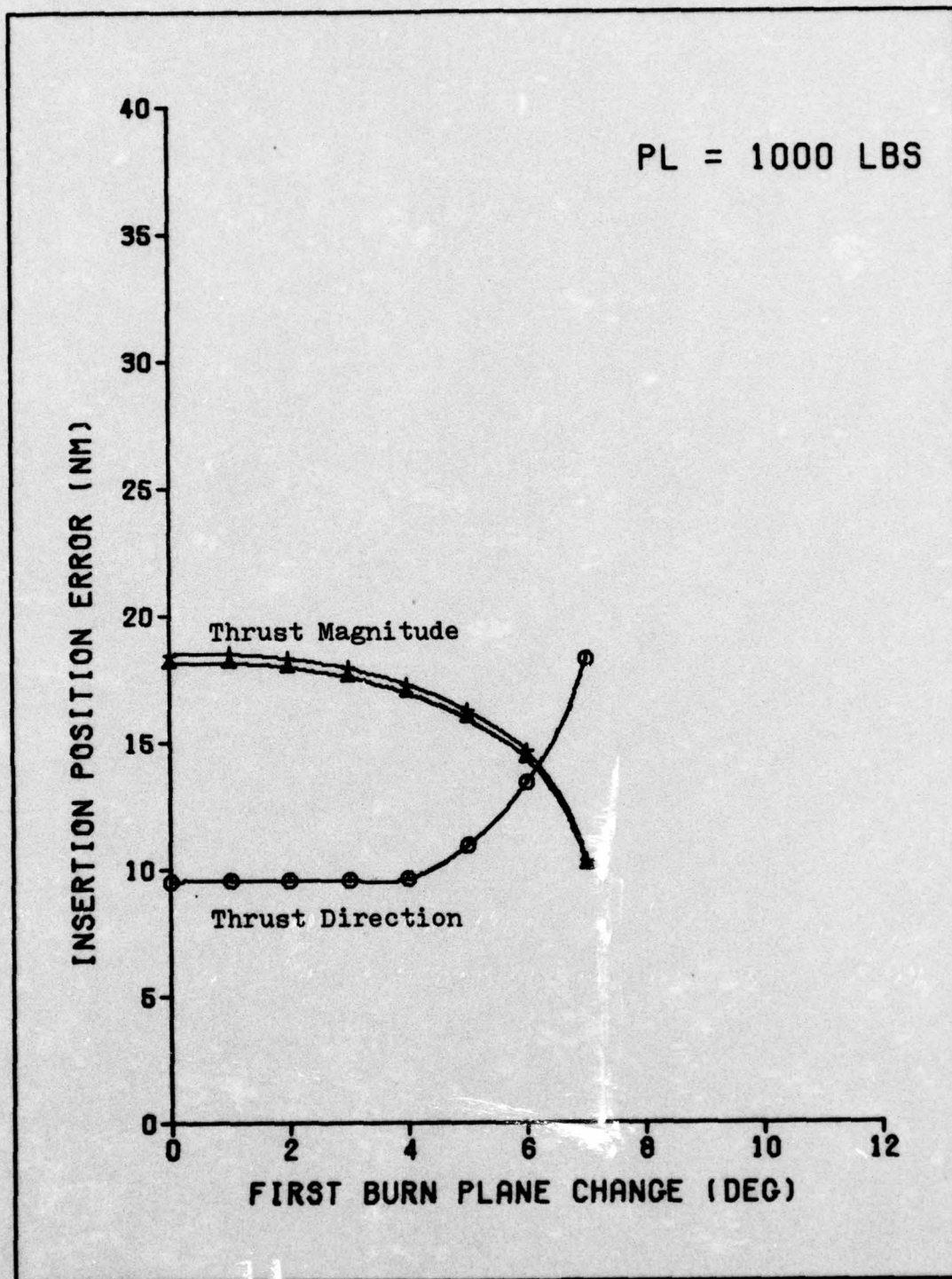


Figure 4-1. Geosynchronous Insertion Error Sensitivities (Position)
(PROP₁ = 17,300 lb, PL = 1000 lb)

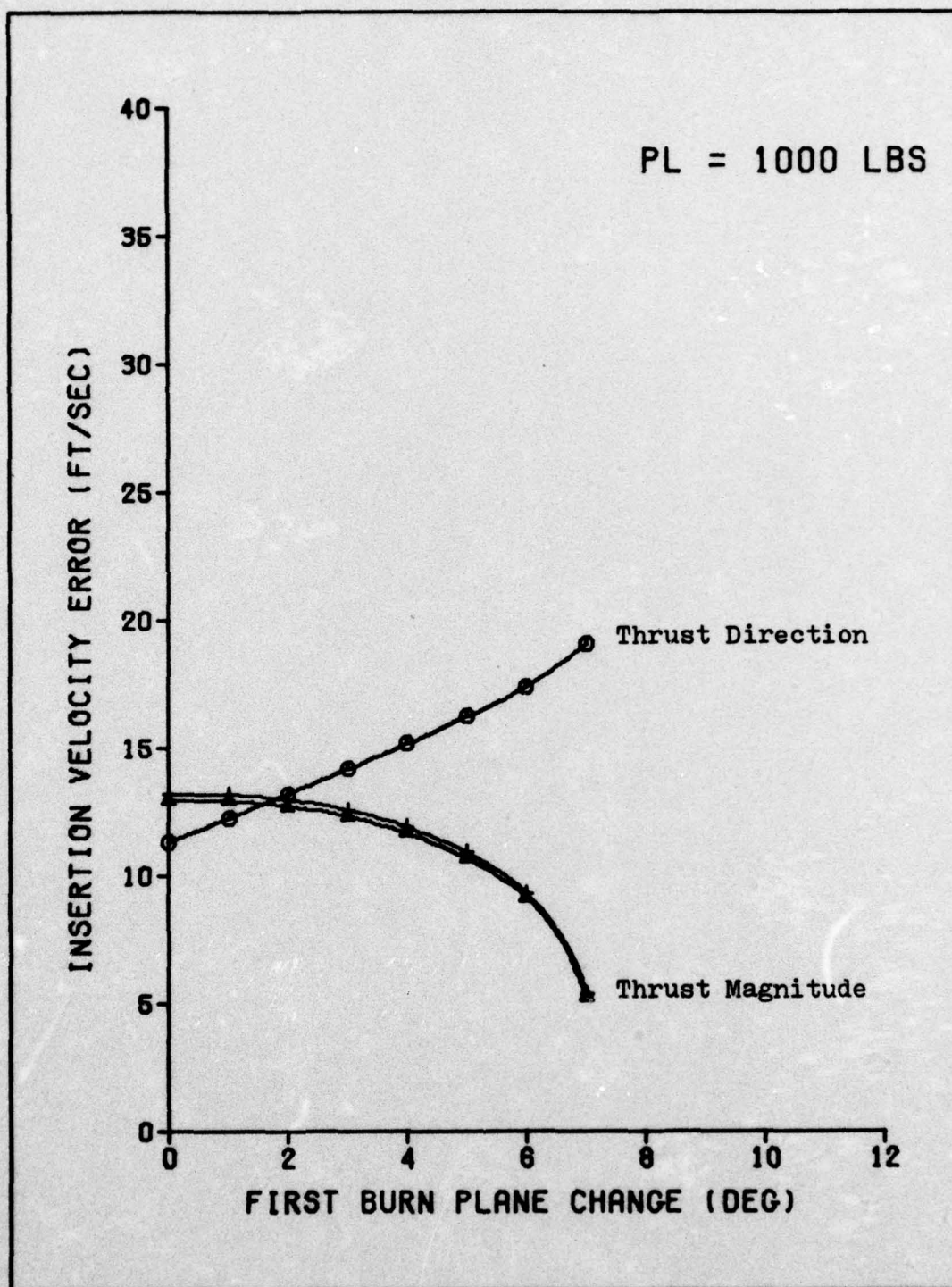


Figure 6-2. Geosynchronous Insertion Error Sensitivities (Velocity)
(PROP₁ = 17,300 lb, PL = 1000 lb)

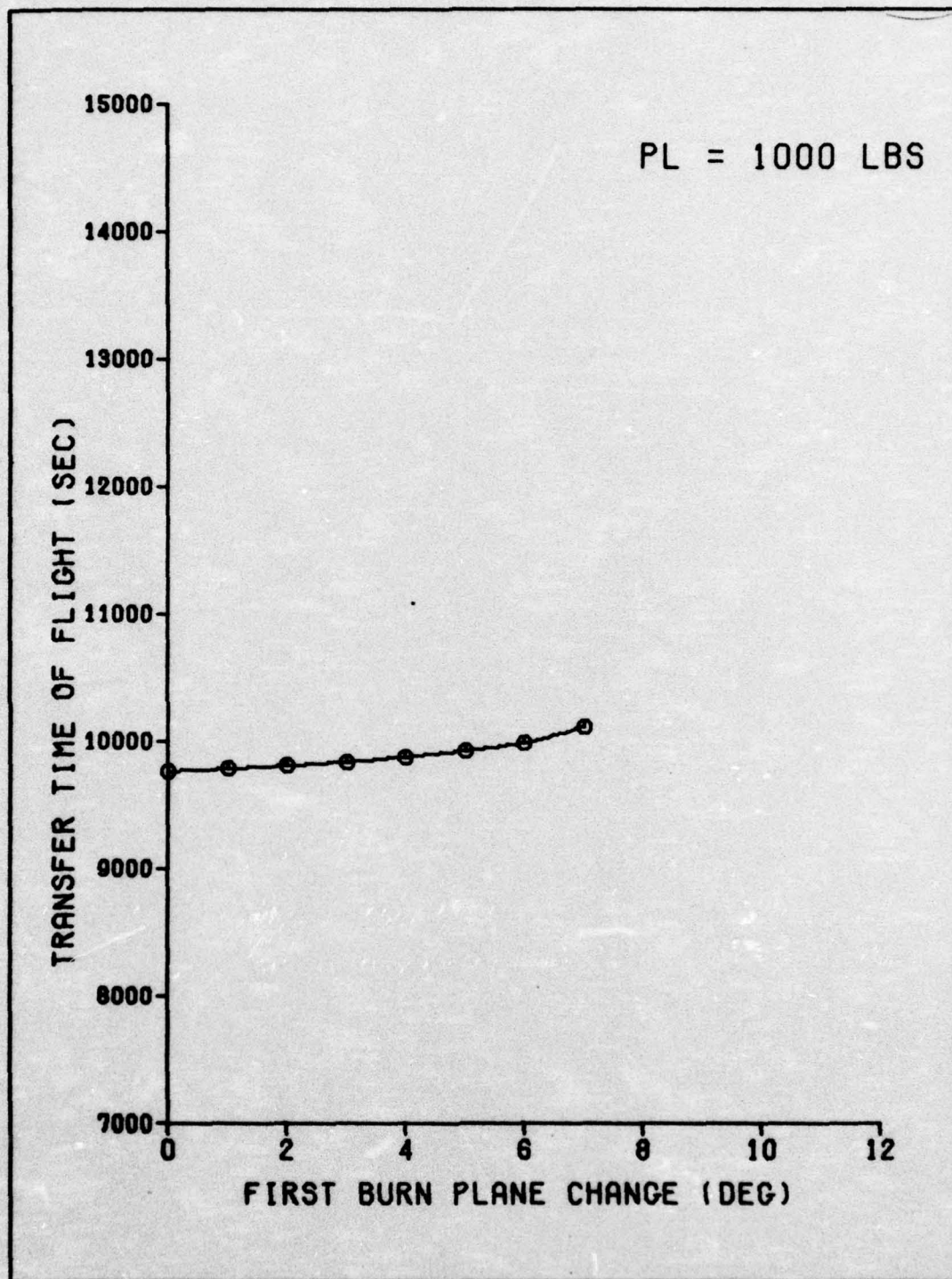


Figure 6-3. Geosynchronous Time of Flight
(PROP₁ = 17,300 lb, PL = 1000 lb)

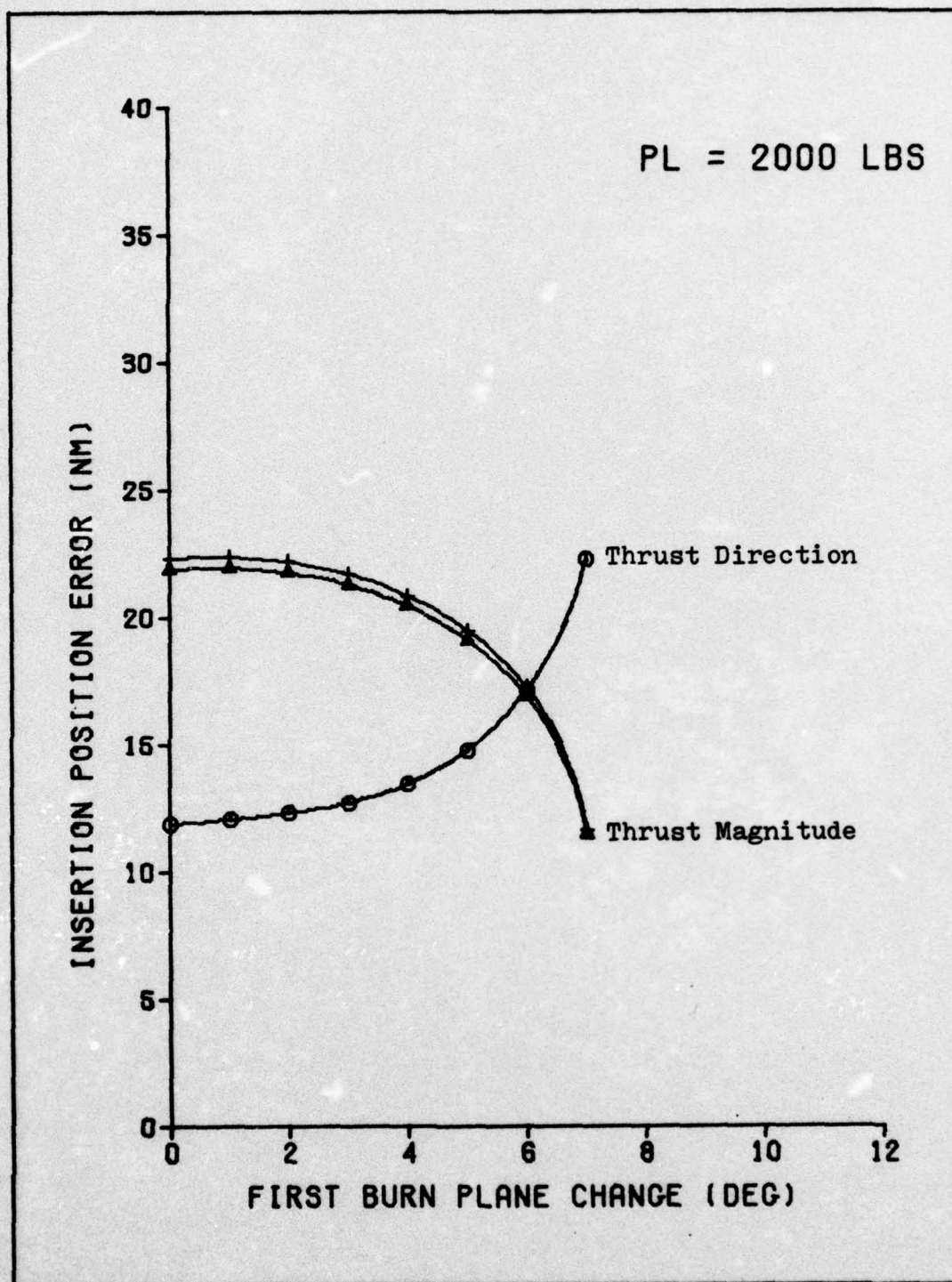


Figure 6-4. Geosynchronous Insertion Error Sensitivities (Position)
(PROP₁ = 17,300 lb, PL = 2000 lb)

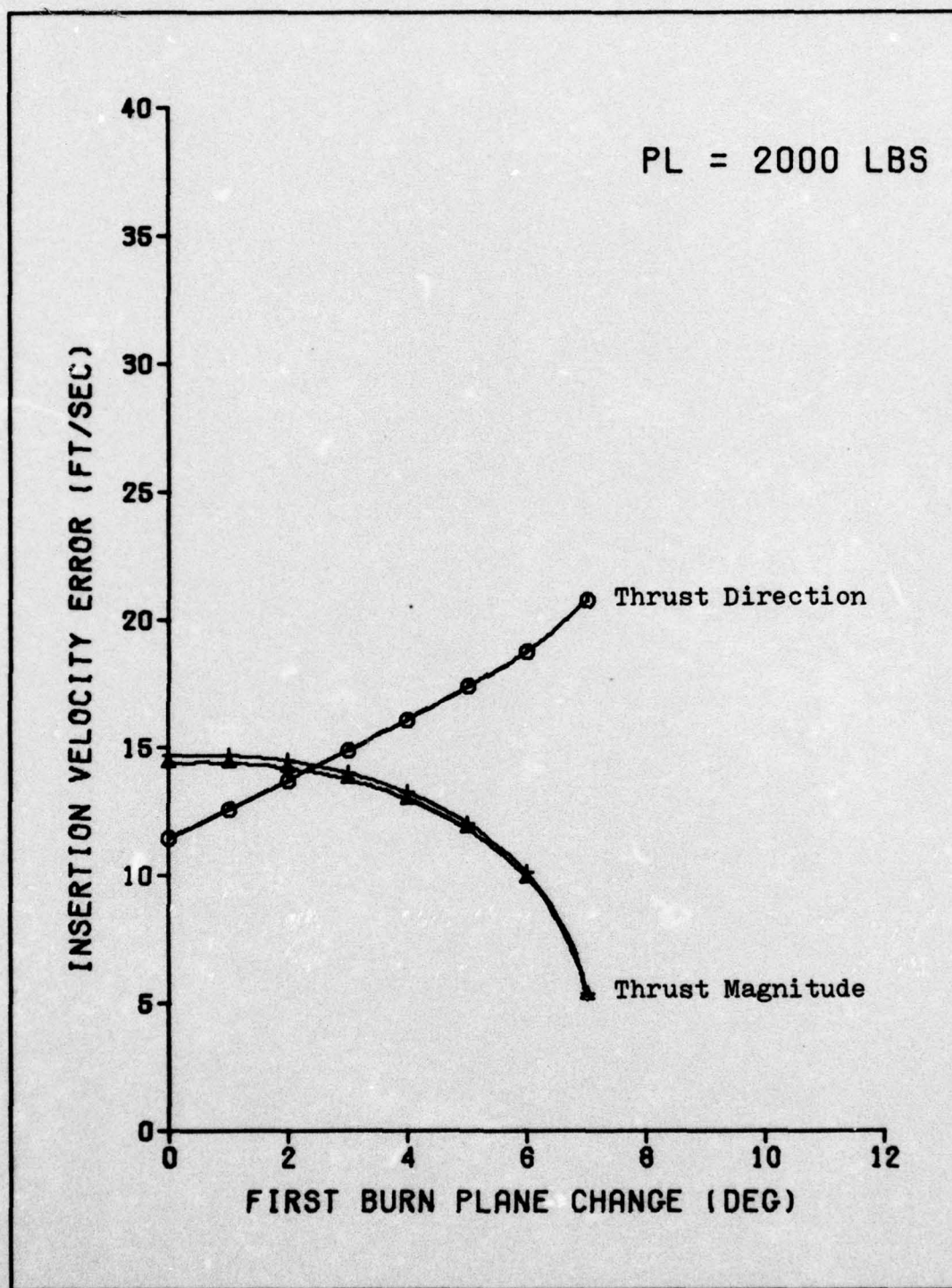


Figure 6-5. Geosynchronous Insertion Error
Sensitivities (Velocity)
(PROP₁ = 17,300 lb, PL = 2000 lb)

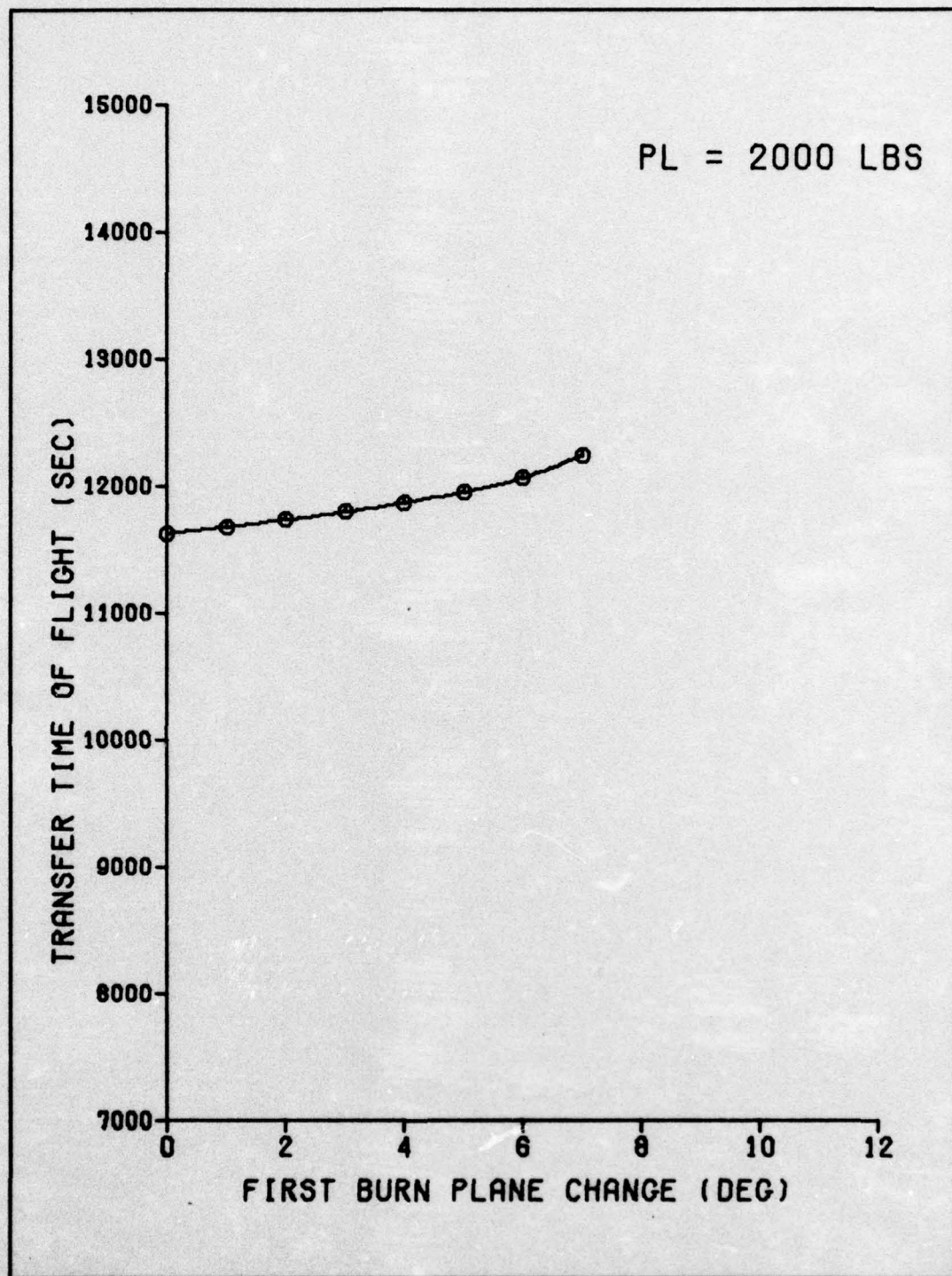


Figure 6-6. Geosynchronous Time of Flight
($PROP_1 = 17,300$ lb, PL = 2000 lb)

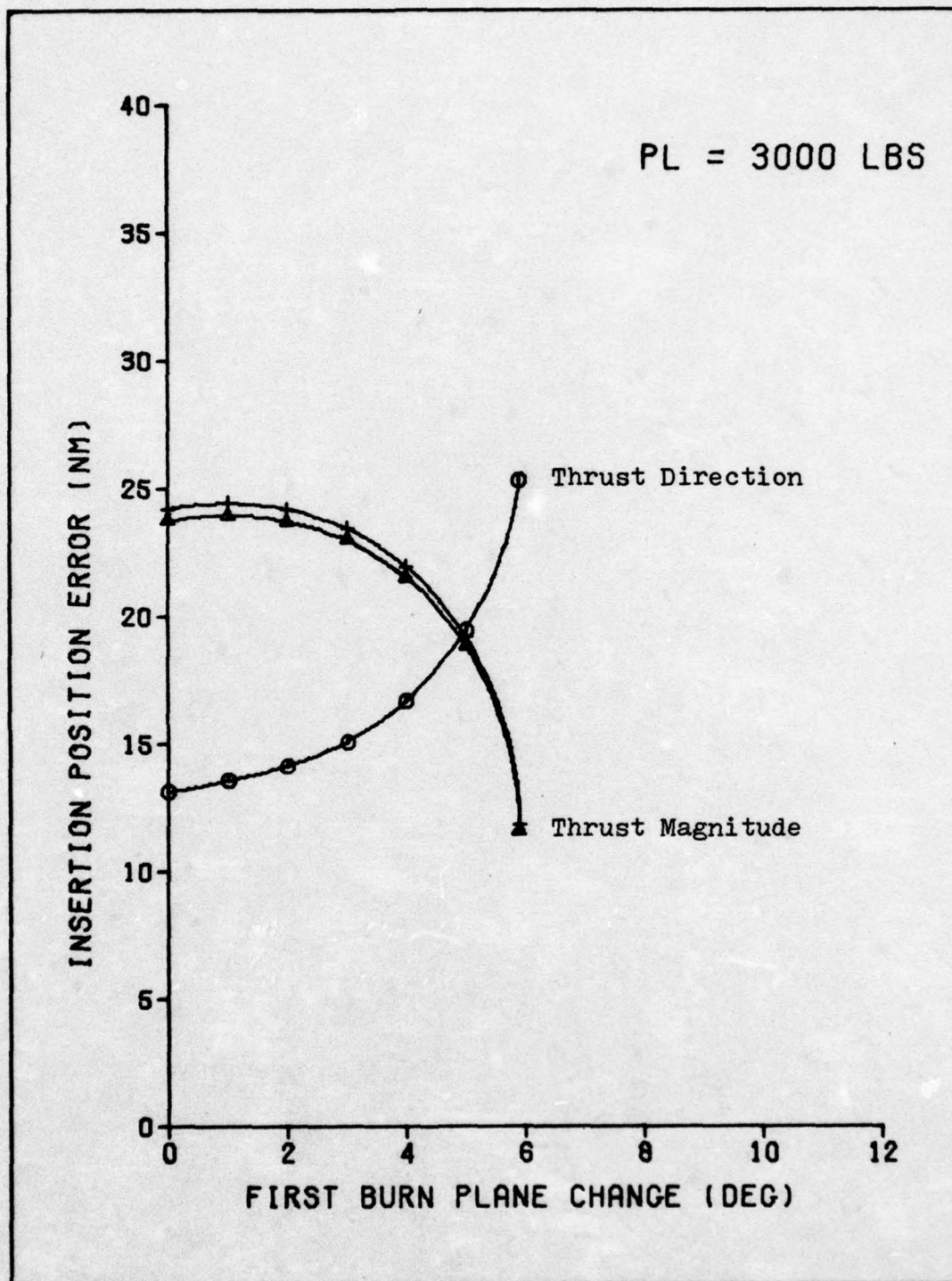


Figure 6-7. Geosynchronous Insertion Error Sensitivities (Position)
(PROP₁ = 17,300 lb, PL = 3000 lb)

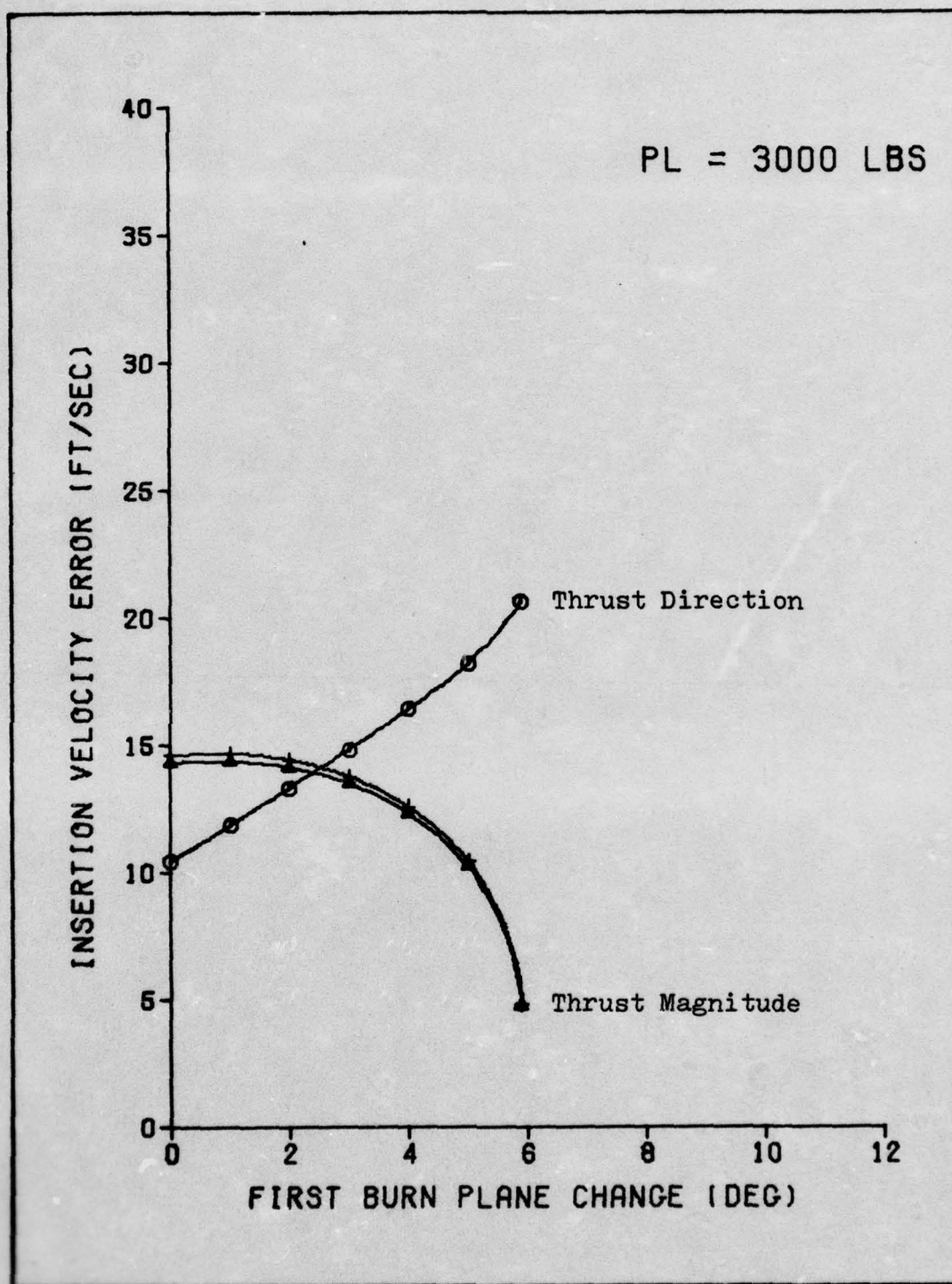


Figure 6-8. Geosynchronous Insertion Error
Sensitivities (Velocity)
(PROP₁ = 17,300 lb, PL = 3000 lb)

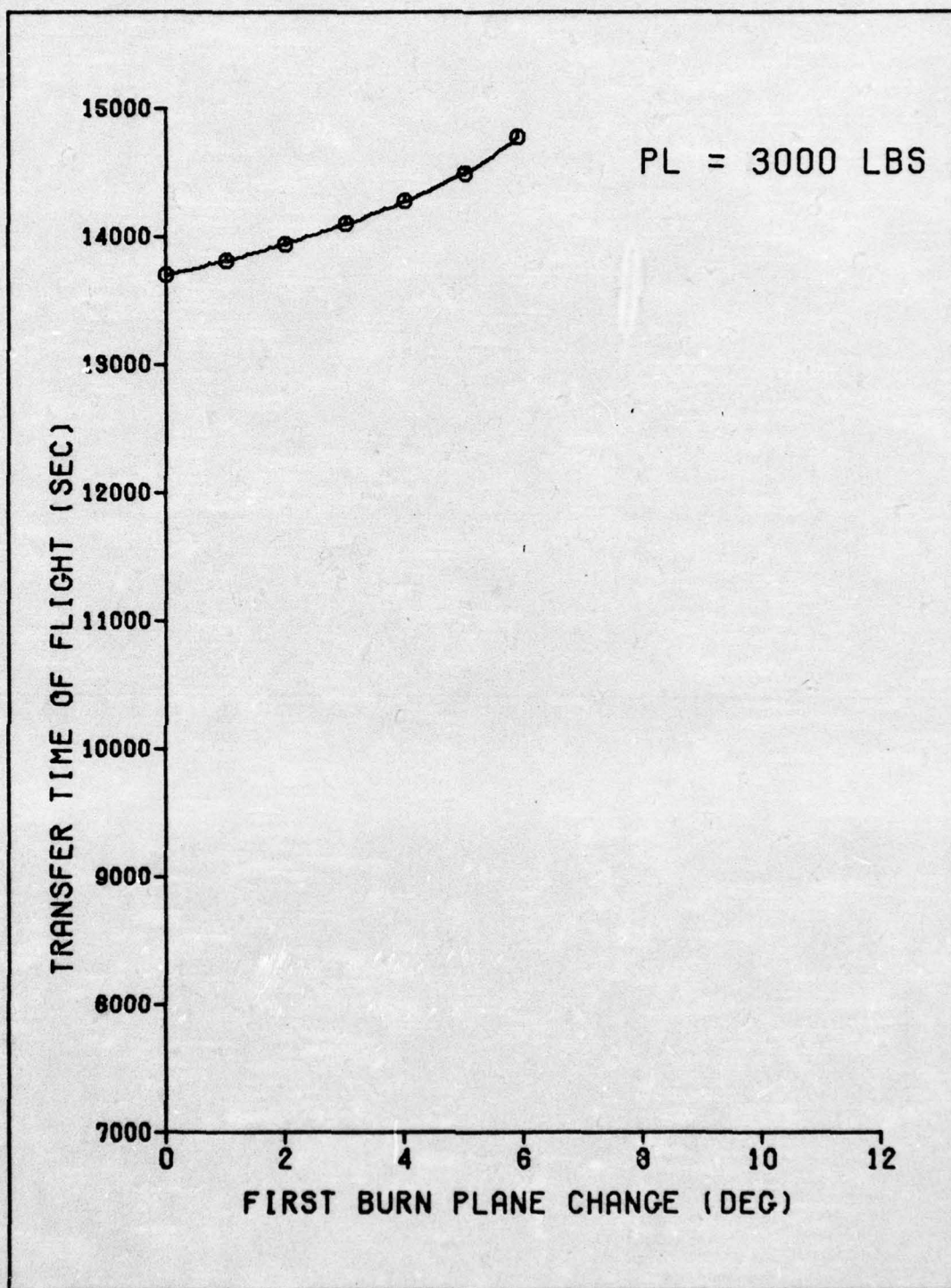


Figure 6-9. Geosynchronous Time of Flight
(PROP₁ = 17,300 lb, PL = 3000 lb)

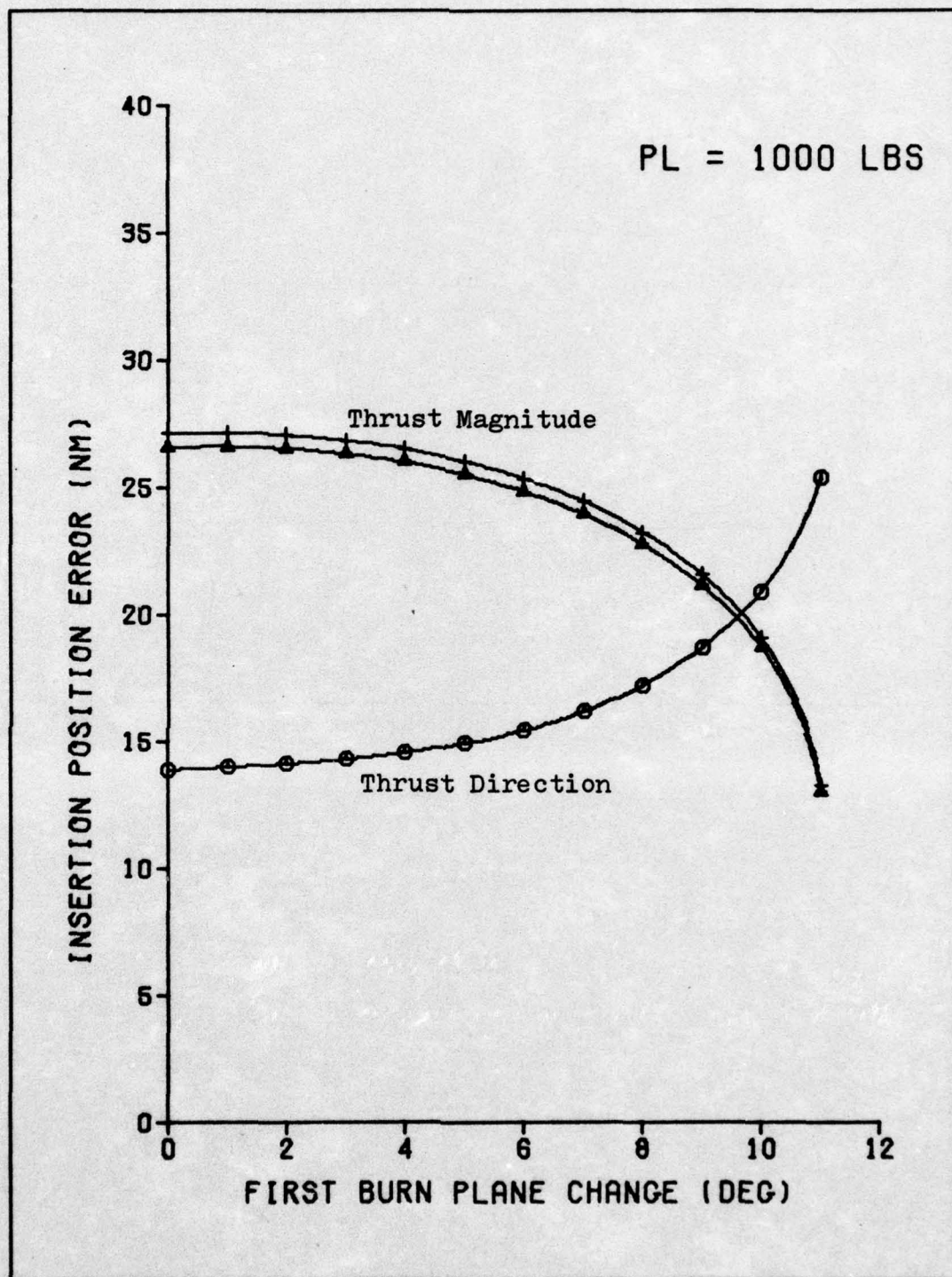


Figure 6-10. Geosynchronous Insertion Error Sensitivities (Position)
PROP₁ = 20,000 lb, PL = 1000 lb

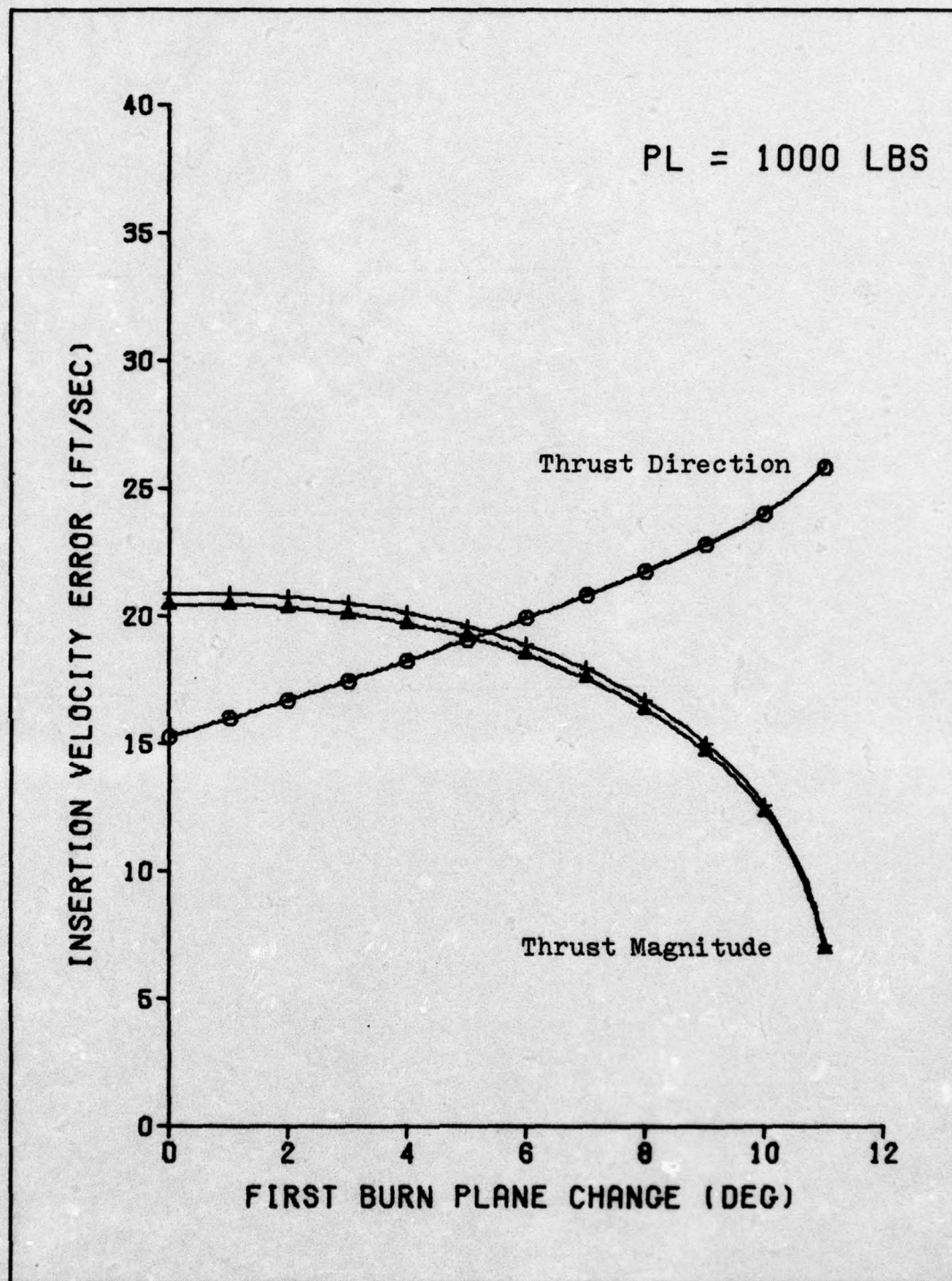


Figure 6-11. Geosynchronous Insertion Error Sensitivities (Velocity)
(PROP₁ = 20,000 lb, PL = 1000 lb)

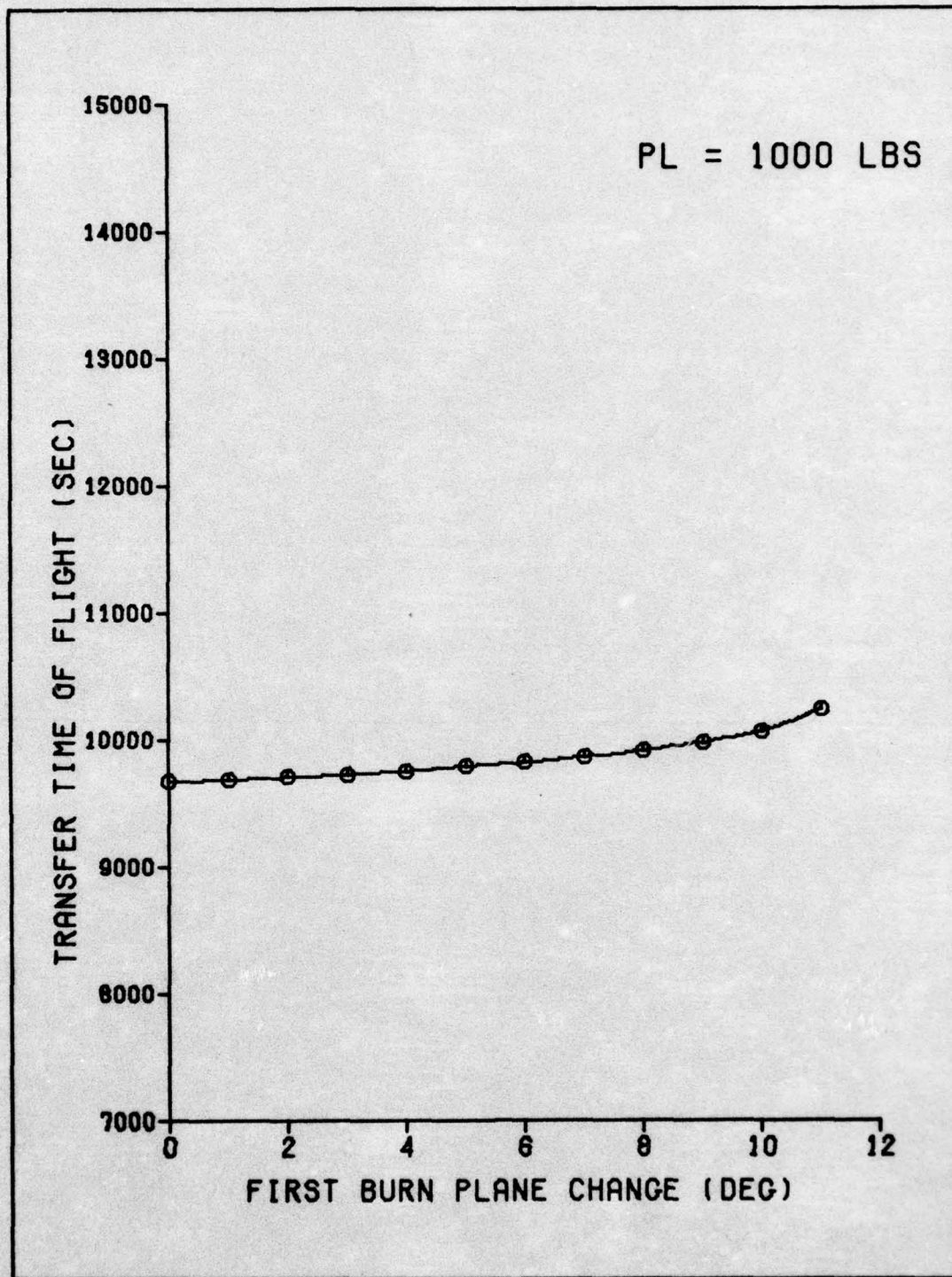


Figure 6-12. Geosynchronous Time of Flight
($PROP_1 = 20,000$ lb, $PL = 1000$ lb)

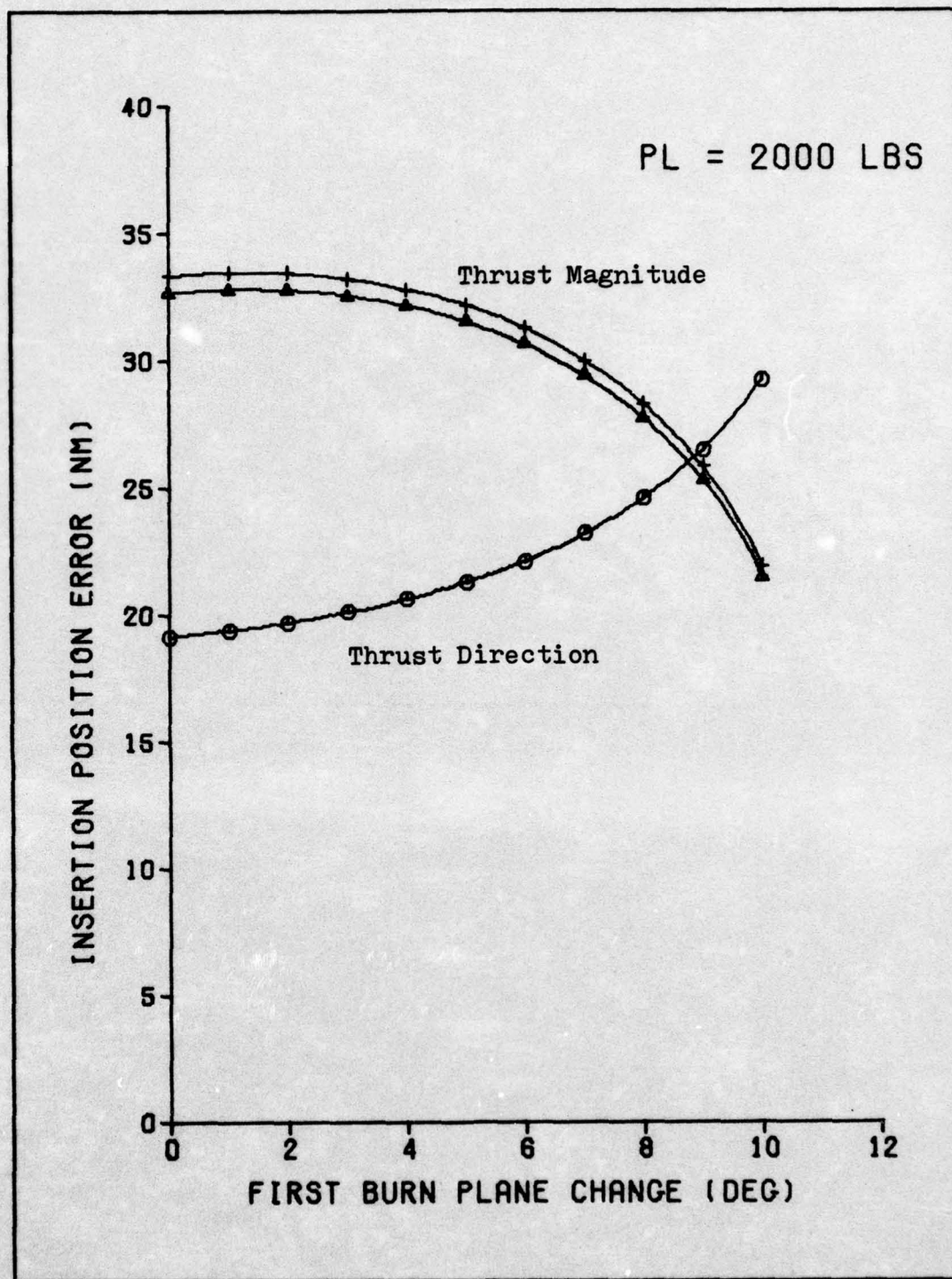


Figure 6-13. Geosynchronous Insertion Error Sensitivities (Position)
(PROP₁ = 20,000 lb, PL = 2000 lb)

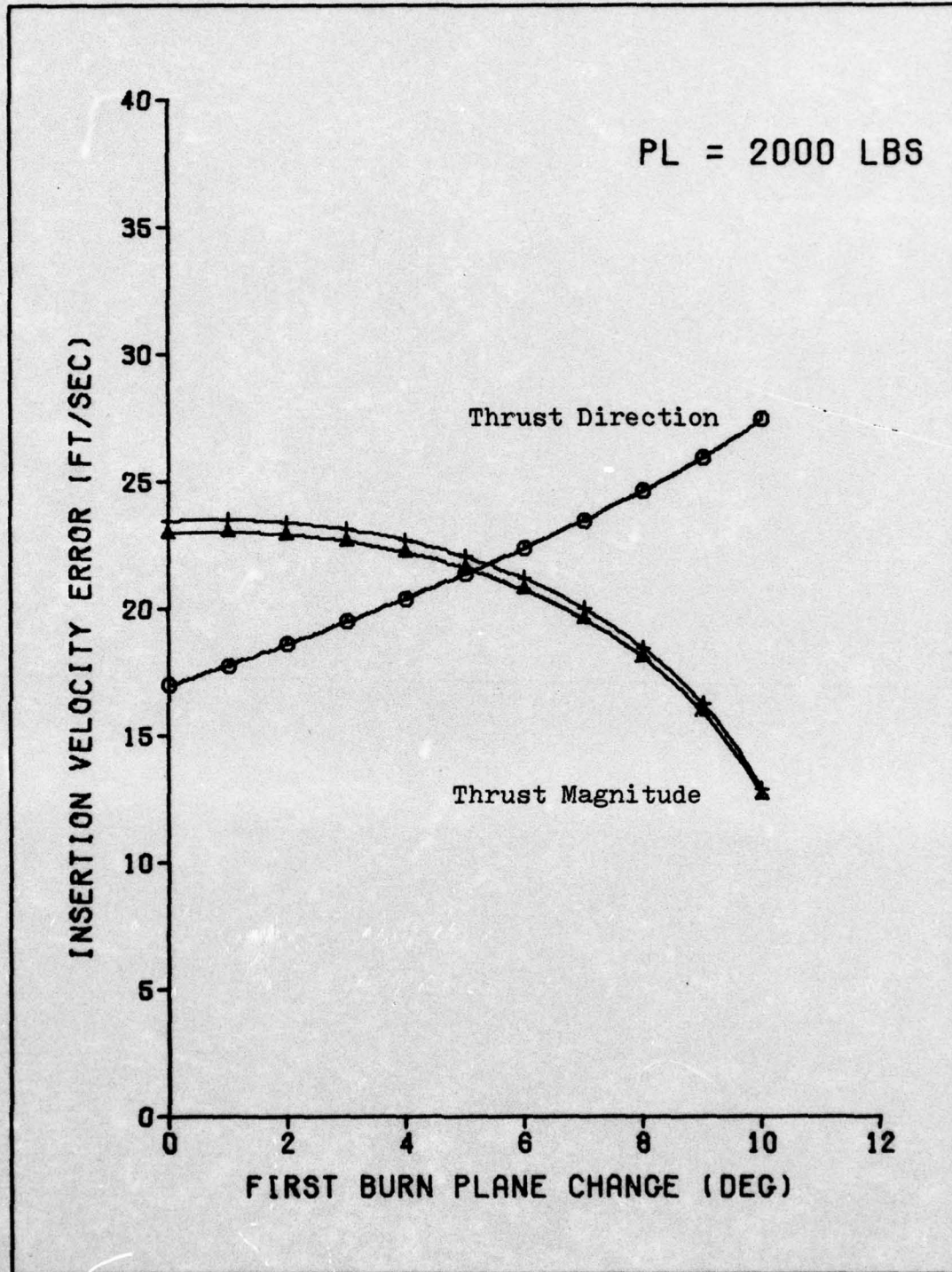


Figure 6-14. Geosynchronous Insertion Error Sensitivities (Velocity)
(PROP₁ = 20,000 lb, PL = 2000 lb)

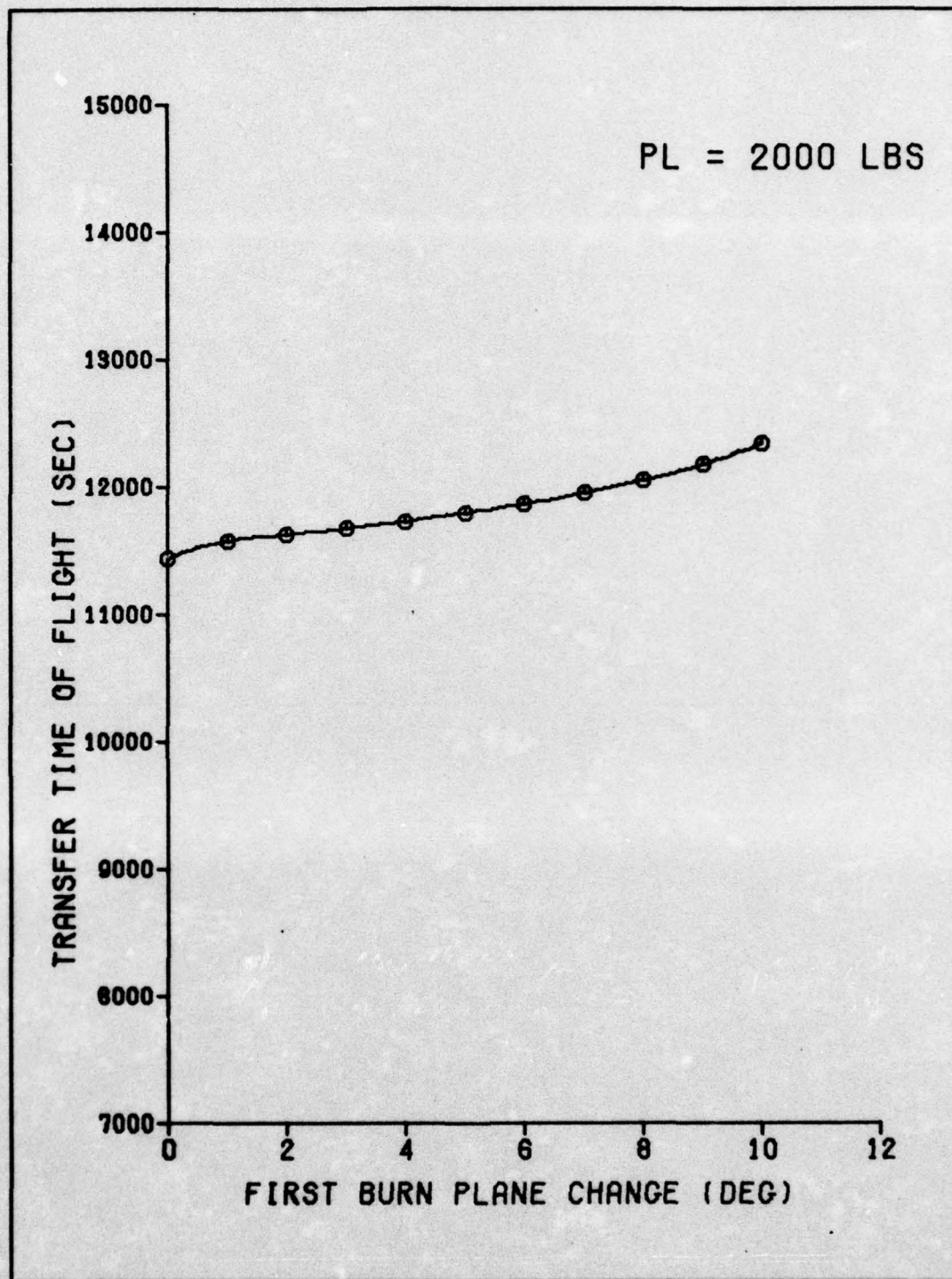


Figure 6-15. Geosynchronous Time of Flight
(PROP₁ = 20,000 lb, PL = 2000 lb)

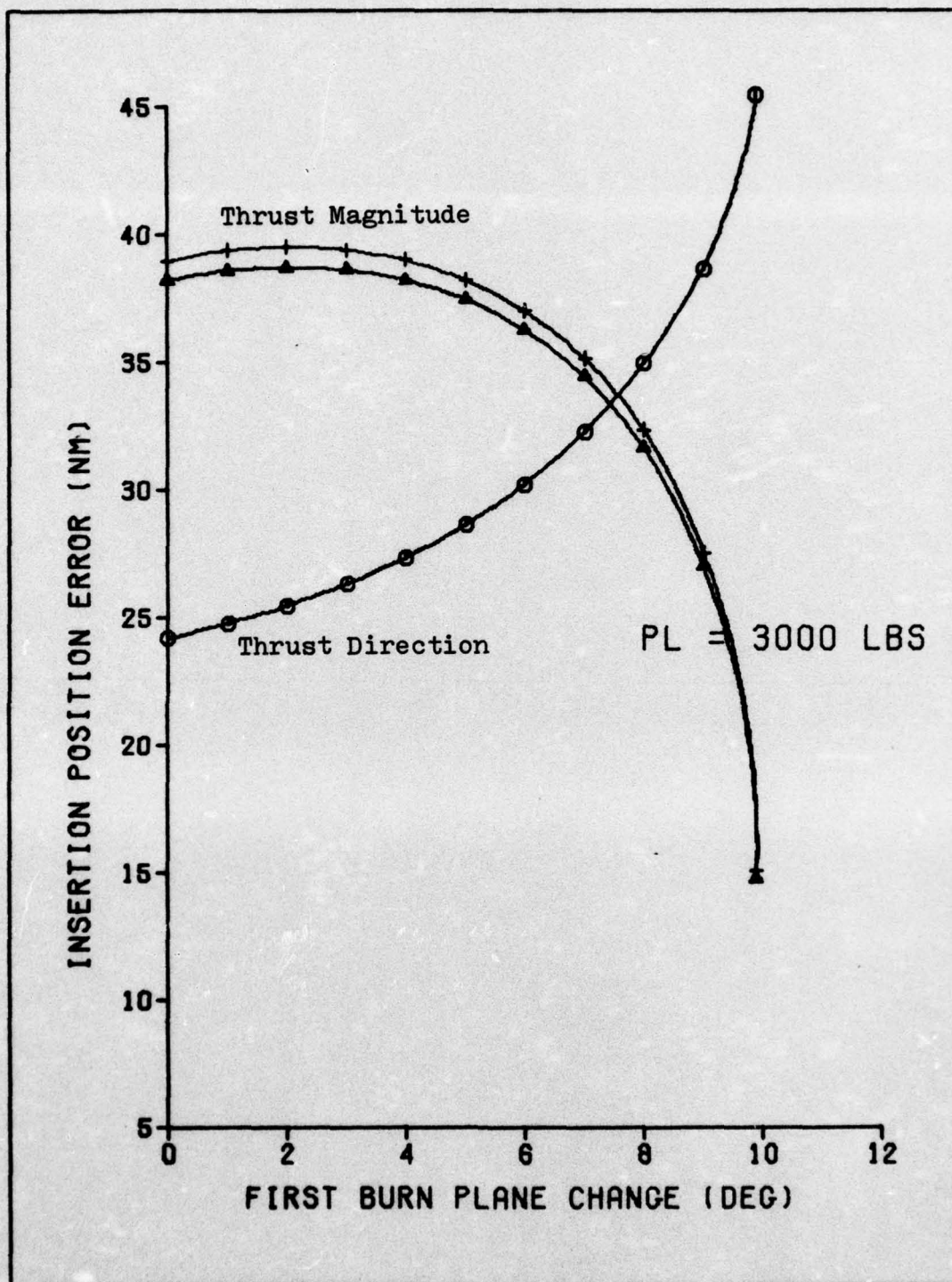


Figure 6-16. Geosynchronous Insertion Error Sensitivities (Position)
(PROP₁ = 20,000 lb, PL = 3000 lb)

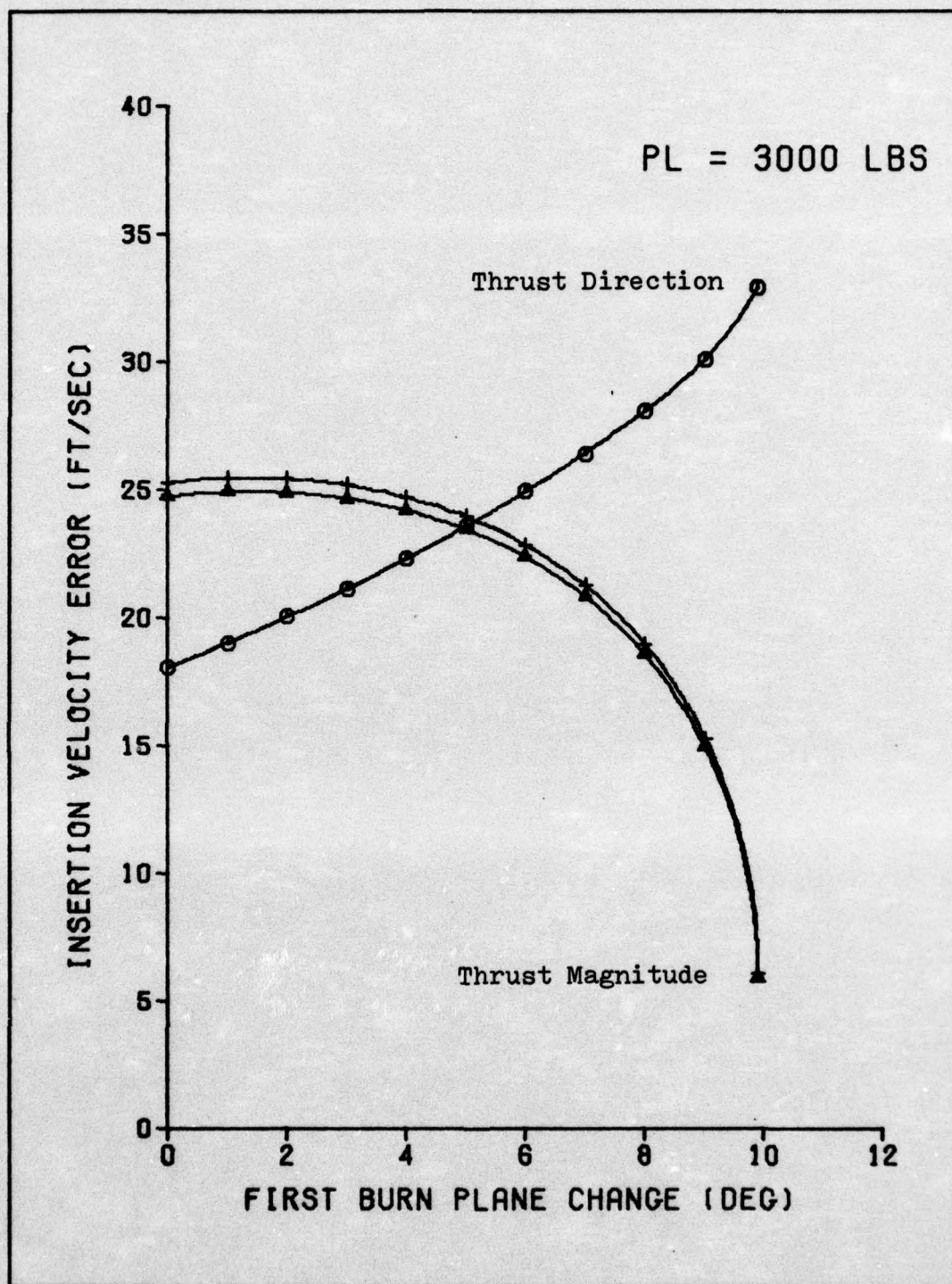


Figure 6-17. Geosynchronous Insertion Error Sensitivities (Velocity)
(PROP₁ = 20,000 lb, PL = 3000 lb)

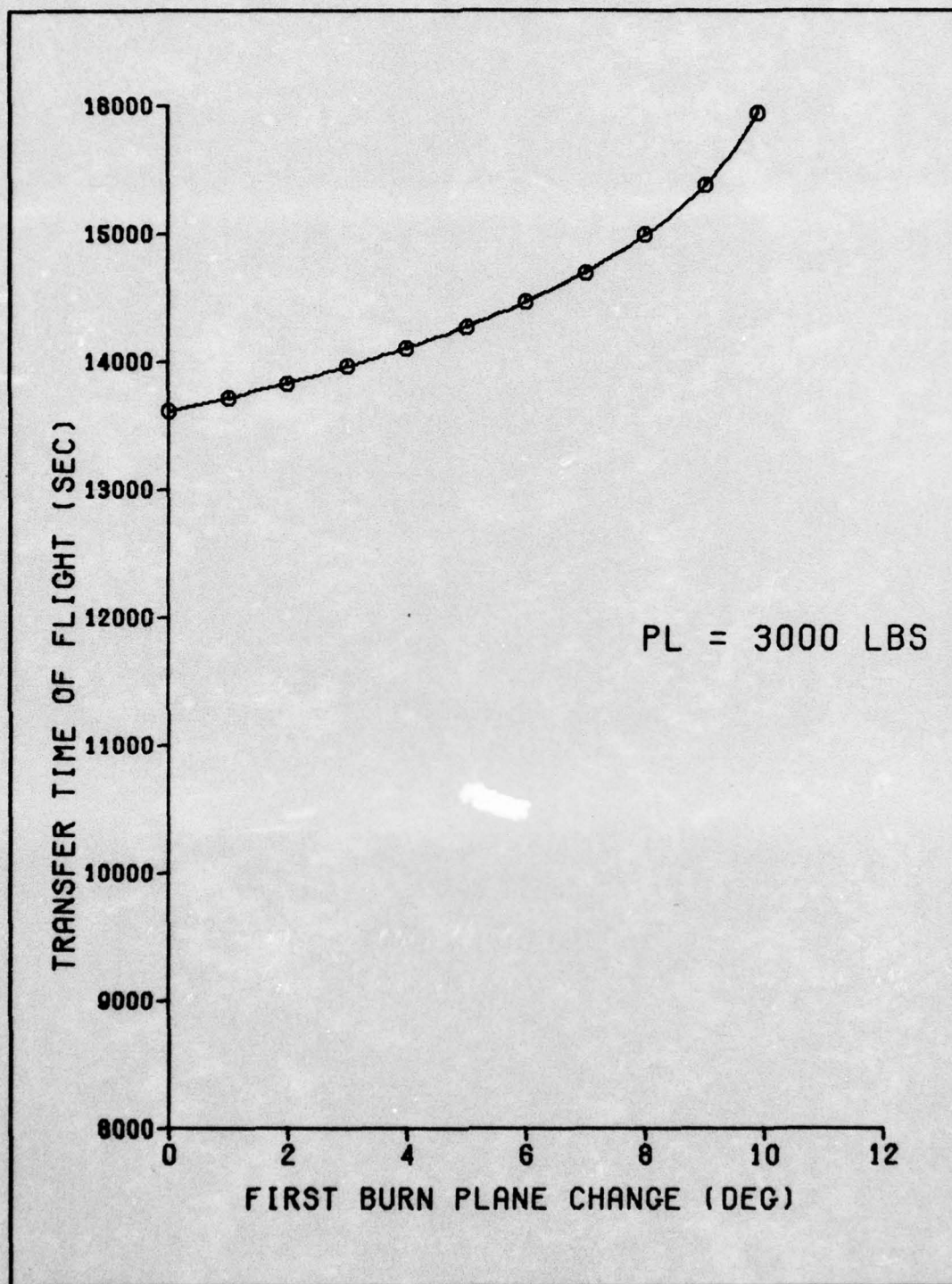


Figure 6-18. Geosynchronous Time of Flight
($PROP_1 = 20,000$ lb, $PL = 3000$ lb)

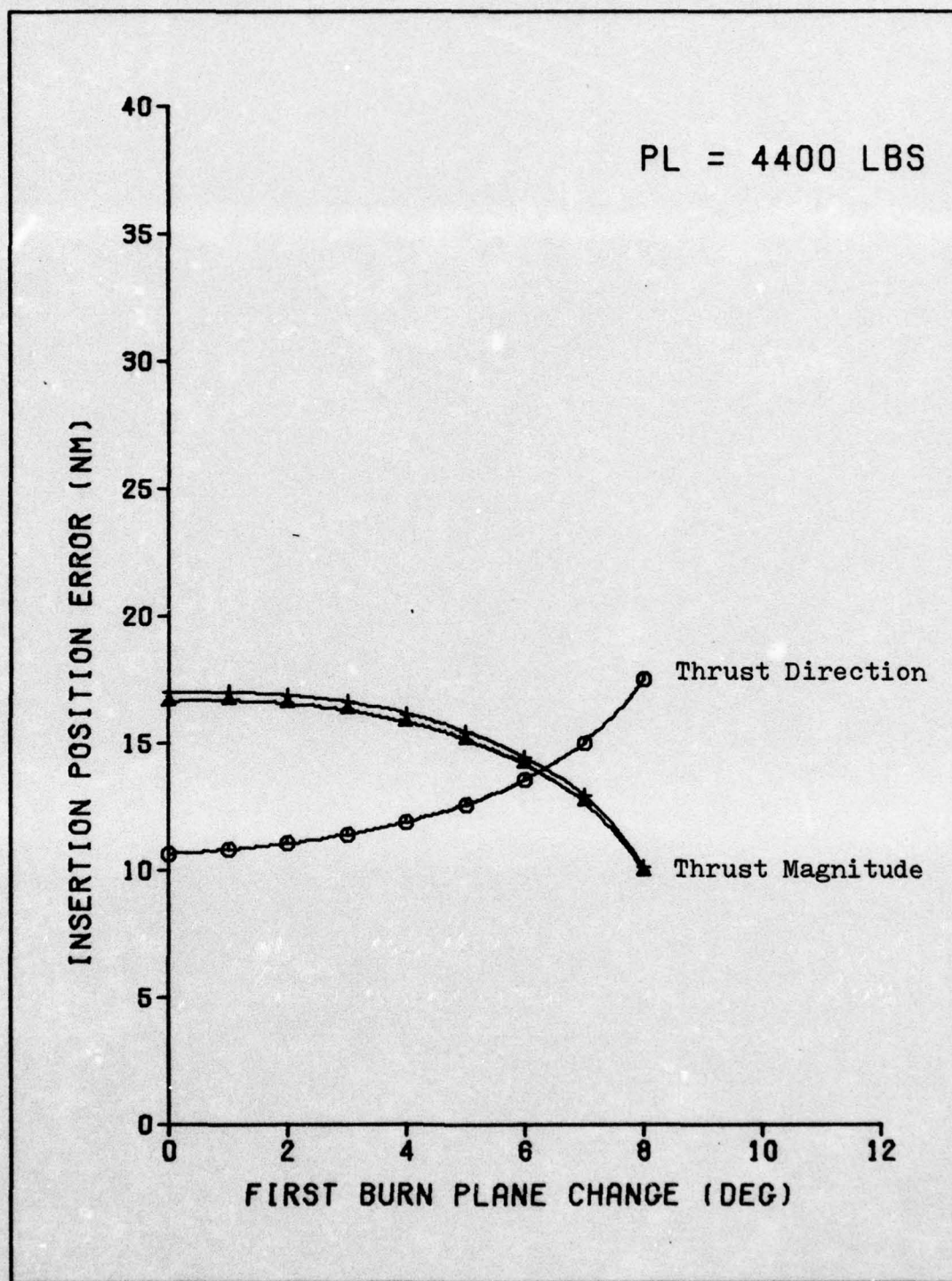


Figure 6-19. Subsynchronous Insertion Error
Sensitivities (Position)
(PROP₁ = 17,300 lb, PL = 4400 lb)

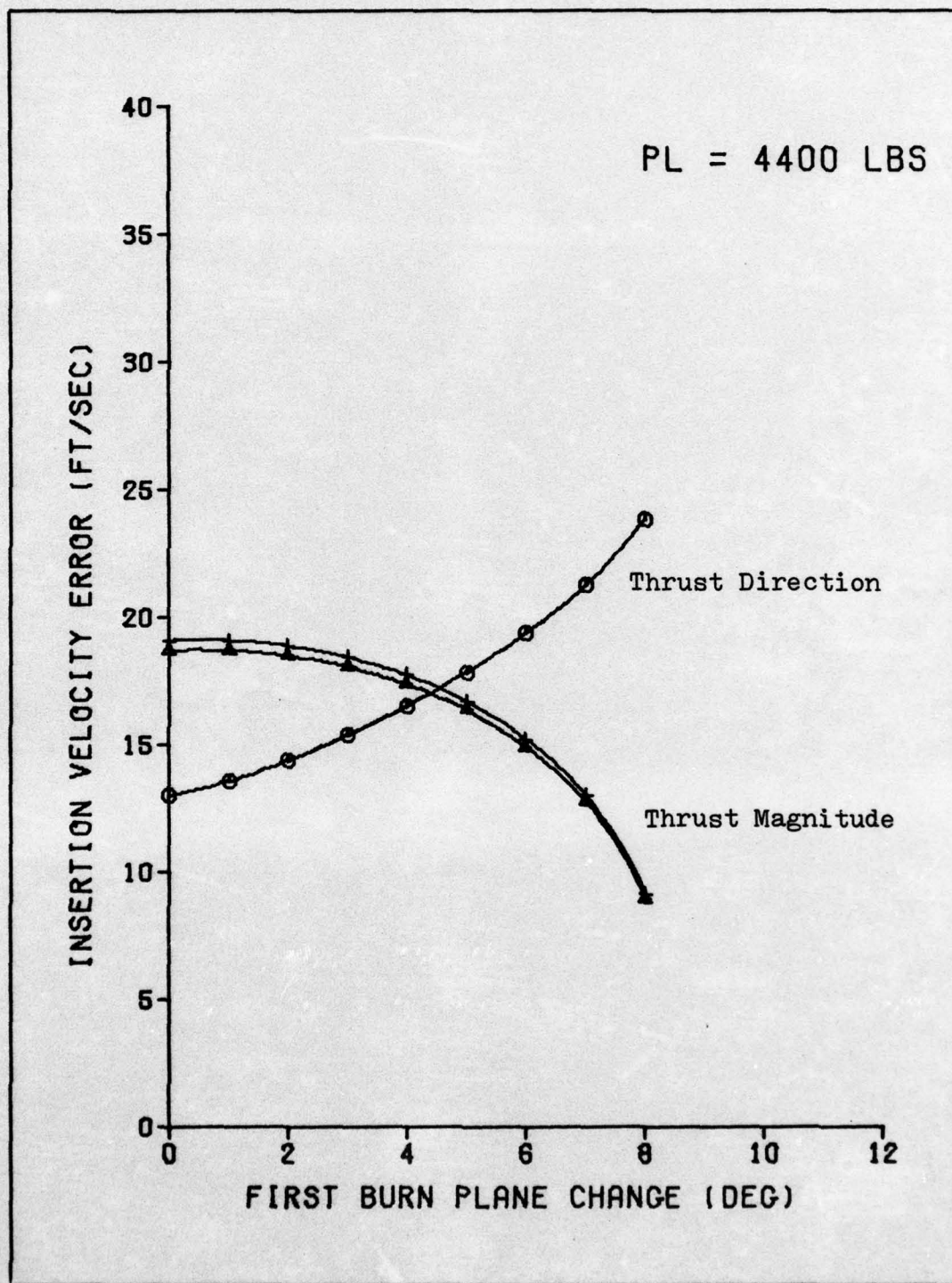


Figure 6-20. Subsynchronous Insertion Error Sensitivities (Velocity)
($PROP_1 \approx 17,300$ lb, PL = 4400 lb)

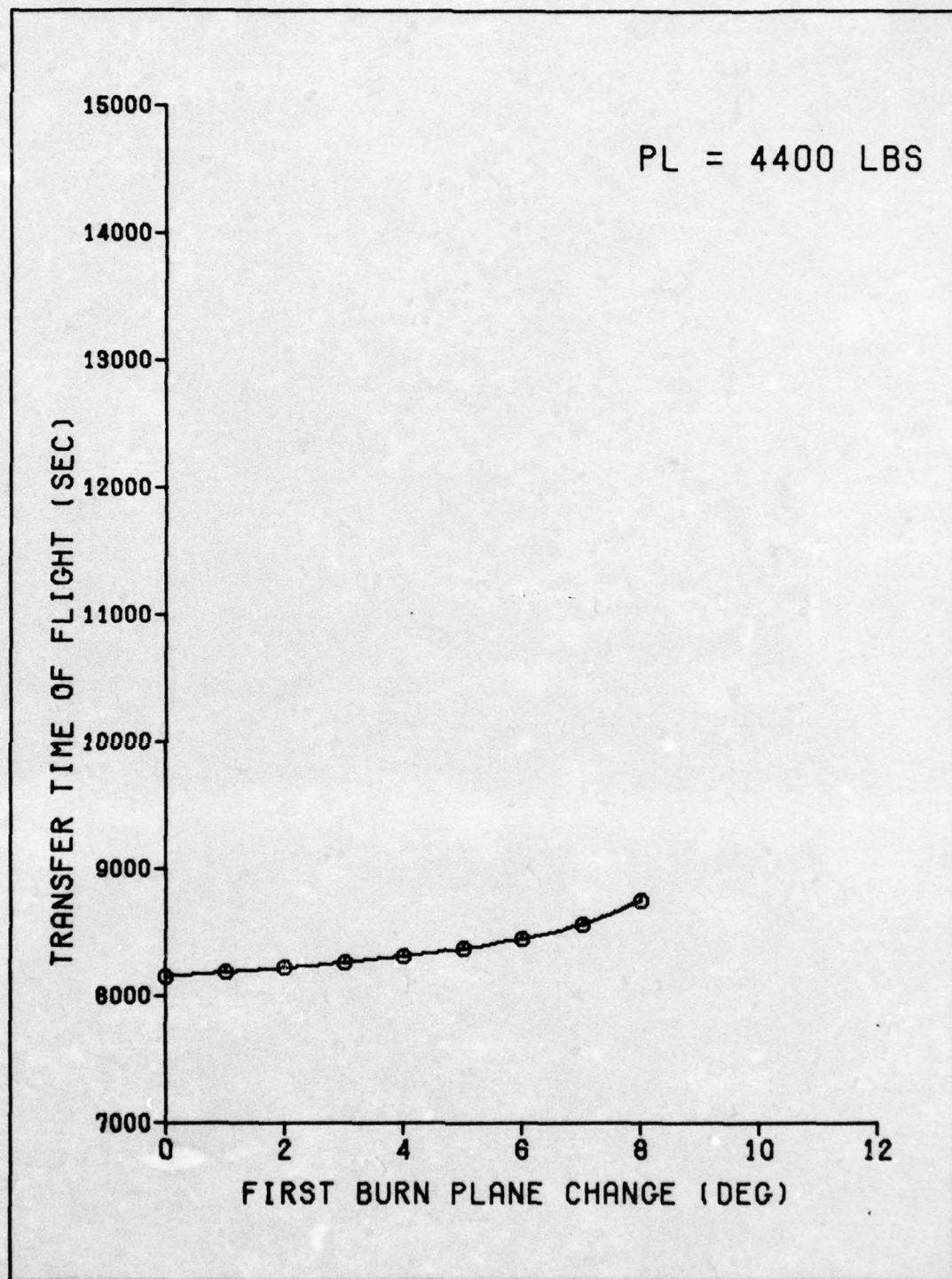


Figure 6-21. Subsynchronous Time of Flight
(PROP₁ = 17,300 lb, PL = 4400 lb)

AD-A034 005

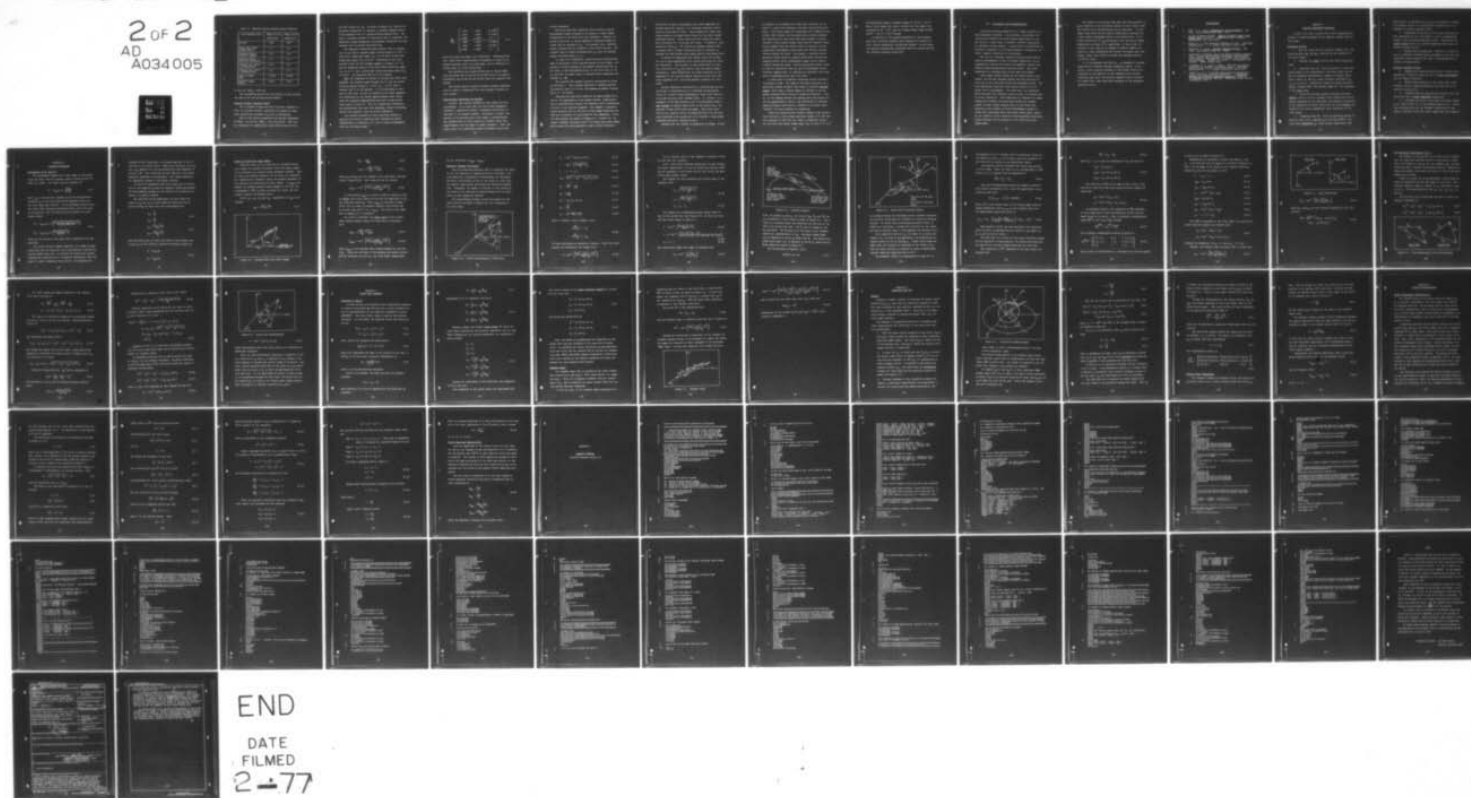
AIR FORCE INST OF TECH WRIGHT-PATTERSON AFB OHIO SCH--ETC F/G 22/3
AN ENERGY MANAGEMENT GUIDANCE SCHEME APPLICABLE TO THE INTERIM --ETC(U)
DEC 76 J L ROBERTS

UNCLASSIFIED

GA/EE/76-1

NL

2 OF 2
AD
A034005



END

DATE
FILMED
2-77

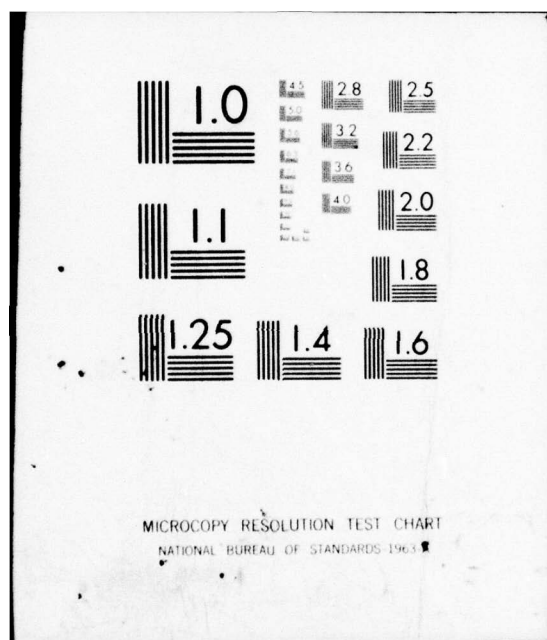


Table IV. Maximum Payload Geosynchronous Transfers

Fuel Loading (lbs)	PROP ₁ =17,300 PROP ₂ =4700	PROP ₁ =20,000 PROP ₂ =4700
Payload	4250	4600
First Burn Plane Change (deg.)	1.7	5.9
Insertion Error, Position (nm/mr)	11.4	36.0
Insertion Error, Velocity (ft/sec/mr)	9.1	21.5
Position Ins. Error, $\pm 1\%$ Thrust Dev.	21.0	32.4
Velocity Ins. Error $\pm 1\%$ Thrust Dev.	10.5	17.3
Time of Flight (sec)	18,954	18,440
Transfer Angle (deg.)	179.9	175.2

17,300 lbs, PROP₂ = 4700 lbs.

The retargeting period for this mission is 5427 seconds, the same as for the geosynchronous mission.

Transfer Between Coplanar Orbits

For a transfer between any two (circular) coplanar orbits, an in-plane transfer trajectory can always be found which matches any allowable ΔV_1 and ΔV_2 combination.

With an IUS vehicle propellant and payload combination of PROP₁ = 20,000 lbs, PROP₂ = 4700 lbs and PL = 3000 lbs, the consequent ΔV capabilities become 9443 ft/sec for ΔV_1 ,

and 7070 ft/sec for ΔV_2 . As shown in Figure 3-4, this is an allowable combination to complete a coplanar transfer from a 160 nm parking orbit to a geosynchronous mission orbit. Because a coplanar transfer is relatively easy to visualize, the applicable energy management (non-Hohmann) trajectory for this transfer will be briefly described here.

The impulsive trajectory which matches this ΔV combination is one with a transfer angle (central angle) of 140° , a first burn flight path angle (ψ_1) of 8.6° and a second burn flight path angle (ψ_3) of 44.5° . Referenced to the local inertial frame (as the transfer appears in Figure 3-1), impulsive targeting yields a first burn thrust direction angle (φ_1) of 57.7° , and a second burn thrust direction angle (φ_3) of -82.9° . The impulsive TOF is 12,107 seconds.

When the targeting is refined to include the finite burn dynamics, the transfer angle becomes 145.2° , and the thrust direction angles become $\varphi_1 = 62.8^\circ$, $\varphi_3 = -77.8^\circ$; with a transfer TOF of 12,230 seconds. It is interesting to note that in this case, as well as nearly all the cases targeted, the differences in the thrust angles between their values using the impulsive approximation and their actual finite burn values is about 5° . This is a significant difference, and demonstrates that open loop targeting, without including finite burn dynamics, would be wholly inadequate.

The accuracy analysis of this trajectory produced a position and velocity insertion error sensitivity matrix ($\partial M / \partial A L$ matrix of Equation 5-2), due to thrust misalignment, with the following values:

$$\frac{\partial M}{\partial AL} = \begin{bmatrix} .0047 & -.0019 & -12.1966 \\ -.0195 & -.0019 & 12.6168 \\ 3.6696 & -1.9258 & 0.0 \\ \hline .0080 & -.0010 & -2.4489 \\ -.0092 & -.0004 & 12.7996 \\ -7.0846 & -1.3990 & 0.0 \end{bmatrix} \quad (6-1)$$

where the units are nm/mr, and (ft/sec)/mr. Combining these into "worst case" sensitivities via Equation 5-7 gave an insertion position error of 17.548 nm/mr, and an insertion velocity error of 13.032 (ft/sec)/mr.

The insertion error sensitivities due to thrust magnitude deviations are 31.331 nm and 20.936 ft/sec for positive deviations; and 31.974 nm and 21.382 ft/sec for negative deviations.

The synodic period (interval between transfer opportunities to effect a rendezvous) for this coplanar transfer is 5791 seconds.

Observations Concerning the Results

Overall, the results obtained by this scheme are very encouraging. It is clear that for most energy management transfers a significant amount of targeting flexibility is available to the mission planner, allowing an "optimal" trajectory to be selected from a wide range of possibilities. The sensitivities to error inputs and transfer times vary significantly over the range of usable transfers. Thus, the final choice of a trajectory would be somewhat vehicle and

mission dependent.

The plots show that insertion errors caused by thrust misalignment always increase as the amount of plane change accomplished by the first burn (ψ_2) increases. However, insertion errors due to thrust magnitude deviations always decrease with an increase in ψ_2 . As a general rule, insertion errors increase with an increase in fuel and/or payload. The transfer time of flight increases with ψ_2 ; with the minimum always occurring where $\psi_2 = 0$.

In order to be meaningful, insertion error sensitivities must be multiplied by the expected amount of error input. Engineers currently working on IUS design indicate that the upper limit on IMU misalignment prior to the first burn is 1.8 mr, and that the upper bound on expected thrust magnitude variations is $\pm \frac{1}{2}\%$.

The required IUS orbital insertion accuracies are given in Reference 5. That document specifies a maximum permissible position error of ± 92 nm, and maximum allowable velocity error of ± 78 ft/sec.

Assuming the only error inputs to be those caused by errors in the application of the thrust vectors, trajectories can be selected which satisfy the insertion error requirements for each of the missions targeted. For example, a geosynchronous transfer with 17,300 lbs of first stage propellant and 3000 lbs of payload is a good baseline for comparison. Plots for this mission are shown in Figures 6-7, 6-8 and 6-9. By using a transfer trajectory with 0° of first burn plane change, and assuming the most pessimistic case in which insertion

errors due to thrust misalignment and thrust magnitude variations would add linearly, the resulting insertion errors would be 36 nm and 26 ft/sec. These figures are worst case values based on the upper bound values for the error inputs mentioned earlier. These errors are well within the allowable tolerances of ± 92 nm and ± 78 ft/sec. In addition, this trajectory (with $\psi_2 = 0^\circ$) yields the minimum transfer time. A minimum time of flight trajectory would be desirable to minimize the IMU platform gyro drift prior to the second burn.

It should be emphasized that thrust vector errors may not be the only significant error inputs affecting the transfer trajectory. Also present to some extent will be insertion errors due to I_{sp} and vehicle (fuel and inert) weight dispersions. These dispersions can cause variations in the magnitude of the velocity impulse applied by each burn (reference Equation 2-1), which was assumed invariant for this study.

Another important consideration in interpreting the sensitivities is determination of a realistic multiplication factor for overall thrust misalignment, which would take into account any gyro drift between burns. If, however, a realignment of the IMU platform could be accomplished using a star tracker or similar means prior to the second burn, the question of gyro drift would not apply. This would leave the velocity impulse errors (as described above) as the only other important error source yet to be applied to this scheme (assuming negligible modeling errors).

Staying with the concept of simplicity in design, it may

be possible to accomplish the burns open loop also, as opposed to closed loop (constant) attitude control during the burns. This would negate the requirement for a Thrust Vector Control (TVC) system, and any associated on-board software. The feasibility of open loop burns would depend on how accurately a fixed nozzle design could keep the applied thrust vector aligned with the vehicle center of gravity, as any significant misalignment would cause some vehicle attitude rotation during the burns. Here again, a realistic multiplication factor could be computed which would include the expected thrust vector misalignment caused by any vehicle rotation during the burns. This multiplication factor could be used in conjunction with the thrust misalignment sensitivities computed here, to indicate the insertion error that would be associated with open loop burns.

A final point of interest concerning mission flexibility should be made. The range of transfers available for a particular mission allows a wide range of possible transfer angles, which adds a limited degree of freedom to non-coplanar transfers which involve a rendezvous maneuver. That is, if the phasing between the parking orbit and mission orbit was approximately correct, the flexibility in transfer angles available would allow a transfer to be chosen which "matches" the exact phasing for rendezvous.

Using the geosynchronous transfer example cited earlier, which involved a first stage propellant weight of 17,300 lbs and a payload of 3000 lbs, the range of admissible values for the first burn plane change angle (ψ_2) is from 0° to 5.9° .

The associated range of transfer angles is $157.0^{\circ} - 172.3^{\circ}$. With a first stage fuel load of 20,000 lbs. the range of ψ_2 increases to $0^{\circ} - 9.9^{\circ}$, and the transfer angle range becomes $148.9^{\circ} - 176.3^{\circ}$; a 27.4° spread.

In addition to the missions presented in this chapter, many other possible transfers were targeted for various orbits, vehicle parameters, and payload weights. In all cases the results obtained were consistent with the results for the two reference missions shown here.

VII. Conclusions and Recommendations

Trajectory matching appears to be a highly effective energy management technique. By selecting a non-Hohmann trajectory which matches the fixed energy capabilities of the IUS vehicle, a wide range of possible transfer trajectories is available for any mission. A great deal of flexibility is, therefore, available to the mission planner, allowing an "optimal" transfer trajectory to be selected.

The use of a nonlinear equation solving routine was extremely advantageous in that it allowed targeting to be accomplished to include the finite burn dynamics, without any inherent algorithm-generated insertion error. This exact targeting is a necessary part of the open loop design.

Using upper bounded values for the thrust vector error inputs, the accuracy analysis showed that the insertion errors were in all cases well within the allowable limits. The most significant insertion error source turned out to be thrust vector misalignment. For this case, the trajectory which minimizes the insertion errors is also the minimum time of flight trajectory. This trajectory is obtained by a plane change split between the burns which places the minimum amount of plane change (usually zero) in the first burn. Insertion errors caused by thrust misalignment always increase with increasing first burn plane change angle, whereas the insertion errors caused by thrust magnitude deviations always decrease with an increase in the first burn plane change angle.

The results of this study show that open loop guidance is quite feasible if the additional effects of error inputs other than thrust vector perturbations can be controlled. In this regard, gyro drift errors could be effectively eliminated by a star tracker realignment prior to the second burn. If insertion errors due to I_{sp} and vehicle (fuel and inert) weight dispersions are found to be significant, it may be more economical in the long run to attempt to achieve tighter tolerances on these dispersions and utilize the simple open loop design, rather than invest in closed loop software and RCS correction burns.

It is recommended that this study be extended to include targeting for transfers between elliptical orbits. In addition, a more rigorous analysis of this scheme could be accomplished by the addition of the remaining error sources (primarily gyro drift and velocity impulse errors) followed by a Monte Carlo type statistical analysis of the subsequent insertion errors.

Bibliography

1. Bate, R. R., et al. Fundamentals of Astrodynamics. New York: Dover Publications, Inc., 1971.
2. Boeing Aerospace Company. Burner II Interim Upper Stage System Study, Volume II. SAMSO TR-75-180. Seattle, Washington: BAC, July 1975.
3. Brand, T. J. "Fuel Depletion Guidance for IUS". Cambridge, Massachusetts: C. S. Draper Laboratory, April 1976.
4. Carnahan, B., et al. Applied Numerical Methods. New York: John Wiley & Sons, Inc., 1969.
5. Department of Defense, Space and Missile Systems Organization. "System Specification Performance and Design Requirements for the Department of Defense Space Transportation System". SS-STC-100, Volume 3. Los Angeles, California: SAMSO, January 1976.
6. Kriegsman, B. A. and K. B. Mahar, "IMU Accuracy Requirements for Two Possible IUS Mission Types". Cambridge, Massachusetts: C. S. Draper Laboratory, March 1976.
7. Powell, M. J. D. "A Fortran Subroutine for Solving Systems of Nonlinear Algebraic Equations." in Numerical Methods for Nonlinear Algebraic Equations, edited by P. Rabinowitz, et al. New York: Gordon and Breach Science Publishers, 1972.

Appendix A

Computer Simulation Algorithm

A verbal flow chart is given here, which summarizes the sequence of steps performed by the computer program used for this study.

Targeting Portion

1. From the input data (as listed in Chapter II), computes available ΔV_1 and ΔV_2 ; corrects ΔV_1 for estimated finite burn losses.
2. Computes the range of first burn plane change possible.
3. Targeting step one: Sets the amount of first burn plane change to be accomplished to the lower limit, and using the impulsive approximation, targets a transfer trajectory to match ΔV_1 and ΔV_2 , which satisfies constraints i_T , r_2 , V_2 , i_2 and e_2 . Results are values for thrust direction angles, transfer TOF*, and transfer angle TA*, all expressed in the local frame.
4. Using the nonlinear equation solving subroutine (NS01A), with its initial guesses as the values from the impulsive targeting of the last step, and numerical integration of the equations of motion, solves for the actual finite burn values of the control parameters, still referenced to the local frame.
5. Targeting step two: From the specified orbital elements of each orbit, computes $\bar{r}_{1C}(t)$ and $\bar{r}_{2C}(t+TOF^*)$, and from these determines t_{b1} (first mission opportunity time

after epoch), to satisfy either Ω_2 if the transfer is between non-coplanar orbits, or to satisfy TA^* (rendezvous) if the transfer is between coplanar orbits.

6. Transforms the values for the thrust direction angles (expressed in the local frame) to their corresponding values in the geocentric-equatorial frame. Outputs are the actual values for the six control parameters which would be stored on-board the IUS.

7. Mission Delay retargeting: Computes the values of the six targeting constants which correspond to the next four sequential mission opportunity times, using appropriate coordinate transformations.

Accuracy Analysis Portion

8. Computes the insertion position and velocity error sensitivity coefficient matrices due to thrust misalignment, for the target trajectory.

9. Reduces these matrices to two "worst case" sensitivities, one for insertion position error and one for insertion velocity error.

10. Computes insertion position and velocity error sensitivities due to thrust magnitude fluxuations.

11. Increases the value of the first burn plane change by 1° , then returns to (1) and repeats steps (1-10). Continues iterating until all the transfer trajectories in the range of possible first burn plane change have been targeted.

Appendix B

Trajectory Matching

Calculation of ΔV_1 and ΔV_2

The performance capability of each stage is calculated using the ideal velocity equation, with a correction for finite burn losses. The ideal velocity equation is:

$$\Delta V = I_{sp} g_0 \ln \left(\frac{m_0}{m_f} \right) \quad (2-1)$$

where I_{sp} is the specific impulse; g_0 is the gravitational constant; m_0 is the total mass before ignition; and m_f is the total mass after burnout. If ST represents vehicle structure mass, PROP represents propellant mass, and PL the mass of the payload, then the ideal velocity equation for each stage becomes:

$$\Delta V_1 = I_{sp1} g_0 \ln \left(\frac{ST_1 + PROP_1 + ST_2 + PROP_2 + PL}{ST_1 + ST_2 + PROP_2 + PL} \right) \quad (B-1)$$

$$\Delta V_2 = I_{sp2} g_0 \ln \left(\frac{ST_2 + PROP_2 + PL}{ST_2 + PL} \right)$$

where all the values on the right side of Equation (B-1) are specified.

The actual velocity change capability of a stage is something less than the ideal ΔV , due to gravitational effects during the finite burn time. To account for finite burn losses, trajectories resulting from a ΔV applied impulsively, were compared to actual integrated trajectories. By comparing the

energies of each trajectory, an estimate was made of the ΔV loss due to the finite burns. Using this technique, the loss for a ΔV_1 applied in a 160 nm parking orbit was estimated to be about .1%. This correction is then applied to ΔV_1 before impulsive targeting is accomplished. The losses during ΔV_2 are negligible because of the higher altitude.

It should be emphasized that this correction for finite loss is only applied to help the impulsive targeting generate the best possible guesses for the values of the mission variables to be given to NSOLA.

For specified thrust magnitudes, the burn times (denoted by t_{ba} and t_{bb}) of each stage are fixed and are obtained through the mass flow rate relationships as:

$$\dot{m}_1 = \frac{T_1}{c_1} \quad (B-2)$$

$$\dot{m}_2 = \frac{T_2}{c_2}$$

$$t_{ba} = \frac{m_{01} - m_{f1}}{\dot{m}_1} \quad (B-3)$$

$$t_{bb} = \frac{m_{02} - m_{f2}}{\dot{m}_2}$$

where \dot{m}_1 and \dot{m}_2 are the mass flow rates of each engine; and c_1 and c_2 are the effective exhaust velocities as given by

$$c_1 = I_{sp1} g_0 \quad (B-4)$$

$$c_2 = I_{sp2} g_0$$

Limits of First Burn Plane Change

Using the value of ΔV_1 corrected for estimated finite burn losses, the maximum attainable first burn plane change is one followed by a minimum energy (Hohmann) transfer. That is, using the minimum component (of the total ΔV_1 available) for completing the transfer, leaves the maximum component of ΔV_1 available for executing the plane change. If $\psi_{2\max}$ represents the maximum possible plane change by burn one, its relationship to $\overline{\Delta V_1}$ is shown in Figure B-1, where the subscript H denotes the Hohmann value.

Given r_{1C} , r_{2C} , V_{1C} and V_{2C} , computation of V_{1TH} is as follows:

$$a_{TH} = \frac{r_{1T} + r_{2T}}{2} \quad (B-5)$$

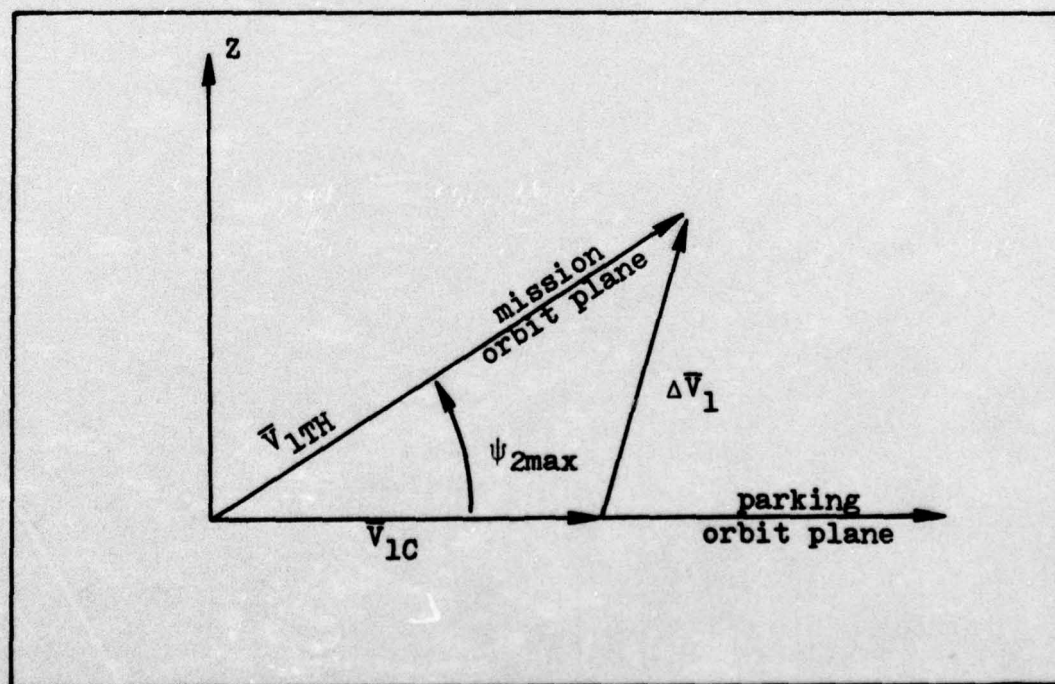


Figure B-1. Maximum First Burn Plane Change

$$E_{TH} = \frac{-\mu}{2a_{TH}} \quad (B-6)$$

$$V_{1TH} = \sqrt{\frac{2\mu}{r_{1T}} + 2 E_{TH}} \quad (B-7)$$

where a_{TH} and E_{TH} are the transfer orbit semi-major axis and energy, respectively. Then using the law of cosines:

$$\psi_{2max} = \cos^{-1} \left[\frac{V_{1C}^2 + V_{1TH}^2 + \Delta V_1^2}{2 V_{1C} V_{1TH}} \right] \quad (B-8)$$

In calculating ψ_{2max} no effort is made in trying to find an actual value which takes into account the magnitude of ΔV_2 and trajectory matching. Thus, ψ_{2max} is strictly an upper limit, and the range of possible transfer trajectories can be no more than for $0^\circ < \psi_2 < \psi_{2max}$. This then is the range that is sampled at 1° intervals.

As a note of interest, the upper limit of the overall plane change possible using both burns may be determined from:

$$V_{2TH} = \sqrt{\frac{2\mu}{r_{2T}} + 2 E_{TH}} \quad (B-9)$$

$$\psi_{4max} = \cos^{-1} \left[\frac{V_{2C}^2 + V_{2TH}^2 - \Delta V_2^2}{2 V_{2C} V_{2TH}} \right] \quad (B-10)$$

where ψ_{4max} is the maximum plane change possible by burn two (ΔV_2). Given the altitudes of the parking and mission orbits, and the available ΔV_1 and ΔV_2 , the total plane change possi-

ble is, therefore, $(\psi_{2\max} + \psi_{4\max})$.

Impulsive Transfer Derivation

Here the governing equations used in targeting the transfer for the impulsive ΔV approximation are developed. Numerous spherical trigonometric relationships are necessary, and their verification is left to the reader in order that the logical steps remain uncluttered by extraneous explanation. Similarly, the reader is referred to the listing in the front of the book and the various Figures for an explanation of any unfamiliar notation.

The relationships between vectors and angles for the first burn are as shown in Figure B-2, all referenced to the local frame.

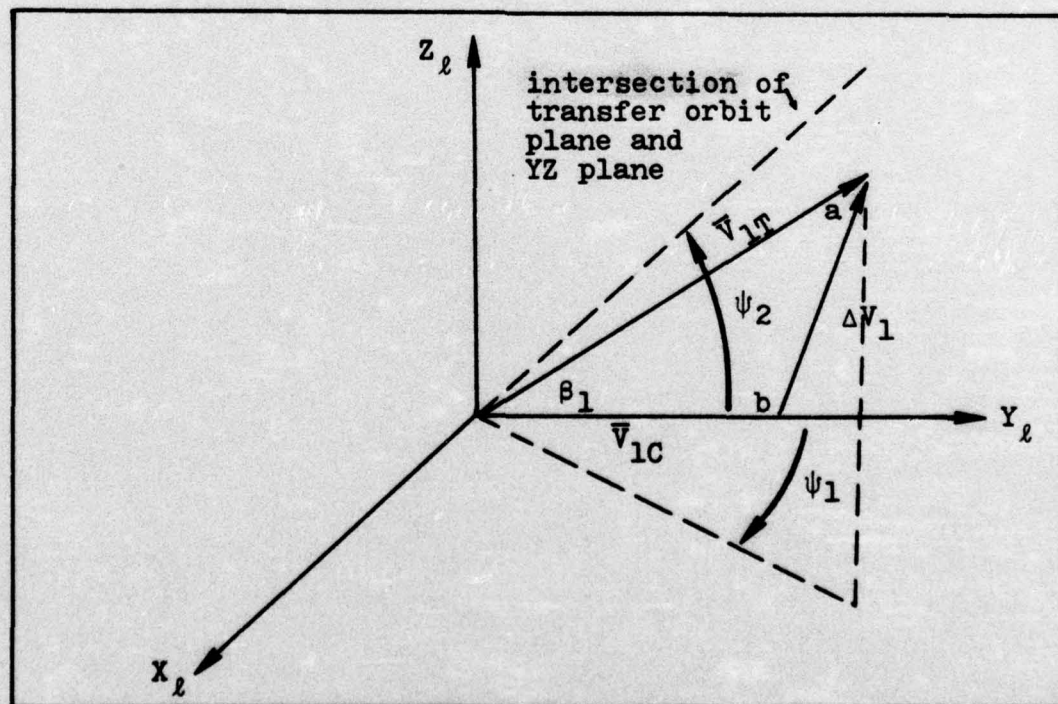


Figure B-2. Vector Relationships at First Burn

$$\beta_1 = \cos^{-1} (\cos \psi_2 \cos \psi_1) \quad (B-11)$$

$$a = \sin^{-1} \left[\frac{V_{1C} \sin \beta_1}{\Delta V_1} \right] \quad (B-12)$$

$$b = \pi - a - \beta_1 \quad (B-13)$$

$$V_{1T} = \sqrt{\Delta V_1^2 + V_{1C}^2 - 2V_{1C} \Delta V_1 \cos b} \quad (B-14)$$

$$E_T = \frac{V_{1T}^2}{2} - \frac{\mu}{r_{1T}} \quad (B-15)$$

$$a_T = \frac{-\mu}{2E_T} \quad (B-16)$$

$$h_T = r_{1T} V_{1T} \cos \psi_1 \quad (B-17)$$

$$p_T = \frac{h_T^2}{\mu} \quad (B-18)$$

$$e_T = \sqrt{1 - (p_T / a_T)} \quad (B-19)$$

Check to assure a valid transfer orbit:

$$\frac{p_T}{1 + e_T} \leq r_{1C} \quad (B-20)$$

$$\frac{p_T}{1 - e_T} \geq r_{2C}$$

If both conditions are satisfied, continue. Check for valid second burn conditions (see Figure B-6):

$$w = \cos^{-1} \left[\frac{V_{2T}^2 + V_{2C}^2 - \Delta V_2^2}{2V_{2T} V_{2C}} \right] \quad (B-21)$$

If the absolute value of the argument of Equation (B-21) is less than one, continue.

Note: Other quite numerous checks must be made throughout these computations, but are not shown here (mainly checking the arguments of arc-cosine and arc-sine terms, and quantities under square roots).

Now compute the true anomalies and central angle of the transfer orbit:

$$v_1 = \sqrt{\frac{(p_T / r_{1T}) - 1}{e_T}} \quad (B-22)$$

$$v_2 = \sqrt{\frac{(p_T / r_{2T}) - 1}{e_T}}$$

$$C_a = v_2 - v_1 \quad (B-23)$$

Now compute the corresponding plane change required (ψ_4) at the second burn (see Figure B-3), so that the total two burn plane change is equal to θ .

$$d = \sin^{-1} \left[\frac{\sin \psi_2 \sin C_a}{\sin \theta} \right] \quad (B-24)$$

$$c = 2 \tan^{-1} \left[\frac{\cos [1/2 (C_a - d)]}{\cos [1/2 (C_a + d)] \tan [1/2 (\theta + \psi_2)]} \right] \quad (B-25)$$

$$\psi_4 = \pi - c \quad (B-26)$$

The second burn flight path angle is obtained from

$$\psi_3 = \cos^{-1} \left[\frac{h_T}{r_{2T} v_{2T}} \right] \quad (B-27)$$

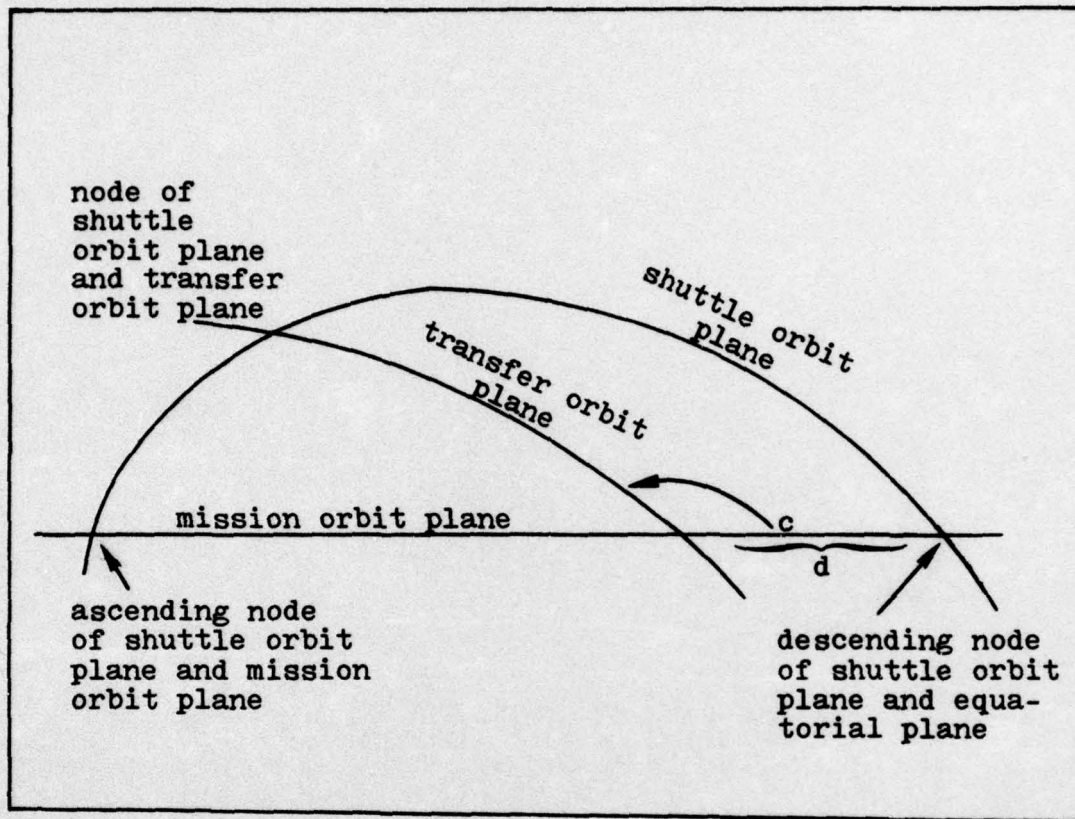


Figure B-3. Transfer Geometry

Here, the angles ψ_4 and ψ_3 , the vectors \bar{V}_{2T} , \bar{V}_{2C} and $\Delta\bar{V}_2$ are all referenced to the \hat{e} frame as shown in Figure B-4. The \hat{e} frame is a rotating frame that describes the position of the IUS at the second burn time. The \hat{e}_r axis is always in the \bar{r}_{2T} direction. The \hat{e}_θ axis is in the plane of the transfer trajectory, perpendicular to \bar{r}_{2T} . The plane change angle (ψ_4) is measured in the $\hat{e}_\theta \hat{e}_z$ plane from \hat{e}_θ . The second burn flight path angle (ψ_3) is measured in the $\hat{e}_r \hat{e}_\theta$ plane from \hat{e}_θ . These angles are shown in Figure B-4.

The relationship of Equation (3-1),

$$\Delta V_2(\Delta V_1, \psi_1, \psi_2) \quad (3-1)$$

relationships of (B-11) through (B-27) to determine values for the angles ψ_3 and ψ_4 in the \hat{e} frame, which are generated by each value of ψ_1 during the one-dimensional search.

The angles ψ_3 and ψ_4 establish the vectors \bar{V}_{2C} and \bar{V}_{2T} in the \hat{e} frame. Thus, the value of ΔV_2 corresponding to that value of ψ_1 is obtained from the magnitude of

$$\overline{\Delta V_2} = \bar{V}_{2C} - \bar{V}_{2T} \quad (B-28)$$

Once the one-dimensional search has roughly bracketed the solution to Equation (2-2), then the Regula-Falsi iterations are used until

$$\left| \Delta V_{2 \ k+1} - \Delta V_2^* \right| < \text{ACCURACY} \quad (B-29)$$

where ΔV_2^* is the actual value of the second stage velocity change capability, and $\Delta V_{2 \ k+1}$ is the iterated value from the Regula-Falsi algorithm, which is

$$\psi_{k+1} = \psi_k - \left[\frac{\psi_k - \psi_{k-1}}{\Delta V_2(\psi_k) - \Delta V_2(\psi_{k-1})} \right] (\Delta V_{2k} - \Delta V_2^*) \quad (B-30)$$

When Equation (B-29) has been satisfied, the trajectory match has been accomplished and the values of the angles ψ_1 , ψ_2 , ψ_3 and ψ_4 are all known.

The last step is to solve for the thrust direction angles. For the impulsive ΔV approximation, the thrust directions are the same as the velocity change directions for each burn.

The components of $\overline{\Delta V_1}$ (expressed in the XYZ_ℓ frame) are obtained from

$$\overline{\Delta V}_1 = \overline{V}_{1T} - \overline{V}_{1C} \quad (B-31)$$

where $\overline{V}_{1C} = V_{1C} \bar{j}$; and the components of \overline{V}_{1T} are given by

$$\begin{aligned} V_{1TX} &= V_{1T} \sin \psi_1 \\ V_{1TY} &= V_{1T} \cos \psi_1 \cos \psi_2 \\ V_{1TZ} &= V_{1T} \cos \psi_1 \sin \psi_2 \end{aligned} \quad (B-32)$$

The direction of $\overline{\Delta V}_1$ is the same as that of \overline{T}_1 in Figure 4-2, so that the first burn thrust direction angles are found from

$$\begin{aligned} \varphi_2 &= \sin^{-1} (\Delta V_{1Z} / \Delta V_1) \\ \varphi_1 &= \sin^{-1} (\Delta V_{1Y} / \Delta V_1 \cos \varphi_2) \end{aligned} \quad (B-33)$$

In analogous fashion, the components of $\overline{\Delta V}_2$ expressed in the \hat{e} frame may be found from Equation (B-28), and the known values of ψ_3 and ψ_4 . Then a coordinate transformation takes $\overline{\Delta V}_2^{\hat{e}}$ to the local frame through

$$\overline{\Delta V}_2^{XYZ}_l = C_{\hat{e}}^{XYZ}_l \overline{\Delta V}_2^{\hat{e}} \quad (B-34)$$

The coordinate transformation matrix is given by

$$C_{\hat{e}}^{XYZ}_l = \begin{bmatrix} c \gamma_2 c \gamma_1 & -s \gamma_2 & -c \gamma_2 s \gamma_1 \\ s \gamma_2 c \gamma_1 & c \gamma_2 & -s \gamma_2 s \gamma_1 \\ s \gamma_1 & 0 & c \gamma_1 \end{bmatrix} \quad (B-35)$$

where cosine is abbreviated as c, and sine as s; and the angles

γ_1 and γ_2 are as shown in Figure B-4.

Manipulation is necessary to obtain the angles γ_1 and γ_2 . A top and side view of Figure B-4 is shown in Figure B-5. Here α is the angle in the plane of the transfer trajectory between \bar{r}_{2C} and the $Y_\ell Z_\ell$ plane, so that

$$\alpha = C_a - \pi / 2 \quad (B-36)$$

$$r_{2TP} = r_{2T} \cos \alpha \quad (B-37)$$

$$r_{2Z} = r_{2TP} \sin \psi_2 \quad (B-38)$$

$$\gamma_1 = \sin^{-1} (r_{2Z} / r_{2T}) \quad (B-39)$$

$$r_{2XY} = r_{2T} \cos \gamma_1 \quad (B-40)$$

$$r_{2Y} = r_{2TP} \cos \psi_2 \quad (B-41)$$

$$\gamma_{2P} = \cos^{-1} (r_{2Y} / r_{2XY}) \quad (B-42)$$

$$\gamma_2 = \pi / 2 + \gamma_{2P} \quad (B-43)$$

Once $\overline{\Delta V}_2$ is expressed in the local frame, the second burn thrust direction angles are obtained from:

$$\varphi_4 = \sin^{-1} (\Delta V_{2Z} / \Delta V_2) \quad (B-44)$$

$$\varphi_3 = \sin^{-1} (\Delta V_{2Y} / \Delta V_2 \cos \varphi_4)$$

Checking for ambiguity, if $\varphi_3 < 0$, then $\varphi_3 = -(\pi + \varphi_3)$.

Finally, the transfer time of flight, TOF, is found from:

$$E_{c1} = \cos^{-1} \left[\frac{e_T + \cos \gamma_1}{1 + e_T \cos \gamma_1} \right] \quad (B-45)$$

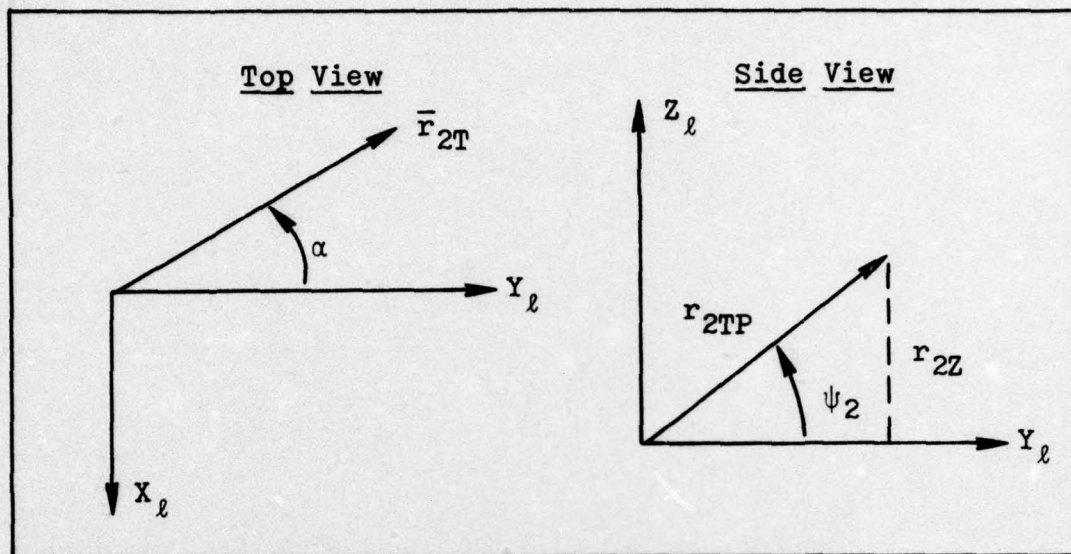


Figure B-5. Angle Definitions

$$E_{c2} = \cos^{-1} \left[\frac{e_T + \cos v_2}{1 + e_T \cos v_2} \right] \quad (B-45)$$

where E_{c1} and E_{c2} are the eccentric anomalies at burn one and two.

$$\begin{aligned} \text{TOF} = \sqrt{a_T^3 / \mu} [& (E_{c2} - e_T \sin E_{c2}) \\ & - (E_{c1} - e_T \sin E_{c1})] \end{aligned} \quad (B-46)$$

The Functional Relationship $\Delta V_2(\psi_1)$

The purpose of this section is to yield further insight into the trajectory matching concept by developing a closed form relationship for $\Delta V_2(\psi_1)$ for the coplanar case, and demonstrating that a similar relationship holds for transfers between non-coplanar orbits when the amount of first burn plane change (ψ_2) is fixed.

Figure B-6 shows the three-dimensional relationships between the associated vectors and angles at each burn. For a coplanar transfer, angle β_1 reduces to ψ_1 , and angle w reduces to ψ_3 . The known quantities are r_{1T} , r_{2T} , V_{1C} , V_{2C} , ΔV_1 and ΔV_2 .

The velocities are related thru the law of cosines (for coplanar transfers) as

$$\Delta V_1^2 = V_{1T}^2 + V_{1C}^2 - 2 V_{1T} V_{1C} \cos \psi_1 \quad (B-47)$$

$$\Delta V_2^2 = V_{2T}^2 + V_{2C}^2 - 2 V_{2T} V_{2C} \cos \psi_3 \quad (B-48)$$

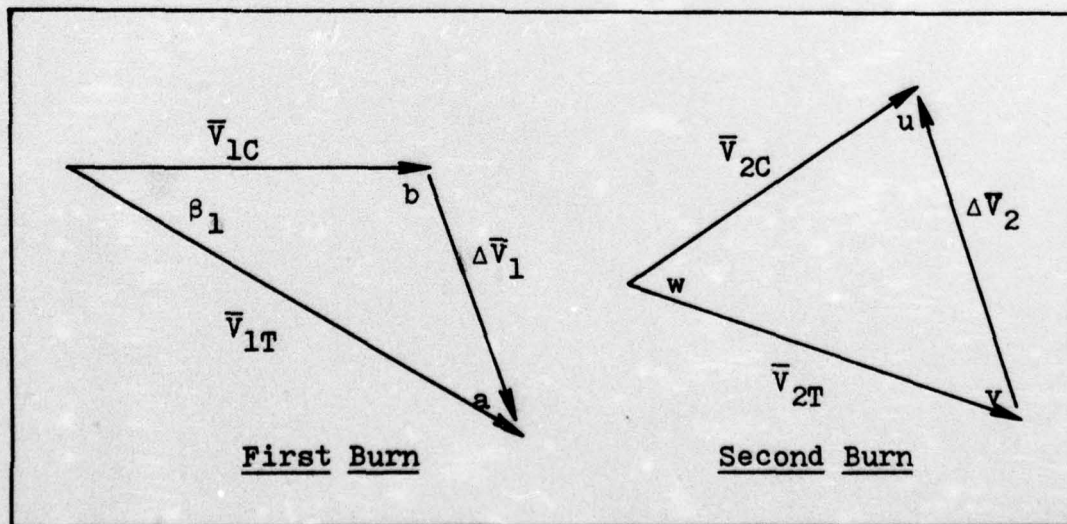


Figure B-6. Three-Dimensional Vector Relationships

The total energy and angular momentum of the transfer orbit may be written as

$$E_T = \frac{V_{1T}^2}{2} - \frac{\mu}{r_{1T}} = \frac{V_{2T}^2}{2} - \frac{\mu}{r_{2T}} \quad (B-49)$$

$$h_T = r_{1T} V_{1T} \cos \psi_1 = r_{2T} V_{2T} \cos \psi_3 \quad (B-50)$$

The task is to develop an analytical relationship between ΔV_2 and ψ_1 , with ψ_1 as the only unknown. Rewriting Equation (B-47) as

$$V_{1T}^2 - 2 V_{1T} V_{1C} \cos \psi_1 = \Delta V_1^2 - V_{1C}^2 \quad (B-51)$$

and completing the squares gives

$$(V_{1T} - V_{1C} \cos \psi_1)^2 = \Delta V_1^2 - V_{1C}^2 + V_{1C}^2 \cos^2 \psi_1 \quad (B-52)$$

Now taking the square root of both sides, using geometrical arguments to determine the proper choice of signs, gives V_{1T} as a function of ψ_1 only:

$$V_{1T} = V_{1C} \cos \psi_1 + \sqrt{\Delta V_1^2 - V_{1C}^2 + V_{1C}^2 \cos^2 \psi_1} \quad (B-53)$$

Using the energy equation, V_{2T}^2 may be expressed as

$$V_{2T}^2 = \frac{2\mu}{r_{2T}} - \frac{2\mu}{r_{1T}} + V_{1T}^2 \quad (B-54)$$

and solving for $\cos \psi_3$ from the angular momentum equation gives

$$\cos \psi_3 = \frac{r_{1T} V_{1T} \cos \psi_1}{r_{2T} V_{2T}} \quad (B-55)$$

Substitution of Equation (B-55) into (B-48) yields

$$\Delta V_2^2 = V_{2T}^2 + V_{2C}^2 - \frac{2 V_{2C} r_{1T} V_{1T} \cos \psi_1}{r_{2T}} \quad (B-56)$$

Finally, Equations (B-53) and (B-54) are used in (B-56) to produce (after tedious manipulation) the desired result of ΔV_2 as a function of ψ_1 only:

$$\begin{aligned} \Delta V_2(\psi_1) = \sqrt{[2 \mu + 2 \cos \psi_1 \{V_{1C}^2 r_{2T} \cos \psi_1 \\ - V_{1C} V_{2C} r_{1T} + \sqrt{\Delta V_1^2 - V_{1C}^2 + V_{1C}^2 \cos \psi_1} \\ (V_{1C} r_{2T} - V_{2C} r_{1T})\}/r_{2T}] - (2 \mu/r_{1T}) \\ + \Delta V_1^2]} \quad (B-57) \end{aligned}$$

Equation (B-57) is a closed form relationship between the first burn flight path angle and the second burn velocity change for coplanar orbits.

An analogous procedure can be used to derive the form of $\Delta V_2(\psi_1)$ for non-coplanar transfers. The major difference is that now Equations (B-47) and (B-48) become the three dimensional relationships

$$\Delta V_1^2 = V_{1T}^2 + V_{1C}^2 - 2 V_{1T} V_{1C} \cos \beta_1 \quad (B-58)$$

$$\Delta V_2^2 = V_{2T}^2 + V_{2C}^2 - 2 V_{2T} V_{2C} \cos w \quad (B-59)$$

where β_1 and w are expressed by (see Figures B-2 and B-7)

$$\beta_1 = \cos^{-1} (\cos \psi_2 \cos \psi_1) \quad (B-60)$$

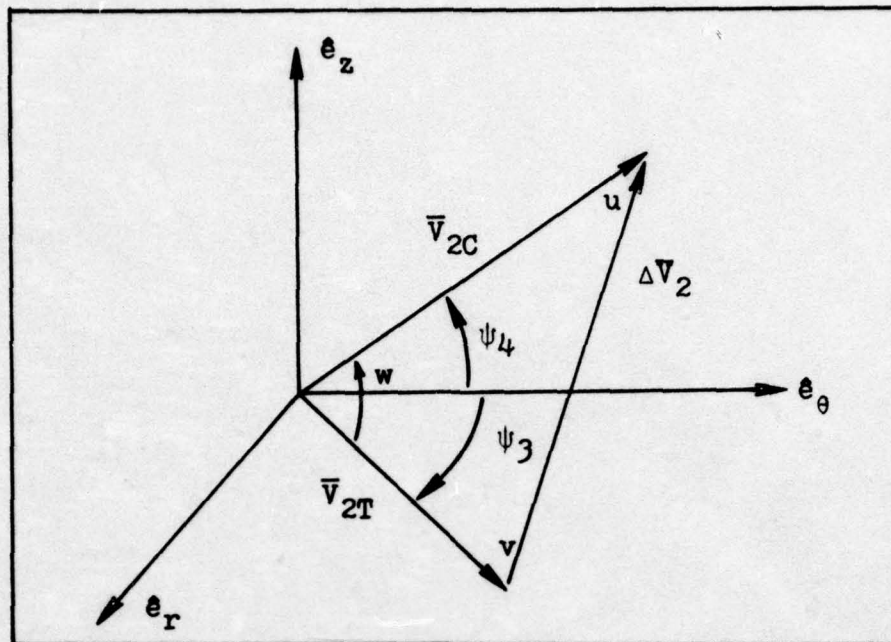


Figure B-7. Second Burn Relationships

$$w = \cos^{-1} (\cos \psi_3 \cos \psi_4) \quad (\text{B-61})$$

These relationships show that now ψ_2 and ψ_4 are introduced as additional variables.

Thus, the three-dimensional equivalent to Equation (B-57) is a function of ψ_2 and ψ_4 , in addition to ψ_1 , giving it the extra degrees of freedom that allow a range of solutions. However, careful analysis shows that if the value of ψ_2 is specified, then the value of ψ_4 is fixed through Equations (B-24, B-25 and B-26). So, by specifying the amount of plane change to be accomplished during the first burn, the amount left for the second burn is fixed by the overall plane change requirement; and again ΔV_2 becomes a function of ψ_1 only.

Appendix C
Finite Burn Dynamics

Equations of Motion

In this section the nonlinear vector differential equation of motion is developed and then put into a state variable format for implementation of the numerical integration routine (SET/STEP). The local (XYZ)_g frame is used as the inertial reference. In this frame, the position vector and thrust vector are

$$\bar{r}(t) = r_x \bar{i} + r_y \bar{j} + r_z \bar{k} \quad (C-1)$$

$$\bar{T} = T_x \bar{i} + T_y \bar{j} + T_z \bar{k} \quad (C-2)$$

Thus, finite burn dynamics are described by

$$\bar{F}_g[\bar{r}(t)] + \bar{T} = m(t) \ddot{\bar{r}}(t) \quad (C-3)$$

where $m(t)$ represents the mass of the vehicle at any time, t , and \bar{F}_g is the force due to gravity, expressible as

$$\bar{F}_g = \frac{-\mu m(t)}{r(t)^3} \bar{r}(t) \quad (C-4)$$

where μ is the gravitational parameter.

Since T is constant, the mass flow rate is constant, yielding

$$m(t) = m_0 - \dot{m}t$$

Thus, Equation (C-3) may be expressed as (omitting time dependency)

$$\ddot{\bar{r}} = \frac{-\mu \bar{r}}{r^3} + \frac{\bar{T}}{m_0 - \dot{m}t} \quad (C-5)$$

Expressing (C-5) in component form gives

$$\begin{aligned} \ddot{r}_x &= \frac{-\mu}{r^3} r_x + \frac{T_x}{m_0 - \dot{m}t} \\ \ddot{r}_y &= \frac{-\mu}{r^3} r_y + \frac{T_y}{m_0 - \dot{m}t} \\ \ddot{r}_z &= \frac{-\mu}{r^3} r_z + \frac{T_z}{m_0 - \dot{m}t} \end{aligned} \quad (C-6)$$

Finally, using a six element state vector (\bar{X}) where the first three elements are the position components, and the last three elements are the velocity components, the equations of motion become:

$$\begin{aligned} X_1 &= X_4 \\ X_2 &= X_5 \\ X_3 &= X_6 \\ X_4 &= \frac{-\mu X_1}{r^3} + \frac{T_x}{m_0 - \dot{m}t} \\ X_5 &= \frac{-\mu X_2}{r^3} + \frac{T_y}{m_0 - \dot{m}t} \\ X_6 &= \frac{-\mu X_3}{r^3} + \frac{T_z}{m_0 - \dot{m}t} \end{aligned} \quad (C-7)$$

During the coast phase of the trajectory, the components of \bar{T} are all zero.

The components of the thrust vector are calculated from

the current values of the thrust direction angles as follows:

For the first burn

$$\begin{aligned}T_x &= T_1 \cos \varphi_2 \cos \varphi_1 \\T_y &= T_1 \cos \varphi_2 \sin \varphi_1 \\T_z &= T_1 \sin \varphi_2\end{aligned}\tag{C-8}$$

and during the second burn as

$$\begin{aligned}T_x &= T_2 \cos \varphi_4 \cos \varphi_3 \\T_y &= T_2 \cos \varphi_4 \sin \varphi_3 \\T_z &= T_2 \sin \varphi_4\end{aligned}\tag{C-9}$$

Thus, the means of accomplishing the targeting for the finite burn case are contained in the equations of motion (C-7). By adjusting the thrust directions through Equations (C-8) and (C-9), and the transfer TOF by varying the integration time, NSOLA repeatedly demands integration of Equations (C-7) until values for the mission variables are found that produce the exact mission orbit desired.

Transfer Angle

The transfer angle (TA) is defined as the angle between the vectors $\bar{r}_{1C}(t)$ and $\bar{r}_{2C}(t + \text{TOF})$, where finite burn dynamics apply. Thus, TA is slightly different from the central angle (C_a), used to describe the angle between these two vectors during impulsive targeting.

To find the value of the transfer angle resulting from

targeting step one (where it was left free), a third vector ($\overline{\Delta r}$) is first formed, as shown in Figure C-1. In the local frame, the component form of $\overline{r}_{1C}(t_{b1})$ is always just $r_{1C} \bar{i}$. The components of $\overline{r}_{2C}(t_{b1} + \text{TOF})$ are known after numerical integration of the transfer trajectory.

The vector $\overline{\Delta r}$ is then determined from

$$\overline{\Delta r} = \overline{r}_{2C} - \overline{r}_{1C} \quad (\text{C-10})$$

and the transfer angle is obtained using the law of cosines as

$$\text{TA}^* = \cos^{-1} \left[\frac{r_{2C}^2 + r_{1C}^2 - \Delta r^2}{2 r_{1C} r_{2C}} \right] \quad (\text{C-11})$$

During the second step of targeting, if the transfer is between coplanar orbits, it is necessary to compute the transfer angle as a function of time, expressed in the perifocal (PQW) frame. In this case, Equation (C-11) takes the form

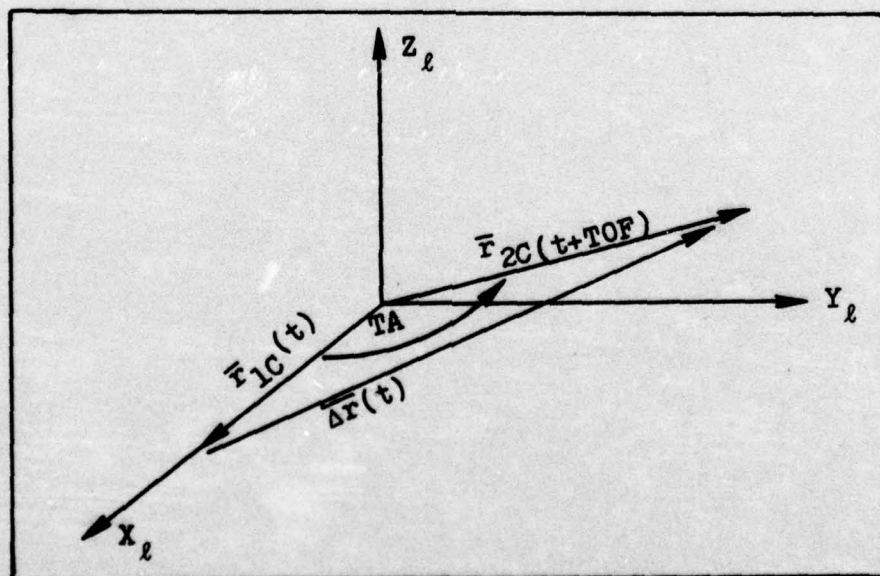


Figure C-1. Transfer Angle

$$TA(t) = \cos^{-1} \left[\frac{r_{2C}^2(t + TOF^*) + r_{1C}^2(t) - \Delta r^2(t)}{2 r_{1C}(t) r_{2C}(t + TOF^*)} \right] \quad (C-12)$$

and is solved for the first burn time (t_{b1}) such that

$$TA(t_{b1}) = TA^* \quad (C-13)$$

Computation of the vectors $\bar{r}_{1C}(t)$ and $\bar{r}_{2C}(t + TOF^*)$ is described in Appendix D.

Appendix D
Targeting Step Two

Phasing

Phasing is simply a matter of selecting the proper launch position $\bar{r}_{1C}(t_{b1})$, such that the trajectory targeted in step one, when initiated at that position, satisfies either the constraint Ω_2 , or the constraint $TA(t)$. Since $\bar{r}_{1C}(t)$ is known, this becomes a problem of finding the proper time (t_{b1}) for first stage ignition.

The sequence of operations carried out in phasing (and their significance) are listed here in the order that they are accomplished:

1. From the given orbital elements of each orbit, $\bar{r}_{1C}(t)$ and $\bar{r}_{2C}(t)$ (when needed) are computed in their respective perifocal (PQW) frames. The vector $\bar{r}_{1C}(t)$ tracks the IUS in the parking orbit, and $\bar{r}_{2C}(t)$ tracks the mission orbit target position, if specified.
2. A value for t_{b1} is found such that $\bar{r}_{1C}(t_{b1})$ becomes the proper launch point to satisfy either Ω_2 (if the orbits are non-coplanar), or $TA^*(t_{b1})$ if transferring between coplanar orbits. In addition to specifying the mission variable t_{b1} , this step fixes the orientation between the local frame and the geocentric-equatorial frame (see Figure D-1).
3. Through knowledge of the orientation between the frames, a coordinate transformation is accomplished to convert the thrust direction angles expressed in the

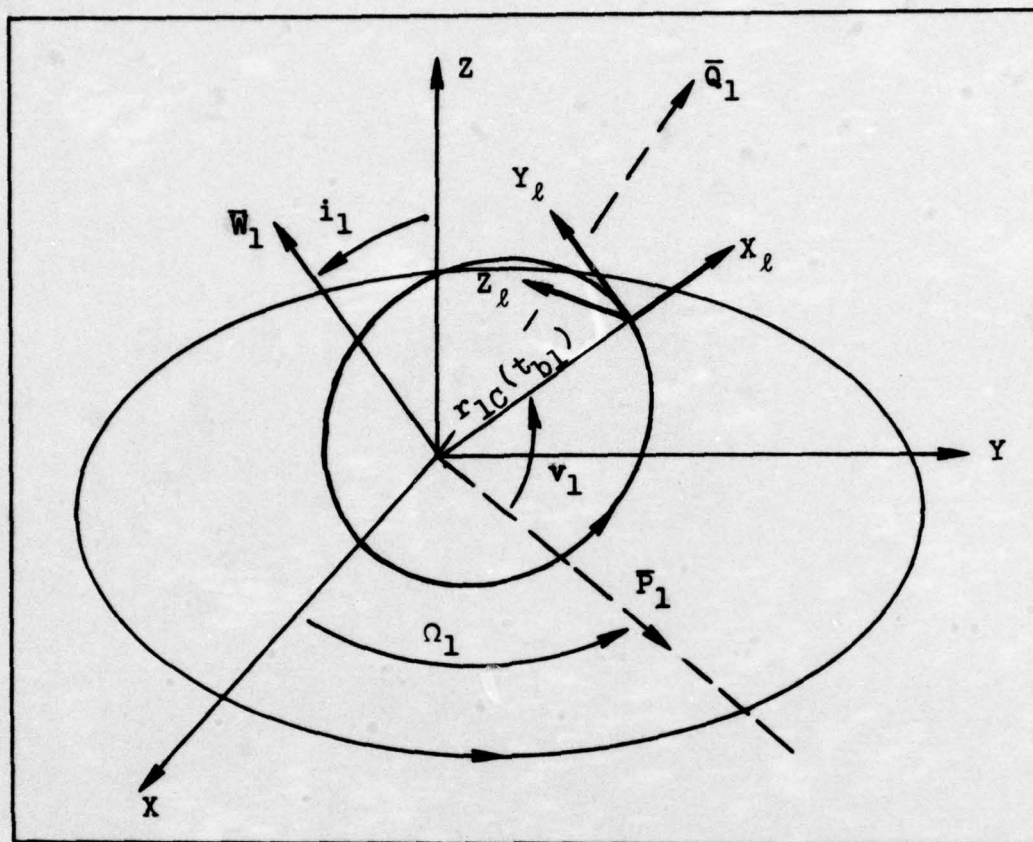


Figure D-1. Orientation Between Frames

local frame, to their corresponding values in the geocentric-equatorial frame.

The actual accomplishment of the phasing steps listed above involves a great deal of computations, and only the highlights will be given here. The reader is referred to the computer code listing if more details are desired.

To compute $\bar{r}_{1C}(t)$ and $\bar{r}_{2C}(t)$ in their perifocal (PQW) frames, epoch time (t_0) is used to fix their initial positions. At epoch, $\bar{r}_{1C}(t_0)$ is directed along the \bar{P}_1 axis, and $\bar{r}_{2C}(t_0)$ is at an angle u_{02} with the \bar{P}_2 axis. First, the angular velocities are determined from

$$\omega_1 = \frac{V_{1C}}{r_{1C}} \quad (D-1)$$

$$\omega_2 = \frac{V_{2C}}{r_{2C}}$$

Then the two vectors can be calculated at any time t as

$$\bar{r}_{1C}(t) = (r_{1C} \cos \omega_1 t) \bar{P}_1 + (r_{1C} \sin \omega_1 t) \bar{Q}_1 \quad (D-2)$$

$$\begin{aligned} \bar{r}_{2C}(t) = & [r_{2C} \cos (\omega_2 t_f + u_{02})] \bar{P}_2 \\ & + [r_{2C} \sin (\omega_2 t_f + u_{02})] \bar{Q}_2 \end{aligned} \quad (D-3)$$

where $t_f = t + \text{TOF}^*$; and TOF^* is the transfer time of flight as targeted in step one.

If Ω_2 is to be satisfied, then t_{b1} may be found as follows:

$$u_1 = \Omega_2 - \Omega_{2G} \quad (D-4)$$

$$t_{b1} = \frac{u_1}{\omega_1} \quad (D-5)$$

Here u_1 represents the angle that $\bar{r}_{1C}(t)$ generates in going from t_0 to t_{b1} ; and Ω_{2G} is the value resulting from step one, where longitude of the ascending node was left free.

If $\text{TA}(t)$ is to be satisfied (coplanar orbits), Equation (C-12) is used. A one-dimensional search on t is made until a solution is bracketed; then a secant technique is used to get the exact t_{b1} such that Equation (C-13) is satisfied.

The last step is to transform the thrust angles from the local frame to the geocentric-equatorial frame. Once t_{b1}

is known, the orientation between the frames is fixed by the given orbital elements of each frame, and $\bar{r}_{1C}(t_{b1})$ as shown in Figure D-1. Here v_1 is the angle between the \bar{P}_1 axis and $\bar{r}_{1C}(t_{b1})$.

To make the transformation, unit thrust vectors, \bar{u}_{T1} and \bar{u}_{T2} , are formed (expressed in the local frame) from the targeted thrust angles. Then these vectors are each transformed to the geocentric-equatorial frame by

$$\bar{u}_T^{XYZ} = C_{XYZ_\ell}^{XYZ} \bar{u}_T^{XYZ_\ell} \quad (D-6)$$

After the transformation, angles are formed again from the unit vectors.

The three Euler angles between the frames are (by order of removal), v_1 , i_1 and Ω_1 . The angle v_1 is obtained, once t_{b1} is known, from the relationship

$$v_1 = \omega_1 t_{b1} \quad (D-7)$$

The transformation matrix is

$$C_{XYZ_\ell}^{XYZ} = \begin{bmatrix} (c\Omega_1 cv_1 + s\Omega_1 ci_1 sv_1) & (c\Omega_1 sv_1 - s\Omega_1 ci_1 cv_1) & (s\Omega_1 si_1) \\ (s\Omega_1 cv_1 - c\Omega_1 ci_1 sv_1) & (s\Omega_1 sv_1 + c\Omega_1 ci_1 cv_1) & (-si_1 c\Omega_1) \\ (-si_1 sv_1) & (si_1 cv_1) & (ci_1) \end{bmatrix} \quad (D-8)$$

Mission Delay Retargeting

For transfer between non-coplanar orbits, the mission opportunity times occur at equal intervals after the first t_{b1}

time. This is because the first burn must occur at the same position in the parking orbit each time. The time interval between the possible launch times is just equal to the period of the parking orbit, which is given by

$$P = \frac{2\pi}{\omega_1} \quad (D-9)$$

and the thrust direct angles are the same at each possible launch time.

For transfer between coplanar orbits (rendezvous assumed), the mission opportunity times are again periodic, but now the interval is equal to the synodic period, which is found by

$$P_s = \frac{2\pi}{|\omega_1 - \omega_2|} \quad (D-10)$$

In this case the launch position changes each time, so that for each sequential opportunity, the corresponding angle v_1 must be computed, and the coordinate transformation of the thrust angles repeated.

Summarizing, the mission opportunity times (times when proper phasing occurs) are, for non-coplanar orbits

$$t_{bl_{k+1}} = t_{bl_k} + P \quad (D-11)$$

and for coplanar orbits

$$t_{bl_{k+1}} = t_{bl_k} + P_s \quad (D-12)$$

for $k = 1, 2, \dots$

Appendix E
Accuracy Determination

Thrust Misalignment Sensitivities

The nominal values of the thrust direction angles (φ_1 , φ_2 , φ_3 and φ_4), expressed in the local frame, are obtained in targeting step one. The procedure used to obtain insertion error sensitivities, due to thrust vector misalignment, is to perturb these nominal values slightly by assuming a one milliradian (mr) alignment error about each axis of the XYZ_ℓ frame, in turn.

To generate perturbed thrust angles, nominal unit thrust vectors (\bar{u}_{T1} and \bar{u}_{T2}) are first formed, with their components expressed in the XYZ_ℓ frame. Then these vectors are coordinated in a frame which is misaligned by one mr about the X_ℓ axis. Next, their components in the misaligned frame are converted to misaligned thrust angles. Lastly, Equations (C-7) are integrated using these misaligned thrust angles, so that the insertion error sensitivities due to a one mr misalignment about the X_ℓ axis are obtained. This gives the first column of the sensitivity matrix in Equation (5-2). The same process is then repeated for misalignments about the Y_ℓ axis and the Z_ℓ axis, generating the second and third columns of the matrix.

The insertion error sensitivity matrix of Equation (5-2) is then partitioned as shown, to form the individual position and velocity matrices. Next, the maximum eigenvalues of these matrices are determined by use of a standard subroutine designed

for that purpose, and the two "worst case" sensitivities are formed using Equation (5-7). The derivation of this equation will now be explained.

The derivation is motivated by formulating the problem as Equation (5-6)

$$\bar{y} = A \bar{x} \quad (5-6)$$

where, for a fixed magnitude of the vector \bar{x} (thrust misalignment vector), it is desired to find the maximum possible magnitude of the vector \bar{y} (representing insertion position or velocity error), caused by the sensitivity matrix, A .

To express the worst case sensitivities with respect to milliradians of misalignment, the problem becomes: Given

$$|\bar{x}| = \sqrt{x_1^2 + x_2^2 + x_3^2} = 1 \text{ mr} \quad (E-1)$$

find the associated value of $|\bar{y}|_{\max}$.

The steps in the development of Equation (5-7) are as follows

$$\bar{y} = A \bar{x} \quad (5-6)$$

$$\bar{y}^T \bar{y} = \bar{x}^T A^T A \bar{x} \quad (E-2)$$

thus $A^T A$ is a symmetric matrix where

$$A^T A = M^{-1} \Lambda M \quad (E-3)$$

where Λ is the diagonal matrix whose elements are the eigenvalues of $A^T A$, and M is the normalized (and dimensionless)

modal matrix of $A^T A$; and is scaled such that

$$M^{-1} = M^T \quad (E-4)$$

substituting (E-3) into (E-2) gives

$$\bar{y}^T \bar{y} = \bar{x}^T M^{-1} \Lambda M \bar{x} \quad (E-5)$$

now let

$$\bar{z} = M \bar{x} \quad (E-6)$$

and taking the transpose of each side

$$\bar{z}^T = \bar{x}^T M^T = \bar{x}^T M^{-1} \quad (E-7)$$

Now, substituting \bar{z} and \bar{z}^T into (E-5) gives

$$\bar{y}^T \bar{y} = |\bar{y}|^2 = \bar{z}^T \Lambda \bar{z} \quad (E-8)$$

and performing the vector matrix multiplications yields

$$y^2 = \lambda_1 z_1^2 + \lambda_2 z_2^2 + \lambda_3 z_3^2 \quad (E-9)$$

But the vectors \bar{x} and \bar{z} are related through

$$\bar{z}^T \bar{z} = \bar{x}^T (M^T M) \bar{x} = \bar{x}^T \bar{x} \quad (E-10)$$

since M is an orthogonal matrix such that

$$M^T M = M^{-1} M = I \quad (E-11)$$

where I is the identity matrix. Thus

$$|\bar{z}| = |\bar{x}| \quad (E-12)$$

and the problem reduces to one of maximizing y^2 in Equation (E-9), subject to the constraint

$$|\bar{z}| = \sqrt{z_1^2 + z_2^2 + z_3^2} = |\bar{x}| = 1 \quad (\text{E-13})$$

which is equivalent to the constraint equation

$$z_1^2 + z_2^2 + z_3^2 = 1 \quad (\text{E-14})$$

Using a Lagrange multiplier (λ_4) to attach (E-14) to (E-9), the problem is transformed to one of maximizing F , where

$$\begin{aligned} F = & \lambda_1 z_1^2 + \lambda_2 z_2^2 + \lambda_3 z_3^2 \\ & + \lambda_4 (z_1^2 + z_2^2 + z_3^2 - 1) \end{aligned} \quad (\text{E-15})$$

The necessary conditions for a maximum of F are

$$\begin{aligned} \frac{\partial F}{\partial z_1} &= 2 \lambda_1 z_1 + 2 \lambda_4 z_1 = 0 \\ \frac{\partial F}{\partial z_2} &= 2 \lambda_2 z_2 + 2 \lambda_4 z_2 = 0 \\ \frac{\partial F}{\partial z_3} &= 2 \lambda_3 z_3 + 2 \lambda_4 z_3 = 0 \end{aligned} \quad (\text{E-16})$$

Thus, the necessary conditions, plus the constraint equation, become four equations in four unknowns

$$\begin{aligned} (\lambda_1 + \lambda_4) z_1 &= 0 \\ (\lambda_2 + \lambda_4) z_2 &= 0 \\ (\lambda_3 + \lambda_4) z_3 &= 0 \end{aligned} \quad (\text{E-17})$$

$$z_1^2 + z_2^2 + z_3^2 = 1$$

The solution involves checking the four possible cases, which are:

Case 1: $z_1 = 0, z_2 = 0, z_3 = 0$. This case is impossible since it violates the constraint Equation (E-14).

Case 2: $z_1 \neq 0, z_2 = 0, z_3 = 0$.

Case 3: $z_1 \neq 0, z_2 \neq 0, z_3 = 0$.

Case 4: $z_1 \neq 0, z_2 \neq 0, z_3 \neq 0$.

For Case 2, Equations (E-17) reduce to

$$\lambda_1 + \lambda_4 = 0 \tag{E-18}$$

$$\lambda_1 = -\lambda_4$$

$$z_1^2 = 1 \tag{E-19}$$

Making these substitutions in Equation (E-15) yields

$$F = y^2 = \lambda_1 \tag{E-20}$$

which gives

$$y = \sqrt{\lambda_1} \tag{E-21}$$

Cases 3 and 4 similarly yield

$$y = \sqrt{\lambda_2} \tag{E-22}$$

$$y = \sqrt{\lambda_3}$$

Thus, the maximum magnitude of \bar{y} must be determined by the largest of the three eigenvalues of the $A^T A$ matrix, and is always

$$|\bar{y}| = \sqrt{\lambda_{\max}} \quad (E-23)$$

for an $|\bar{x}|$ of one mr.

Thrust Magnitude Sensitivities

Here the magnitudes of the thrust vectors of each stage (T_1 and T_2) are changed by $\pm 1\%$, and Equations (C-7) integrated for the nominal time (TOF^*) so that insertion errors may again be computed. The thrusts of both engines are assumed to deviate by the same plus amount or the same minus amount, so that insertion position and velocity error sensitivities may be determined for both positive and negative thrust magnitude deviations.

The burn times in Equations (C-7) are also changed by thrust magnitude variations and must be recomputed prior to each integration as

$$\dot{m}_{1p} = \frac{T_{1p}}{c_1} \quad (E-24)$$

$$\dot{m}_{2p} = \frac{T_{2p}}{c_2}$$

$$T_{bap} = \frac{m_{01} - m_{f1}}{\dot{m}_{1p}} \quad (E-25)$$

$$T_{bbp} = \frac{m_{02} - m_{f2}}{\dot{m}_{2p}}$$

where the subscript p denotes the perturbed value.

Appendix F

Computer Listing
(Fortran Extended Version IV)


```

C      PROGRAM TARGET(INPUT,OUTPUT,TAPE5=INPJ,TAPE5=OUTPJ)
C
C      XXXXXXXXXXXXXXXXXXXXXXXXXXXXXXXXXXXXXXXXXXXXXXXXXXXXXXXXXXXXXXX
C
C      --- THIS PROGRAM TARGETS THE CONSTANT THRUST, CONSTANT BURN
C      ATTITUDE SIMPLE OPEN LOOP GUIDANCE SCHEME FOR THE ACTUAL
C      FINITE BURN VELOCITY CHANGES, USING A TWO STAGE VEHICLE TO
C      TRANSFER BETWEEN TWO CIRCULAR COPLANAR OR NON-COPLANAR ORBITS.
C      AN ACCURACY ANALYSIS OF EACH TRAJECTORY THIS TARGETED IS THEN
C      ACCOMPLISHED, AND MISSION DELAY RETARGETING IS DONE. ---
C
C      XXXXXXXXXXXXXXXXXXXXXXXXXXXXXXXXXXXXXXXXXXXXXXXXXXXXXXXXXXXXXXX
C
C      DIMENSION F(5),F(5),AJINV(5,5),W(75),Z(5),SNS(6,3),X(6),A(3,3),B(3
C      5,3),WORK(5),ATP(3,3),BTP(3,3),C(3,3),J(3,3)
C      COMPLEX EIGVAL(3),EIGVEC(3,3)
C      EXTERNAL S.OPE
C      REAL ISP1,ISP2,I1,I2N,M1,M2,M01,M02,MF1,MF2,M01,M02,I2,I1A,L02
C      COM4CON/TT/ENJ,PI,CNMF,RO,DR,R1T,V1T,R1C,V1C,R2T,V2T,R2C,V2C,DV1,
C      DV2,TNU1,TNU2,F,CA,AT,SY1,SY2,SY3,SY4,I2N,THETA
C      COM4CON/ODD/ R2CC,V2CC,R2CA,R2CP,I2,E2CC,I1A,I1,TA,J2G
C      COM4CON/TE/C,SNS
C      COM4CON/SL/M01,M02,MF1,MF2,T1,T2,M01,M02,T0A,T0B
C      COM4CON/TTB1/AI1,AI2,O1,O2,L02,T22,TEST
C      COM4CON/CH/4AXPL
C      ENJ=1.407634E13
C      RE=3443.93
C      PI=3.1415926535898
C      CNMF=6076.115496
C      RO=190./PI
C      TR=PI/180.
C      GO=32.1464
C      J12=0
C
C      READ IN THE INPUT DATA AS FOLLOWS:
C
C      (1) ORBITAL ELEMENTS FOR EACH ORBIT
C      (2) TWO STAGE VEHICLE SPECIFICATIONS.
C      (3) DESIRED FUEL AND PAYLOAD HEIGHTS IN LBS.
C      (4) PLANE CHANGE TO BE ACCOMPLISHED DURING THE FIRST BURN IN DEG.
C      (5) CHOICE OF HIT CONDITIONS (0 -IF CONSTRAINT, 1 -MAXPAYLOAD )
C
C      READ*,M1,M2,AI1,AI2,O1,O2,L02
C      READ*,ISP1,ISP2,ST1,ST2,T1,T2
C      READ*,PROPL,PROP2,PL
C      READ*,SY2
C      READ*,MAXPL
C
C      COMPUTE ORBIT PARAMETERS:
C
C      THETA=AI2-AI1
C      TEST=THETA
C      T4ET4=ABS(THETA)
C      I1=0.
C      I2N=THETA
C      R1C=(RE+M1)*CNMF.
C      R2C=(RE+M2)*CNMF.
C      V1C=SQRT(E4U/R1C)
C      V2C=SQRT(E4U/R2C)

```

```

C      COMPUTE MOHANN TRANSFER VELOCITIES AND TDFH
C
R1T=R1C
R2T=R2C
ATH=(R1T+R2T)/2.
ET4=-EMU/(2.*ATH)
V1TH=SQRT(2.*(EMU/R1T+ETH))
DV1H=V1TH-V1C
V2TH=SQRT(2.*(EMU/R2T+ETH))
DV2H=V2C-V2T4
TDFH=PI*SQRT(ATH**3/EMU)

C
C      COMPUTE DV1 AND DV2 (IDEAL), AND THE SR4 BURN TIMES.
C
PRCP1=PROPL/GO $ PROP2=PRO2/GO $ PL=P./GO
M1=ST1+PRO21
M2=ST2+PRO22
M01=M1+M2+PL
M02=M2+PL
MF1=M01-PRCP1
MF2=M02-PRCP2
C1=ISP1*GO
C2=ISP2*GO
M01=T1/C1
M02=T2/C2
TBA=(M01-MF1)/M01
TB3=(M02-MF2)/M02
DV1=ISP1*GO*ALOG(M01/MF1)
DV2=ISP2*GO*ALOG(M02/MF2)

C
C      CORRECT FOR FINITE BURN LOSSES OF DV1, FINITE LOSSES OF DV2 NEGL.
C
FILOSS=.001
DV1=DV1-(DV1*FILOSS)

C
C      COMPUTE THE MAXIMUM POSSIBLE PLANE CHANGE DURING THE FIRST BURN
C
SY2MAX=ACOS((V1C**2+V1TH**2-DV1**2)/(2.*V1C*V1TH))
SY4MAX=ACOS((V2C**2+V2TH**2-DV2**2)/(2.*V2C*V2TH))
SYTOT=SY2MAX+SY4MAX

C
C      PRINT INPUTS:
C
PRINT*, "XXXXXXXXXXXXXXXXXXXXXXXXXXXXXXXXXXXXXXXXXXXXXXXXXXXXXXXXXXXXX"
5XXXXXXXXXXXXXXXXXXXXXXXXXXXXXXXXXXXXX"
PRINT*, "XXXXXXXXXXXXXXXXXXXXXXXXXXXXX OUTPJT XXXXXXXXXXXXXXXXXXXXXXXX"
5XXXXXXXXXXXXXXXXXXXXXXXXXXXXXXXXXXXXX"
PRINT*
PRINT*
IF(MAXPL.E2.0)GO TO 341
PRINT*, "THIS IS A MAXIMUM PAYLOAD RUN USING HIT CONDITION SET TWO"
PRINT*
PRINT*
341 CONTINUE
PRINT*, "THE ORBIT PARAMETERS ARE: "
PRINT*
PRINT*, "M1= ",M1," NM. AND M2= ",M2," NM."
PRINT*, "R1C= ",R1C/CNMF," V.M. AND R2C= ",R2C/CNMF," V.M. "
PRINT*, "V1C= ",V1C," FT/SEC. AND V2C= ",V2C," FT/SEC. "
PRINT*, "COPLANAR MOHANN TRANSFER VELOCITIES ARE: "

```



```

PRINT*, "V1TH= ", V1TH, " FT/SEC. AND V2TH= ", V2TH, " FT/SEC. "
PRINT*, "DV1H= ", DV1H, " FT/SEC. AND DV2H= ", DV2H, " FT/SEC. "
PRINT*, "INCLINATION OF ORBIT ONE IS: ", AI1, " DEG. "
PRINT*, "INCLINATION OF ORBIT TWO IS: ", AI2, " DEG. "
PRINT*, "LONGITUDE OF ORBIT ONE IS: ", J1, " DEG. "
PRINT*, "LONGITUDE OF ORBIT TWO IS: ", J2, " DEG. "
PRINT*, "LONG. AT EPOCH OF ORBIT TWO IS: ", L2, " DEG. "
PRINT*, "REQUIRED PLANE CHANGE IS: ", THETA, " DEG. "
PRINT*
PRINT*
PRINT*, "THE SRM SPECIFICATIONS ARE: "
PRINT*
PRINT*, "ISP1= ", ISP1, " AND ISP2= ", ISP2, " SEC. "
PRINT*, "FIRST STAGE STRUCTURE WEIGHT IS ", ST1*G0, " LBS "
PRINT*, "SECOND STAGE STRUCTURE WEIGHT IS ", ST2*G0, " LBS "
PRINT*, "FIRST STAGE THRUST IS ", T1, " LBS "
PRINT*, "SECOND STAGE THRUST IS ", T2, " LBS "
PRINT*
PRINT*
PRINT*, "THE VEHICLE LOADING IS TO BE: "
PRINT*
PRINT*, "FIRST STAGE PROPELLANT WEIGHT IS ", PROP1*G0, " LBS "
PRINT*, "SECOND STAGE PROPELLANT WEIGHT IS ", PROP2*G0, " LBS "
PRINT*, "PAYLOAD WEIGHT IS ", PL*G0, " LBS "
PRINT*
PRINT*
PRINT*, "THE VELOCITY CAPABILITIES OF EACH STAGE ARE: "
PRINT*
PRINT*, "DV1= ", DV1, " FT/SEC. "
PRINT*, "DV2= ", DV2, " FT/SEC. "
PRINT*
PRINT*
PRINT*, "THE SRM BURN TIMES ARE: "
PRINT*
PRINT*, "TBA= ", TBA, " SEC. "
PRINT*, "TBB= ", TBB, " SEC. "
PRINT*
PRINT*
PRINT*, "THE LIMITS OF POSSIBLE PLANE CHANGE WITH THESE VELOCITIES
ARE: "
PRINT*
PRINT*, "MAXIMUM PLANE CHANGE ATTAINABLE DURING FIRST BURN IS: ",
SSY2MAX*RD, " DEG. "
PRINT*, "MAXIMUM PLANE CHANGE ATTAINABLE DURING SECOND BURN IS: ",
SSY4MAX*RD, " DEG. "
PRINT*, "THE TOTAL POSSIBLE PLANE CHANGE IS: ", SYTOT*RD, " DEG. "
PRINT*
PRINT*
PRINT*, "XXXXXXXXXXXXXXXXXXXXXXXXXXXXXXXXXXXXXXXXXXXXXXXXXXXXXXXXXXXX"
THETA=THETA*JR $ I1=I1*DR $ I2N=I2N*JR $ AI1=AI1*DR $ AI2=AI2*DR
O1=O1*DR $ O2=O2*DR $ L2=L2*DR
PRINT*
PRINT*

```

C
C
C

ITERATE THRU THE RANGE OF POSSIBLE FIRST BURN PLANE CHANGE:

1

```

SY2=(SY2-1.)*DR
OSY2=1.*DR
SY2=SY2+OSY2
IF(SY2.GT.SSY4MAX)GO TO 30.

```

```

IF(JUMP.GE.1)GO TO 123
C
C CALL SUBROUTINE AGUESS WHICH COMPUTES INITIAL GUESSES FOR NS01A
C
C CALL AGUESS(PHI1,PHI2,PHI3,PHI4,TOF)
C
C CHECK IF TRANSFER POSSIBLE FOR THIS VALUE OF SY2:
C
C IF(CA.EQ.0.)GO TO 1
C
C   TCF=TOF+TBA
C   SF=1.
C   ST=1.0E5
C   Y(1)=PHI1/SF
C   Y(2)=PHI2/SF
C   Y(3)=PHI3/SF
C   Y(4)=PHI4/SF
C   Y(5)=TOF/SF
123 CONTINUE
C
C CALL THE NON-LINEAR EQUATION SOLVING ROUTINE, NS01A
C
C CALL NS01A(S,Y,F,AJINV,1.E-6,1.E7,1.E-5,250,0,W)
C
C ACHECK=(ABS(R2CA-R2CP))/CNMF
C IF(ACHECK.LT.10.)GO TO 19
C PRINT*,"FOR SY2= ",SY2*2," NO FINITE TRAJECTORY IS POSSIBLE"
C PRINT*,"ACHECK= ",ACHECK," N.M. DIFFERENCE "
C IF(JUMP.GT.0)GO TO 30
C PRINT*
C PRINT*
C GO TO 1
19 CONTINUE
C   TCF=Y(5)*SF
C   T22=TOF-TB3
C   PHI1=Y(1)*SF
C   PHI2=Y(2)*SF
C   PHI3=Y(3)*SF
C   PHI4=Y(4)*SF
C   PRINT*
C   PRINT*
C   CSY2=SY2*2)
C   PRINT(6,24) CSY2
24 FORMAT(2X,"***** FOR FIRST BURN PLANE CHANGE OF: ",F5.1," DEG
5. *****",//)
C PRINT*,"THE FINAL ACQUIRED ORBIT DATA IS: "
C PRINT*
C PRINT*,"FINAL POSITION AND VELOCITY ARE: "
C PRINT*,"POSITION IN XYZ: ",X(1)/CNMF,X(2)/CNMF,X(3)/CNMF
C PRINT*,"VELOCITY IN XYZ: ",X(4),X(5),X(5)
C PRINT*," R2C= ",R2CC/CNMF," N.M. "
C PRINT*," V2C= ",V2CC," FT/SEC. "
C PRINT*,"R2CA= ",R2CA/CNMF," N.M. "
C PRINT*,"R2CP= ",R2CP/CNMF," N.M. "
C PRINT*,"I1= ",I1A*RD," DEG. "
C PRINT*,"I2= ",I2*RD," DEG. "
C PRINT*,"O2= ",O2G*RD," DEG. "
C PRINT*,"F2CC= ",E2CC
C PRINT*,"TA= ",TA*RD," DEG. "
C PRINT*

```



```

PRINT*
PRINT*
PRINT*, "THE RESULTS OF TARGETING ARE: "
PRINT*
PRINT*
P4I1F=PHI1*RD
P4I2F=PHI2*RD
P4I3F=PHI3*RD
P4I4F=PHI4*RD
PRINT*, "THE FIRST STAGE THRUST DIRECTION ANGLES ARE: "
PRINT*
PRINT(6,75) P4I1F,P4I2F
76 FORMAT(10X,"P4I1= ",F10.5," DEG.",9X,"P4I2= ",F10.5," DEG. ")
PRINT*
PRINT*
PRINT*, "THE SECOND STAGE THRUST DIRECTION ANGLES ARE: "
PRINT*
PRINT(6,85) P4I3F,P4I4F
86 FORMAT(10X,"P4I3= ",F10.5," DEG.",9X,"P4I4= ",F10.5," DEG. ")
PRINT*
PRINT*
PRINT*, "BURN T40 OCCURS AT TIME: ",T22," SEC. "
PRINT*
PRINT*, "TOTAL TOF IS: ",TOF," SEC. "
PRINT*
PRINT*

C
C
C CALL SUBROUTINE ERROR WHICH COMPUTES INSERTION ERROR SENSITIVITIES
C
CALL ERRORS(PHI1,PHI2,PHI3,P4I4,TOF)
PRINT*
PRINT*, "THE RESULTS OF THE ERROR STUDY IS THE SENSITIVITY MATRIX:"
PRINT*, "UNITS ARE N.M. OR FT/SEC. PER MILIRADIAN OF MISALIGNMENT."
PRINT*
PRINT*
DO 20 K=1,5
PRINT(6,11) (SNS(K,J),J=1,3)
11 FORMAT(10X,3(3X,F13.4),/)
20 CONTINUE
PRINT*
PRINT*
PRINT*, "-----"

C
C
C NOW COMPUTE THE WORST CASE INSERTION ERRORS USING EIGENVALUES
C OF THE SENSITIVITY MATRIX
C
PRINT*
PRINT*
DO 3 I=1,3
DO 4 J=1,3
A(I,J)=SNS(I,J)
K=I+3
A(I,J)=SNS(K,J)
4 CONTINUE
3 CONTINUE
CALL MTSP(1,3,3,ATP)
CALL MTSP(3,3,3,BTP)
CALL MHPY(ATP,4,C,3,3,3)
CALL MHPY(BTP,3,D,3,3,3)
T40=1

```



```

C      CONVERT TARGETING INFORMATION TO THE G-E FRAME
C      VIA SUBROUTINE BURN1
C
      PRINT*
      PRINT*
      PRINT*,"THE TARGETING INFORMATION CONVERTED TO THE GEOCENTRIC "
      PRINT*,"EQUATORIAL FRAME FOR THE FIRST FIVE TRANSFER START TIMES:"
      PRINT*
      PRINT*
      IF(THETA.GT.0.)GO TO 250
      CALL BURN1(PHI1,PHI2,PHI3,PHI4,TOF,TA,R1C,V1C,R2C,V2C)
      GO TO 251
250    CALL BURN1(PHI1,PHI2,PHI3,PHI4,02G,R1C,V1C,R2C,V2C)
251    CONTINUE
      PRINT*
      PRINT*
      PRINT*,"*****"
5*****
      PRINT*,"*****"
5*****
      JUMP=JUMP+1
C
C      STEP TO THE NEXT INCREMENT OF FIRST BURN PLANE CHANGE
C
      GO TO 1
      CONTINUE
30    PRINT*
      PRINT*
      PRINT*,"THE FULL RANGE OF POSSIBLE TRANSFERS HAS BEEN EVALUATED. "
      PRINT*
      PRINT*
      PRINT*,"XXXXXXXXXXXXXXXXXXXXX END XXXXXXXXXXXXXXXXXXXXXXXXXXXXXXXX
5XXXXXXXXXXXXXXXXXXXXXXXXXXXXXXXXXXXXX "
      END
      SUBROUTINE AGUESS(PHI1,PHI2,PHI3,PHI4,TOF)
C
C      XXXXXXXXXXXXXXXXXXXXXXXXXXXXXXXXXXXXXXXXXXXXXXXXXXXXXXXXXXXXXXXX
C      THIS ROUTINE TARGETS VALUES FOR THE IMPULSIVE TRANSFER, WHERE
C      FINITE BURN LOSSES FOR FIRST STAGE BURN ARE INCLUDED.
C      XXXXXXXXXXXXXXXXXXXXXXXXXXXXXXXXXXXXXXXXXXXXXXXXXXXXXXXXXXXXXXXX
C
      DIMENSION X(5)
      COMMON/TT/EMJ,PI,CNMF,RO,OR,R1T,V1T,R1C,V1C,R2T,V2T,R2C,V2C,OV1,
5OV2,TNU1,TNU2,E,CA,AT,SY1,SY2,SY3,SY4,I2N,THETA
      REAL I2N
      PRINT*
      PRINT*
C
C      NOW CALL SUBROUTINE IGUESS:
C
      SY1=0.
      SY3=0.
      CALL IGUESS
C
C      CHECK IF TRANSFER POSSIBLE FOR THIS VALUE OF SY2:
C
      IF(CA.EQ.0.)GO TO 269
C
      NOW COMPUTE TOF

```

```

IF (E.GT.1.) GO TO 4
EC1=ACOS((E+COS(TNU1))/(1.+E*COS(TNU1)))
EC2=ACOS((E+COS(TNU2))/(1.+E*COS(TNU2)))
TC=SQRT(AT**3/EMU)*((EC2-E*SIN(EC2))-(EC1-E*SIN(EC1)))
GO TO 7

C
C
C
4
Y1=(E+COS(TNU1))/(1.+E*COS(TNU1))
F1=ALOG(Y1+SQRT(Y1**2-1.))
Y2=(E+COS(TNU2))/(1.+E*COS(TNU2))
F2=ALOG(Y2+SQRT(Y2**2-1.))
TCF=SQRT((-AT)**3/EMU)*((E*SINH(F2)-F2)-(E*SINH(F1)-F1))
7
CONTINUE

C
C
C
THE FIRST BURN THRUST DIRECTION ANGLES ARE:

V1TX=V1T*SIN(SY1)
V1TY=V1T*COS(SY1)*COS(SY2)
V1TZ=V1T*COS(SY1)*SIN(SY2)
DV1X=V1TX
DV1Y=V1TY-1.0
DV1Z=V1TZ
DV1XYZ=SQRT(DV1X**2+DV1Y**2+DV1Z**2)
PHI2=ASIN(DV1Z/DV1)
PHI1=ASIN(DV1Y/(DV1*COS(PHI2)))

C
C
C
NOW COMPUTE DV2 IN THE E FRAME:

55
V2CX=0.
V2CY=V2C*COS(SY4)
V2CZ=V2C*SIN(SY4)
V2TX=V2T*SIN(SY3)
V2TY=V2T*COS(SY3)
V2TZ=0.
DV2XE=V2CX-V2TX
DV2YE=V2CY-V2TY
DV2ZE=V2CZ-V2TZ

C
C
C
NOW COORDINATIZE DV2 IN THE INERTIAL FRAME:

DEL=CA-PI/2.
R2TP=R2T*COS(DEL)
R2Z=R2TP*SIN(SY2)
GA1A1=ASIN(R2Z/R2T)
R2Y=R2TP*COS(SY2)
R2XY=R2T*COS(GA1A1)
G2P=ACOS(R2Y/R2XY)
GA1A2=PI/2.+G2P
R2X=-R2XY*SIN(G2P)
DV2X=DV2XE*COS(GA1A2)*COS(GA1A1)-DV2YE*SIN(GA1A2)-DV2ZE*COS(GA1A2)
5
5*SIN(GA1A1)
DV2Y=DV2XE*SIN(GA1A2)*COS(GA1A1)+DV2YE*COS(GA1A2)-DV2ZE*SIN(GA1A2)
5
5*SIN(GA1A1)
DV2Z=DV2XE*SIN(GA1A1)+DV2ZE*COS(GA1A1)
DV2E=SQRT(DV2X**2+DV2YE**2+DV2ZE**2)
DV2XYZ=SQRT(DV2X**2+DV2Y**2+DV2Z**2)

C
C
C
NOW COMPUTE THE THRUST DIRECTION ANGLES FOR 2ND BURN:

```



```

PRINT*
P4I4=ASIN(JV2Z/DV2)
P4I3=ASIN(JV2Y/(DV2*COS(PHI4)))
IF(DV2X.LT.0.) P4I3=-(PI+PHI3)

C
C
C
NOW PRINT RESULTS:

PRINT*, "XXXXXXXXXXXXXXXXXXXXXXXXXXXXXXXXXXXXXXXXXXXXXXXXXXXXXXXXXXXX"
PRINT*, "THE TARGETING RESULTS IN THE ---LOCAL--- FRAME ARE: "
PRINT*, "XXXXXXXXXXXXXXXXXXXXXXXXXXXXXXXXXXXXXXXXXXXXXXXXXXXXXXXXXXXX"
PRINT*
PRINT*, " FOR A PLANE CHANGE ANGLE (SY2) DURING THE FIRST BURN OF
5** ",SY2*RD," ** DEGREES, THE RESULTS ARE: "
PRINT*
PRINT*
PRINT*, "XXXXXXXXXX FOR IMPULSIVE TRANSFER XXXXXXXXXXXXXXXXXXXXXXX"
PRINT*
PRINT*
PRINT*, "THE TRANSFER ORBIT CHARACTERISTICS ARE: "
PRINT*
PRINT*, "THE ECCENTRICITY OF THE TRANSFER ORBIT IS: ",E
PRINT*, "THE TRANSFER ANGLE IS: ",CA*RD," DEG. "
PRINT*, "V1T= ",V1T," FT/SEC. "
PRINT*, "V2T= ",V2T," FT/SEC. "
PRINT*
PRINT*, "THE R2T COMPUTED ANALYTICALLY IS: "
PRINT*, "R2TX= ", R2X/CNMF," N.M. "
PRINT*, "R2TY= ", R2Y/CNMF," N.M. "
PRINT*, "R2TZ= ", R2Z/CNMF," N.M. "
PRINT*
PRINT*
PRINT*, "THE COMPUTED ANGLES ARE: "
PRINT*, " THE ANGLE SY1 IS: ",SY1*RD," DEG. "
PRINT*, " THE ANGLE SY3 IS: ",SY3*RD," DEG. "
PRINT*, " THE ANGLE SY4 IS: ",SY4*RD," DEG. "
PRINT*
PRINT*, "-----"
PRINT*
PRINT*, "THE TARGETING INFORMATION IS: "
PRINT*
PRINT*, "THE FIRST BURN INERTIAL THRUST DIRECTION ANGLES ARE: "
PRINT*, " P4I1= ",PHI1*RD," DEG. "
PRINT*, " P4I2= ",PHI2*RD," DEG. "
PRINT*, "THE 2 ND BURN INERTIAL THRUST DIRECTION ANGLES ARE: "
PRINT*, " P4I3= ",PHI3*RD," DEG. "
PRINT*, " P4I4= ",PHI4*RD," DEG. "
PRINT*
PRINT*, " THE TDF IS: ",TDF," SEC. "
PRINT*
PRINT*, "-----"
PRINT*
PRINT*
PRINT*, "XXXXXXXXXXXXXXXXXXXXXXXXXXXXXXXXXXXXXXXXXXXXXXXXXXXXXXXXXXXX"
PRINT*
PRINT*
PRINT*
PRINT*
PRINT*
PRINT*, "*****"

```

```

PRINT*, "THE FOLLOWING RESULTS ARE FOR --FINITE THRUST-- BURNS: "
PRINT*, "*****"
PRINT*
PRINT*
PRINT*
269 RETURN
END
SUBROUTINE IGUESS
C
C XXXXXXXXXXXXXXXXXXXXXXXXXXXXXXXXXXXXXXXXXXXXXXXXXXXXXXXXXXXXXXXX
C THIS SUBROUTINE GENERATES THE COMPATIBLE TRANSFER TRAJECTORY FOR
C THE FIXED VELOCITY CHANGE INCREMENTS BY A REGULA FALSI ITERATION
C OF DV2 (SY1), SECOND BURN DELTA VELOCITY AS A FUNCTION OF THE FIRST
C BURN FLIGHT PATH ANGLE, UNTIL ITERATED DV2 MATCHES ACTUAL DV2.
C XXXXXXXXXXXXXXXXXXXXXXXXXXXXXXXXXXXXXXXXXXXXXXXXXXXXXXXXXXXXXXXX
C
C COM40N/TT/ENJ,PI,CNMF,RO,DR,R1T,V1T,R1C,V1C,R2T,V2T,R2C,V2C,DV1,
C DV2,TNU1,TNU2,E,CA,AT,SY1,SY2,SY3,SY4,I2N,THETA
C REAL I2N
C
C COMPUTE MAXIMUM POSSIBLE SY1
C SY1MAX=ATAN(DV1/V1C)
C
C PRINT*
C PRINT*
C IC=0
C CRIT=.01
C SY1=-.2*DR
C DS1=.2*DR
1 SY1=SY1+DS1
IF (SY1.GE.SY1MAX) GO TO 20
GO TO 10
5 SY1V=SY1C-((SY1C-SY1P)/(DV2C-DV2P))*(DV2C-DV2)
SY1=SY1V
10 B1=ACOS(COS(SY2)*COS(SY1))
QUANT0=(V1C/DV1)*SIN(B1)
IF (ABS(QUANT0) .GT. 1.) GO TO 2
A=ASIN(QUANT0)
B=PI-A-B1
QUANT1=DV1**2+V1C**2-2.*V1C*DV1*COS(B)
IF (QUANT1.LT.0) GO TO 2
V1T=SQRT(QUANT1)
ET=(V1T**2)/2.-EMU/R1T
QUANT2=2.*(EMU/R2T+ET)
IF (QUANT2.LT.0) GO TO 2
V2T=SQRT(QUANT2)
AT=-EMU/(2.*ET)
H=R1T*V1T*COS(SY1)
D=4**2/EMU
E=SQRT(1.-D/AT)
C
C CHECK TO ASSURE VALID TRANSFER ORBIT:
C
C IF (D/(1.+E).GT.R1T) GO TO 2
C IF (D/(1.-E).LT.R2T) GO TO 2
C QUANTH=(V2T**2+V2C**2-DV2**2)/(2.*V2T*V2C)
C IF (ABS(QUANTH).GT.1) GO TO 2
C
C COMPUTE TRUE ANOMOLIES AND CENTRAL ANGLE:

```



```

C      TNJ1=ACOS((P/R1T-1.)/E)
      TNJ2=ACOS((P/R2T-1.)/E)
      CA=TNU2-TNJ1
C
C      CHECK FOR PLANAR OR NON-COPLANAR TRANSFER:
C
      IF(THETA.E2.0.)GO TO 55
      NOW COMPUTE THE RESULTANT PLANE CHANGE REQUIRED AT SECOND BURN:
C
      QJANT3=(SIN(SY2)/SIN(THETA))*SIN(CA)
      IF(ABS(QJANT3).GT.1.)GO TO 2
      D=ASIN(QJANT3)
      C=2.*ATAN((COS(.5*(CA-D)))/(COS(.5*(CA+D))*TAN(.5*(THETA+SY2))))
      SY4=PI-C
      GO TO 56
55      SY4=SY2
56      QUANT4=H/(R2T*V2T)
      IF(ABS(QUANT4).GT.1.)GO TO 2
      SY3=ACOS(QUANT4)
      IF(SY3.LT.(20.*DR))DSY1=.01*DR
C
C      NOW COMPUTE DV2 IN THE E FRAME:
C
      V2CX=0.
      V2CY=V2C*COS(SY4)
      V2CZ=V2C*SIN(SY4)
      V2TX=V2T*SIN(SY3)
      V2TY=V2T*COS(SY3)
      V2TZ=0.
      DV2XE=V2CX-V2TX
      DV2YE=V2CY-V2TY
      DV2ZE=V2CZ-V2TZ
      DV2E=SQRT(DV2XE**2+DV2YE**2+DV2ZE**2)
      IF(ICO.GT.0)GO TO 5
      IF(DV2E.GT.DV2)GO TO 7
      SY1P=SY1-.2*DR
      SY1C=SY1
      DV2C=DV2E
      ICO=ICO+1
      GO TO 6
7      DV2P=DV2E
      GO TO 1
5      DV2N=DV2E
      IF(ABS(DV2V-DV2).LT.CRIT)GO TO 11
      SY1P=SY1C
      SY1C=SY1N
      DV2P=DV2C
      DV2C=DV2N
      GO TO 6
2      GO TO 1
20      PRINT*,"FOR SY2= ",SY2*RD," NO IMPULSIVE TRAJECTORY IS POSSIBLE"
6      PRINT*
      CA=0.
      GO TO 169
11      CONTINUE
      PRINT*
      PRINT*
      DV2=DV2E
169      RETURN

```

```

      END
      SUBROUTINE CALFUN(N,Y,F)

C
C
C
C
C
      XXXXXXXXXXXXXXXXXXXXXXXXXXXXXXXXXXXXXXXXXXXXXXXXXXXXXXXXXXXXXXXX
      THIS ROUTINE CONTAINS THE NONLINEAR EQUATIONS (INIT CONDITIONS)
      TO BE SOLVED BY NS01A.
      XXXXXXXXXXXXXXXXXXXXXXXXXXXXXXXXXXXXXXXXXXXXXXXXXXXXXXXXXXXXXXXX

      EXTERNAL SLOPE
      DIMENSION Y(N),F(N),X(6),Z(5),SNS(5,3)
      REAL M0,M1,M01,M02,M02,MF1,MF2,I2,I2N,I1A,I1
      COMMON/TT/EMJ,PI,CNMF,RD,DR,R1T,V1T,R1C,V1C,R2T,V2T,R2C,V2C,DV1,
      DV2,TNU1,TNU2,E,CA,AT,SY1,SY2,SY3,SY4,I2N,THETA
      COMMON/SLC/Z
      COMMON/SL/M01,M02,MF1,MF2,T1,T2,M01,M02,TB1,TB8
      COMMON/TE/K,SNS
      COMMON/ODAD/ R2CC,V2CC,R2CA,R2CP,I2,E2CC,I1A,I1,TA,D26
      COMMON/CH/MAXPL
      T=0.
      SF=1.
      ST=1.0E5
      Z(1)=Y(1)*SF
      Z(2)=Y(2)*SF
      Z(3)=Y(3)*SF
      Z(4)=Y(4)*SF
      Z(5)=Y(5)*ST
      X(1)=R1C
      X(2)=0.
      X(3)=0.
      X(4)=0.
      X(5)=V1C
      X(6)=0.
      DT=TRA/512.
      CALL SET(5,T,X,DT,SLOPE,D,.T.,D,D)
      DO 10 K=1,512
      CALL STEP(5,T,X,DT,SLOPE,D,.T.,D,D)
      CONTINUE
10
C
C
      COMPUTE INCLINATION OF TRANSFER ORBIT:

      M1X=X(2)*X(5)-X(3)*X(5)
      M1Y=X(3)*X(4)-X(1)*X(6)
      M1Z=X(1)*X(5)-X(2)*X(4)
      M1=SQRT(M1X**2+M1Y**2+M1Z**2)
      I1A=ACOS(M1Z/M1)
      DT=(Z(5)-(TB1+TB8))/10240.
      CALL SET(5,T,X,DT,SLOPE,D,.T.,D,D)
      DO 20 K=1,10240
      CALL STEP(5,T,X,DT,SLOPE,D,.T.,D,D)
      CONTINUE
20
      DT=TB8/512.
      CALL SET(5,T,X,DT,SLOPE,D,.T.,D,D)
      DO 30 K=1,512
      CALL STEP(5,T,X,DT,SLOPE,D,.T.,D,D)
      CONTINUE
30
C
C
      COMPUTE RESULTING MISSION ORBIT ELEMENTS:

      R2CC=SQRT(X(1)**2+X(2)**2+X(3)**2)
      V2CC=SQRT(X(4)**2+X(5)**2+X(6)**2)

```



```

H2X=X(2)*X(6)-X(3)*X(5)
H2Y=X(3)*X(4)-X(1)*X(6)
H2Z=X(1)*X(5)-X(2)*X(4)
H2=SQRT(H2X**2+H2Y**2+H2Z**2)
XN=SQRT(H2X**2+H2Y**2)
IF(THETA.E1.0.)GO TO 40
O25=ACOS(-H2Y/XN)
IF(H2X.LT.0.)O26=2.*PI-O25
40 CONTINUE
I2=ACOS(H2Z/H2)
RDV=X(1)*X(4)+X(2)*X(5)+X(3)*X(6)
RKT=V2CC**2-E4J/R2CC
EX=(1./EMU)*(RKT*X(1)-RDV*X(4))
EY=(1./EMJ)*(RKT*X(2)-RDV*X(5))
EZ=(1./EMU)*(RKT*X(3)-RDV*X(5))
E2CC=SQRT(EX**2+EY**2+EZ**2)
P2=H2**2/E4U
R2CP=P2/(1.+E2CC)
R2CA=P2/(1.-E2CC)
DR1X=X(1)-R1C
DR1Y=X(2)
DR1Z=X(3)
DR1=SQRT(DR1X**2+DR1Y**2+DR1Z**2)
TA=ACOS((R2C**2+R1C**2-DR1**2)/(2.*R2CC*R1C))
C
C
C FIRST COMPUTE A UNIT VECTOR IN R2,H2, AND V2C DIRECTIONS
UR2X=X(1)/R2CC
UR2Y=X(2)/R2CC
UR2Z=X(3)/R2CC
UH2X=H2X/H2
UH2Y=H2Y/H2
UH2Z=H2Z/H2
UV2X=UH2Y*UR2Z-UH2Z*UR2Y
UV2Y=UH2Z*UR2X-UH2X*UR2Z
UV2Z=UH2X*UR2Y-UH2Y*UR2X
C
C
C NOW COMPUTE NOMINAL V2 CORRESPONDING TO CURRENT R2 DIRECTION.
V2VX=V2C*UV2X
V2VY=V2C*UV2Y
V2VZ=V2C*UV2Z
C
C
C COMPUTE F(I) FOR CHOICE OF HIT CONDITIONS
IF(MAXPLST.0)GO TO 50
F(1)=(I1A-(I1+SY2))*(1.E5)
F(2)=(R2CC-R2C)/(1.E5)
F(3)=V2CC-V2C
F(4)=E2CC*(1.E2)
F(5)=(I2N-I2)*(1.E5)
GO TO 60
C
50 CONTINUE
F(1)=V2NX-((1)
F(2)=V2NY-X(3)
F(3)=V2NZ-((3)
F(4)=E2CC*(1.E2)
F(5)=(I2N-I2)*(1.E5)

```

```

C
50 RETURN
END
SUBROUTINE S.OPE(N,T,X,OX)

C
C
C
C
C
C
XXXXXXXXXXXXXXXXXXXXXXXXXXXXXXXXXXXXXXXXXXXXXXXXXXXXXXXXXXXXXXXXXXXX
THIS ROUTINE CONTAINS THE EQUATIONS OF MOTION TO BE
INTEGRATED BY SET/STEP.
XXXXXXXXXXXXXXXXXXXXXXXXXXXXXXXXXXXXXXXXXXXXXXXXXXXXXXXXXXXXXXXXXXXX

DIMENSION X(N), OX(N), Z(5)
REAL M0,M0,M01,M01,M02,M02,MF1,MF2,I2,I2N
COMMON/SL/401,402,MF1,MF2,T1,T2,401,402,TB1,TBB
COMMON/SLC/Z
ENJ=1.407534E15
TF=T1      S      TS=T2
IF(T.GT.TB1)TF=0.
TX=TF*COS(Z(2))*COS(Z(1))
TY=TF*COS(Z(2))*SIN(Z(1))
TZ=TF*SIN(Z(2))
40=401
40=401
TIME=T
IF(T.LT.(Z(5)-TBB))GO TO 2
TX=TS*COS(Z(4))*COS(Z(3))
TY=TS*COS(Z(4))*SIN(Z(3))
TZ=TS*SIN(Z(4))
40=402
40=402
TIME=T-(Z(5)-TBB)
2 CONTINUE
R=SQRT(X(1)**2+X(2)**2+X(3)**2)
OX(1)=X(4)
OX(2)=X(5)
OX(3)=X(6)
OX(4)=-ENJ*X(1)/R**3+TX/(M0-40*TIME)
OX(5)=-ENJ*X(2)/R**3+TY/(M0-40*TIME)
OX(6)=-ENJ*X(3)/R**3+TZ/(40-40*TIME)
RETURN
END
SUBROUTINE ERRORS(PHI1,PHI2,PHI3,PHI4,TOF)

C
C
C
C
C
C
XXXXXXXXXXXXXXXXXXXXXXXXXXXXXXXXXXXXXXXXXXXXXXXXXXXXXXXXXXXXXXXXXXXX
THIS ROUTINE COMPUTES INSERTION ERROR SENSITIVITIES DUE TO
TARGET VECTOR MISALIGNMENT.
XXXXXXXXXXXXXXXXXXXXXXXXXXXXXXXXXXXXXXXXXXXXXXXXXXXXXXXXXXXXXXXXXXXX

EXTERNAL S.OPE
DIMENSION XNF(5),SNS(6,3),X(5),Z(5)
REAL M0,M0,M01,M01,M02,M02,MF1,MF2,I2,I2N
COMMON/TT/ENJ,PI,CNMF,RO,OR,R1T,V1T,R1C,V1C,R2T,V2T,R2C,V2C,OV1,
SV2,TNU1,TNU2,F,CA,AT,SY1,SY2,SY3,SY4,I2N,THETA
COMMON/SL/401,402,MF1,MF2,T1,T2,401,402,TB1,TBB
COMMON/TF/K,SNS
COMMON/SLC/Z
I=0
TR=.001

C
C
C
STORE THE TARGETED NOMINAL R2C AND V2C:

```



```

10      GO TO J=1,3
      XNF(J)=X(J)
C
C      COMPUTE UNIT VECTORS IN THE INERTIAL FRAME USING THRUST ANGLES:
C
      U1X=COS(PHI2)*COS(PHI1)
      U1Y=COS(PHI2)*SIN(PHI1)
      U1Z=SIN(PHI2)
      U2X=COS(PHI4)*COS(PHI3)
      U2Y=COS(PHI4)*SIN(PHI3)
      U2Z=SIN(PHI4)
C
C      COORDINATIZE THE UNIT VECTORS IN THE MISALIGNED FRAME
C      FOR ALIGNMENT ERROR ABOUT X AXIS:
C
      U1XM=U1X
      U1YM=U1Y*COS(TR)-U1Z*SIN(TR)
      U1ZM=U1Y*SIN(TR)+U1Z*COS(TR)
      U2XM=U2X
      U2YM=U2Y*COS(TR)-U2Z*SIN(TR)
      U2ZM=U2Y*SIN(TR)+U2Z*COS(TR)
      GO TO 20
C
C      FOR ALIGNMENT ERROR ABOUT THE Y AXIS:
C
      U1XM=U1X*COS(TR)+U1Z*SIN(TR)
      U1YM=U1Y
      U1ZM=-U1X*SIN(TR)+U1Z*COS(TR)
      U2XM=U2X*COS(TR)+U2Z*SIN(TR)
      U2YM=U2Y
      U2ZM=-U2X*SIN(TR)+U2Z*COS(TR)
      GO TO 20
C
C      FOR ALIGNMENT ERROR ABOUT Z AXIS
C
      U1XM=U1X*COS(TR)-U1Y*SIN(TR)
      U1YM=U1X*SIN(TR)+U1Y*COS(TR)
      U1ZM=U1Z
      U2XM=U2X*COS(TR)-U2Y*SIN(TR)
      U2YM=U2X*SIN(TR)+U2Y*COS(TR)
      U2ZM=U2Z
C
C      COMPUTE THE MISALIGNED THRUST ANGLES:
C
      PHI2M=ASIN(U1ZM)
      PHI1M=ACOS(U1XM/COS(PHI2M))
      PHI4M=ASIN(U2ZM)
      PHI3M=ASIN(U2YM/COS(PHI4M))
      IF (J2XM.LT.0.) PHI3M=-(PI+PHI3M)
      T(1)=PHI1M
      T(2)=PHI2M
      T(3)=PHI3M
      T(4)=PHI4M
      T(5)=TOP
      GO TO 100
C
C      COMPUTE R2C AND V2C USING MISALIGNED THRUSTS:
C
      T=).
      X(1)=R1C

```

```

X(2)=0.
X(3)=0.
X(4)=0.
X(5)=V1C
X(6)=0.
DT=TBA/512.
CALL SET(5,T,X,DT,SLOPE,D,,T,,D,D)
DO 70 K=1,512
70 CALL STEP(5,T,X,DT,SLOPE,D,,T,,D,D)
CONTINUE
DT=(TOF-(TBA+TBB))/10240.
CALL SET(5,T,X,DT,SLOPE,D,,T,,D,D)
DO 80 K=1,10240
80 CALL STEP(5,T,X,DT,SLOPE,D,,T,,D,D)
CONTINUE
DT=TBB/512.
CALL SET(5,T,X,DT,SLOPE,D,,T,,D,D)
DO 90 K=1,512
90 CALL STEP(5,T,X,DT,SLOPE,D,,T,,D,D)
CONTINUE
C
C COMPUTE SENSITIVITY COEFFICIENTS BY COLUMN
C
I=I+1
SVS(1,I)=(X(1)-XNF(1))/6075.115496
SVS(2,I)=(X(2)-XNF(2))/6075.115496
SVS(3,I)=(X(3)-XNF(3))/6075.115486
SVS(4,I)=X(4)-XNF(4)
SVS(5,I)=X(5)-XNF(5)
SVS(6,I)=X(6)-XNF(6)
IF(I.EQ.1) GO TO 2
IF(I.EQ.2) GO TO 3
RETURN
END
SUBROUTINE BURN1(PHI1,PHI2,PHI3,PHI4,TOF,TA,R1C,V1C,R2C,V2C)
C
C
C
C
C
C
XXXXXXXXXXXXXXXXXXXXXXXXXXXXXXXXXXXXXXXXXXXXXXXXXXXXXXXXXXXXXXXXXXXX
THIS SUBROUTINE COMPUTES THE FIRST BURN TIME (TB1) FOR COPLANAR
TRANSFERS, AND THEN COMPUTES THE ACTUAL CORRESPONDING INERTIAL
THRUST DIRECTION ANGLES FROM TB1 AND SPECIFIED ORBITAL ELEMENTS.
XXXXXXXXXXXXXXXXXXXXXXXXXXXXXXXXXXXXXXXXXXXXXXXXXXXXXXXXXXXXXXXXXXXX
COMMON/TT31/AI1,AI2,O1,O2,L02,T22,TEST
REAL I1,I2,L02
PI=3.1415926535898
R1=190./PI
R2=PI/180.
DT=50.
CRIT=.0001
ITER=0
IC=0
I1=AI1
I2=AI2
IF(TEST.GT.0.) GO TO 14
PHI2=-PHI2
PHI4=-PHI4
14 CONTINUE
W1=V1C/R1C
W2=V2C/R2C
DE2=(2.*PI)/(ABS(W1-W2))

```



```

PRINT*
PRINT*,"THE COPLANAR SYNODIC PERIOD IS: ",PER," SEC. "
PRINT*
PRINT*
U02=L02-02
T=0.

C
C COMPUTE T01
C
GO TO 10
5 TN=TC-((TC-T0)/(TAC-TAP))*(TAC-TA)
T=TN
10 TF=T+TOF
R1CP=R1C*COS(W1*T)
R1CQ=R1C*SIN(W1*T)
R2CP=R2C*COS(U02+W2*TF)
R2CQ=R2C*SIN(U02+W2*TF)
DEL RP=R2CP-R1CP
DEL RQ=R2CQ-R1CQ
R1C=SQRT(R1CP**2+R1CQ**2)
R2C=SQRT(R2CP**2+R2CQ**2)
DEL R=SQRT(DEL RP**2+DEL RQ**2)
TRA=ACOS((R1C**2+R2C**2-DEL R**2)/(2.*R1C*R2C))
IF(ICO.GT.0)GO TO 5
IF((TAP.GE.TA.AND.TRA.LT.TA))GO TO 8
GO TO 7
8 TP=T-DT
TC=T
TAC=TRA
ICO=1
GO TO 6
7 TAP=TRA
T=T+DT
GO TO 10
5 TAN=TRA
IF(ABS(TAN-TA).LT.CRIT)GO TO 15
TP=TC
T0=TN
TAP=TAC
TAC=TAN
GO TO 6
15 T01=T
T02=T01+T02
V1=W1*T01

C
C NOW COMPUTE THE THRUST DIRECTION UNIT VECTORS IN THE LOCAL FRAME
C
X01=COS(PHI1)*COS(PHI2)
Y01=SIN(PHI1)*COS(PHI2)
Z01=SIN(PHI2)
X02=COS(PHI3)*COS(PHI4)
Y02=SIN(PHI3)*COS(PHI4)
Z02=SIN(PHI4)

C
C NOW COORDINATIZE THESE THRUST VECTORS IN THE GEOCENTRIC-EQUATORIAL
C FRAME FOR CORRESPONDING R1C(T01).
X1=(COS(I01)*COS(V1)+SIN(I01)*COS(I1)*SIN(V1))*X01+(COS(I01)*SIN(V1)-
SIN(I01)*COS(I1)*COS(V1))*Y01+(SIN(I01)*SIN(I1))*Z01
Y1=(SIN(I01)*COS(V1)-COS(I01)*COS(I1)*SIN(V1))*X01+(SIN(I01)*SIN(V1)+

```

```

5COS(O1)*COS(I1)*COS(V1))*Y51+(-SIN(I1)*COS(O1))*Z51
Z1=(-SIN(I1)*SIN(V1))*XG1+(SIN(I1)*COS(V1))*Y51+(COS(I1))*ZG1
X2=(COS(O1)*COS(V1)+SIN(O1)*COS(I1)*SIN(V1))*XG2+(COS(O1)*SIN(V1)-
5SIN(O1)*COS(I1)*COS(V1))*YG2+(SIN(O1)*SIN(I1))*ZG2
Y2=(SIN(O1)*COS(V1)-COS(O1)*COS(I1)*SIN(V1))*XG2+(SIN(O1)*SIN(V1)+
5COS(O1)*COS(I1)*COS(V1))*Y52+(-SIN(I1)*COS(O1))*ZG2
Z2=(-SIN(I1)*SIN(V1))*XG2+(SIN(I1)*COS(V1))*Y52+(COS(I1))*ZG2

```

C
C
C

NOW COMPUTE THE ACTUAL INERTIAL THRUST ANGLES

```

PHI2A=ASIN(Z1)
PHI1A=ASIN(Y1/COS(PHI2A))
IF((X1.AND.V1).LT.0.)PHI1A=-(PI+PHI1A)
IF((X1.LT.0.).AND.(Y1.GT.0.))PHI1A=(PI/2.+PHI1A)
PHI4A=ASIN(Z2)
PHI3A=ASIN(Y2/COS(PHI4A))
IF((X2.AND.Y2).LT.0.)PHI3A=-(PI+PHI3A)
IF((X2.LT.0.).AND.(Y2.GT.0.))PHI3A=(PI/2.+PHI3A)
PRINT*
PRINT*
ITER=ITER+1
PRINT*," ***** "
PRINT*
PRINT*,"FOR NOMINAL MISSION START TIME NO. ",ITER," TARGETING IS:"
PRINT*
PRINT*,"1ST BURN POSITION ANGLE = ",V1*RD," DEG. "
PRINT*
PRINT*,"T31",ITER,"= ",T31," SEC. "
PRINT*,"T32",ITER,"= ",T32," SEC. "
PRINT*
PRINT*,"THE THRUST DIRECTION ANGLES ARE: "
PRINT*,"PHI1A= ",PHI1A*RD," DEG. "
PRINT*,"PHI2A= ",PHI2A*RD," DEG. "
PRINT*,"PHI3A= ",PHI3A*RD," DEG. "
PRINT*,"PHI4A= ",PHI4A*RD," DEG. "
T=T+PER
IF(ITER.LT.5)GO TO 15
RETURN
END
SUBROUTINE BURYN(PHI1,PHI2,PHI3,PHI4,C23,R1C,V1C,R2C,V2C)

```

C
C
C
C
C
C

```

XXXXXXXXXXXXXXXXXXXXXXXXXXXXXXXXXXXXXXXXXXXXXXXXXXXXXXXXXXXXXXXXXXXX
THIS SUBROUTINE COMPUTES THE FIRST BURN TIME AND CORRESPONDING
THRUST DIRECTION ANGLES FROM T31 AND SPECIFIED ORBITAL ELEMENTS,
FOR NON-COPLANAR TRANSFERS.
XXXXXXXXXXXXXXXXXXXXXXXXXXXXXXXXXXXXXXXXXXXXXXXXXXXXXXXXXXXXXXXXXXXX

```

```

COMMON/T31/A11,A12,O1,O2,L02,T22,TEST
REAL I1,I2,L02
PI=3.1415926535898
RD=180./PI
GR=PI/180.
I1=A11
I2=A12
ITER=0
IF(TEST.GT.0.)GO TO 14
PHI2=-PHI2
PHI4=-PHI4
CONTINUE
W1=V1C/R1C

```

14


```

      W2=V2C/R2C
C
C      COMPUTE T91
C
      U1=02-02G
      IF(U1.GE.0.)ARC=U1
      IF(U1.LT.0.)ARC=(2.*PI-U1)
      T91=ARC/W1
      PER=(2.*PI)/41
      T92=T91+T22
C
C      NOW COMPUTE THE THRUST DIRECTION UNIT VECTORS IN THE LOCAL FRAME
C
      XG1=COS(PHI1)*COS(PHI2)
      YG1=SIN(PHI1)*COS(PHI2)
      ZG1=SIN(PHI2)
      XG2=COS(PHI3)*COS(PHI4)
      YG2=SIN(PHI3)*COS(PHI4)
      ZG2=SIN(PHI4)
C
C      NOW COORDINATIZE THESE THRUST VECTORS IN THE GEOCENTRIC-EQUATORIAL
C      FRAME FOR CORRESPONDING R1C(T81).
C
      X1=(COS(O1)*COS(V1)+SIN(O1)*COS(I1)*SIN(V1))*XG1+(COS(O1)*SIN(V1)-
5SIN(O1)*COS(I1)*COS(V1))*YG1+(SIN(O1)*SIN(I1))*ZG1
      Y1=(SIN(O1)*COS(V1)-COS(O1)*COS(I1)*SIN(V1))*XG1+(SIN(O1)*SIN(V1)+
6COS(O1)*COS(I1)*COS(V1))*YG1+(-SIN(I1)*COS(O1))*ZG1
      Z1=(-SIN(I1)*SIN(V1))*XG1+(SIN(I1)*COS(V1))*YG1+(COS(I1))*ZG1
      X2=(COS(O1)*COS(V1)+SIN(O1)*COS(I1)*SIN(V1))*XG2+(COS(O1)*SIN(V1)-
5SIN(O1)*COS(I1)*COS(V1))*YG2+(SIN(O1)*SIN(I1))*ZG2
      Y2=(SIN(O1)*COS(V1)-COS(O1)*COS(I1)*SIN(V1))*XG2+(SIN(O1)*SIN(V1)+
5COS(O1)*COS(I1)*COS(V1))*YG2+(-SIN(I1)*COS(O1))*ZG2
      Z2=(-SIN(I1)*SIN(V1))*XG2+(SIN(I1)*COS(V1))*YG2+(COS(I1))*ZG2
C
C      NOW COMPUTE THE ACTUAL INERTIAL THRUST ANGLES:
C
      PHI2A=ASIN(Z1)
      PHI1A=ASIN(Y1/COS(PHI2A))
      IF((X1.AND.Y1) LT.0.)PHI1A=-(PI+PHI1A)
      IF((X1.LT.0.).AND.(Y1.GT.0.))PHI1A=(PI/2.+PHI1A)
      PHI4A=ASIN(Z2)
      PHI3A=ASIN(Y2/COS(PHI4A))
      IF((X2.LT.0.).AND.(Y2.GT.0.))PHI3A=-(PI+PHI3A)
      IF((X2.AND.Y2) LT.0.)PHI3A=-(PI+PHI3A)
      IF((X2.LT.0.).AND.(Y2.GT.0.))PHI3A=(PI/2.+PHI3A)
      PRINT*
      PRINT*
      PRINT*," ***** "
      PRINT*
      PRINT*,"FOR NOMINAL MISSION START TIME T91, THE TARGETING IS: "
      PRINT*
      PRINT*,"1ST BURN POSITION ANGLE = ",J1*RD," DEG. "
      PRINT*,"THE PERIOD= ",PER," SEC. "
      PRINT*
      PRINT*
      ITER=ITER+1
10      PRINT*,"T91",ITER,"= ",T91," SEC. "
      PRINT*,"T92",ITER,"= ",T92," SEC. "
      PRINT*
      T91=T91+PER

```

```

T82=T81+T22
IF(ITER.LT.5)GO TO 10
PRINT*
PRINT*
PRINT*,"THE THRUST DIRECTION ANGLES ARE: "
PRINT*,"PHI1A= ",PHI1A*RD," DEG. "
PRINT*,"PHI2A= ",PHI2A*RD," DEG. "
PRINT*,"PHI3A= ",PHI3A*RD," DEG. "
PRINT*,"PHI4A= ",PHI4A*RD," DEG. "
PRINT*
PRINT*
RETURN
END
SUBROUTINE THRJSTF(R1C,V1C,TJF,C1,C2)
C
C XXXXXXXXXXXXXXXXXXXXXXXXXXXXXXXXXXXXXXXXXXXXXXXXXXXXXXXXXXXXXXX
C THIS ROUTINE COMPUTES INSERTION ERROR SENSITIVITIES DUE
C TO THRUST MAGNITUDE DEVIATIONS.
C XXXXXXXXXXXXXXXXXXXXXXXXXXXXXXXXXXXXXXXXXXXXXXXXXXXXXXXXXXXXXXX
C
EXTERNAL SLOPE
DIMENSION XN(5),X(6),SNS(6,3),Z(5)
COMMON/TE/K,SNS
COMMON/SL/M01,M02,MF1,MF2,T1,T2,M01,M02,TB1,TB3
COMMON/SLC/Z
REAL M01,M02,MF1,MF2,M01,M02,M01N,M02N
CNMF=6076.115486
ISKIP=0
M01N=M01
M02N=M02
TBAN=TBA
TB3N=TB3
T1N=T1
T2N=T2
DO 10 J=1,5
10 XN(J)=X(J)
T1=T1+(.01)*T1
T2=T2+(.01)*T2
M01=T1/C1
M02=T2/C2
TBA=(M01-MF1)/M01
TB3=(M02-MF2)/M02
100 T=J,
X(1)=R1C
X(2)=0.
X(3)=0.
X(4)=0.
X(5)=V1C
X(6)=0.
DT=TBA/512.
CALL SET(5,T,X,DT,SLOPE,D,.T.,D,D)
DO 70 K=1,512
70 CALL STEP(5,T,X,DT,SLOPE,D,.T.,D,D)
CONTINUE
DT=(TOF-(TB1+TB3))/10240.
CALL SET(5,T,X,DT,SLOPE,D,.T.,D,D)
DO 80 K=1,10240
80 CALL STEP(5,T,X,DT,SLOPE,D,.T.,D,D)
CONTINUE
DT=TB3/512.

```



```

CALL SET(5,T,X,DT,SLOPE,D,.T.,D,D)
DO 30 K=1,512
CALL STEP(5,T,X,DT,SLOPE,D,.T.,D,D)
90 CONTINUE
IF(ISKIP.GT.0)GO TO 2
DR2=(SQRT((X(1)-XN(1))**2+(X(2)-XN(2))**2+(X(3)-XN(3))**2))/CNMF
DV2=SQRT(((X(4)-XN(4))**2+(X(5)-XN(5))**2+(X(6)-XN(6))**2)
T1=T1N
T2=T2N
T1=T1-(.01)*T1
T2=T2-(.01)*T2
M01=T1/C1
M02=T2/C2
T01=(M01-MF1)/M01
T02=(M02-MF2)/M02
IS<IP=1
GO TO 100
2 CONTINUE
DR4=(SQRT((X(1)-XN(1))**2+(X(2)-XN(2))**2+(X(3)-XN(3))**2))/CNMF
DV4=SQRT(((X(4)-XN(4))**2+(X(5)-XN(5))**2+(X(6)-XN(6))**2)
PRINT*
PRINT*
PRINT*
PRINT*,"THE INSERTION POSITION AND VELOCITY ERROR SENSITIVITIES "
PRINT*,"FOR -THRUST MAG. DEVIATIONS- , BOTH PLJS AND MINUS ARE: "
PRINT*
PRINT*
PRINT*,"DR2= ",DRP," (N.Y.)/(+1X) "
PRINT*,"DV2= ",DVP," (FT/SEC.)/(+1X) "
PRINT*,"DR4= ",DRM," (N.Y.)/(-1X) "
PRINT*,"DV4= ",DVM," (FT/SEC.)/(-1X) "
PRINT*
PRINT*
PRINT*,"-----"
T1=T1N
T2=T2N
M01=M01N
M02=M02N
T01=T01N
T02=T02N
RETURN
END
SUBROUTINE MTSP(A,M,N,AT)
DIMENSION A(4,4),AT(N,M)
DO 2 I=1,M
DO 3 J=1,4
3 AT(J,I)=A(I,J)
2 CONTINUE
RETURN
END
SUBROUTINE M4PY(A,B,C,M,K,N)
DIMENSION A(4,4),B(K,N),C(4,4)
DO 10 J=1,4
DO 10 I=1,M
C(I,J)=0.0
DO 10 L=1,K
10 C(I,J)=C(I,J)+A(I,L)*B(L,J)
RETURN
END

```

Vita

Jackie L. Roberts was born 16 June 1944 in Hamilton, Montana. Upon graduation from Hamilton High School in 1962, he enlisted in the United States Air Force and served nearly two years in the Security Service. In June of 1964 he entered the United States Air Force Academy. He was awarded a Bachelor of Science Degree in Engineering Sciences, and received a Regular Commission in the United States Air Force upon graduation in 1968.

Upon completion of pilot training at Craig AFB, Selma, Alabama, he was assigned to Norton AFB, California, in the C-141 aircraft. In 1971 he was reassigned to Tan Son Nhut AB, Vietnam, as a pilot on the HH-43 rescue helicopter. He spent an extended tour in Vietnam flying as both a rescue pilot and instructor pilot, and was awarded the Distinguished Flying Cross and Eight Air Medals for his service.

In January 1973 he returned to the United States and served as an Aircraft Commander on the C-5/A aircraft at Dover AFB, Delaware. While serving in this capacity he was selected to attend the Air Force Institute of Technology.

He began study towards a Master of Science Degree in Astronautics at the resident School of Engineering, Wright-Patterson AFB, in June of 1975.

Permanent address: 102 Daly Avenue
Hamilton, Montana 59840

Unclassified

SECURITY CLASSIFICATION OF THIS PAGE (When Data Entered)

REPORT DOCUMENTATION PAGE		READ INSTRUCTIONS BEFORE COMPLETING FORM
1. REPORT NUMBER GA/EE/76-1	2. GOVT ACCESSION NO.	3. RECIPIENT'S CATALOG NUMBER
4. TITLE (and Subtitle) AN ENERGY MANAGEMENT GUIDANCE SCHEME APPLICABLE TO THE INTERIM UPPER STAGE.	5. TYPE OF REPORT & PERIOD COVERED MS Thesis	
7. AUTHOR(s) 10 Jackie L. Roberts	6. PERFORMING ORG. REPORT NUMBER	
9. PERFORMING ORGANIZATION NAME AND ADDRESS Air Force Institute of Technology (AFIT- EN) Wright-Patterson AFB, Ohio 45433	8. CONTRACT OR GRANT NUMBER(s) Master's thesis	
11. CONTROLLING OFFICE NAME AND ADDRESS Space and Missile Systems Organization (LVR) Los Angeles AFS, Ca.	10. PROGRAM ELEMENT, PROJECT, TASK AREA & WORK UNIT NUMBERS	
14. MONITORING AGENCY NAME & ADDRESS (if different from Controlling Office) 11 Dec 76 12 165p.	12. REPORT DATE December 1976	
	13. NUMBER OF PAGES 150	
	15. SECURITY CLASS. (of this report) Unclassified	
	15a. DECLASSIFICATION/DOWNGRADING SCHEDULE	
16. DISTRIBUTION STATEMENT (of this Report) Approved for public release; distribution unlimited		
17. DISTRIBUTION STATEMENT (of the abstract entered in Block 20, if different from Report)		
18. SUPPLEMENTARY NOTES Approved for public release: IAWAFR 190-17 Jerald F. Guess, Captain, USAF Director of Information		
19. KEY WORDS (Continue on reverse side if necessary and identify by block number) Orbit Transfers		
20. ABSTRACT (Continue on reverse side if necessary and identify by block number) A workable open loop guidance scheme for orbital transfer maneuvers is developed for a two stage solid-rocket vehicle which has no thrust termination capability. The scheme effectively manages any excess energy by matching a non-Hohmann transfer trajectory to the fixed energy (AV) capabilities of the vehicle. The entire burden of effecting the transfer is put on prelaunch targeting, so that during the burns the thrust is (contin. p 152)		

DD FORM 1473 EDITION OF 1 NOV 65 IS OBSOLETE

Unclassified 012 225
SECURITY CLASSIFICATION OF THIS PAGE (When Data Entered)

151

Cont p1
p151

Unclassified

SECURITY CLASSIFICATION OF THIS PAGE(When Data Entered)

can be directed along a precomputed direction using constant attitude maneuvers only.

(6)
A computer program has been developed which employs a nonlinear equation solving routine to accomplish exact targeting for the finite-thrust transfer maneuver. The transfer trajectory is characterized by ~~six~~ control parameters (the outputs of targeting), and the final orbit is defined by a set of 'hit conditions'. The values of the control parameters which drive the vehicle state vector to satisfy the hit conditions become the guidance system target parameters.

In addition, an error analysis is performed on the scheme throughout the range of possible trajectories which exist for excess energy missions. These trajectories are then compared on the basis of optimality, such as minimum insertion errors and transfer time. Results are presented for geosynchronous and subsynchronous transfers between circular orbits.

A

152

Unclassified

SECURITY CLASSIFICATION OF THIS PAGE(When Data Entered)